

Test of the Rossby Centre Regional Atmospheric Climate
Model's Land Surface Scheme

Karolina Nilsson

Department of Physics
Lund University, 2006
Supervisor: Fredrik Lagergren



LUNDS UNIVERSITET

Abstract

There is an economic interest in the development of reliable climate models that can give us a good estimation of the present and future climate. Farmers, electricity- and insurance- companies are some of the clients that need long term (monthly) weather information from the Swedish Meteorological and Hydrological Institute (SMHI).

This work focuses on the evaluation of the Rossby Centre Regional Atmospheric Climate Model's land surface scheme. The main purpose with the land surface scheme is to provide the atmosphere with sensible and latent heat (heat fluxes) in a representative manner for different vegetation types. Meteorological data from a boreal forest in Sweden, Norunda, and an open pasture area in the Netherlands, Cabauw, are together with site specific information used as input to the model. The modelled output data, such as heat fluxes, air temperature, soil temperatures and soil water are then compared to observations performed at each site.

Since it is important to have access to continuous meteorological data during the model run a detailed preparation description for a data set from a forest in Finland, Hyytiälä, is presented.

A sensitivity test performed for Norunda shows that the land surface scheme is highly sensitive to specific humidity, global radiation and temperature. Extra care must therefore be attended to these variables during data preparation. It is also shown that extra care must be attended to leaf area index, displacement height and heat capacity of trees since these are the model parameters that mostly affect heat fluxes during the sensitivity test.

The land surface scheme generally performs well for both land types, but especially for the open pasture area, when heat fluxes are considered. However, the result is less satisfying when modelled soil temperatures and soil water are compared to observations. The diurnal variation amplitudes for soil temperatures are higher for the model than for observations even though the former represents deeper depths. Modelled soil water is also represented at a deeper depth than the observations, yet the volume of water is higher in the former case.

Acknowledgements

This work has been carried out during my master thesis in physics at Lund University. First of all, I would like to thank my supervisor, Dr Fredrik Lagergren, at the Department of Physical Geography and Ecosystems Analysis, for his support and providing me with data from Norunda. Further on, I would like to thank Dr Patrick Samuelsson at Rosaby Centre for providing me with the climate model as well as the data from Cabauw, Dr Stefan Gollvik at the Research Department of SMHI, for letting me use his wet bulb program and his contribution to the discussion, and all persons who have provided me with data, especially Dr Pasi Kolari, at the Department of Forest Ecology University of Helsinki, Dr Lisbeth Lewan Department of Soil Sciences at Uppsala and Dr David Gustafsson Department of Land and Water Resources at the Royal Institute of Technology.

A grateful thanks to the staff and friends at Department of Physical Geography and Ecosystems Analysis, especially MSc Janno Tuulik, Associate Professor Lars Barring, who have contributed with their LINUX knowledge, professor Anders Lindroth and Mr Patrik Westin for suggestions and ideas. Finally, I would like to thank Associate Professor Margareta Hellström at Department of Physics, for interesting discussions and sharing her MATLAB programming skills with me.

Contents

ABSTRACT -----	III
ACKNOWLEDGEMENTS -----	IV
CONTENTS -----	IV
SYMBOLS & ABBREVIATIONS -----	VII
1. INTRODUCTION -----	1
2. THEORY -----	3
2.1 DEFINITION OF LATENT AND SENSIBLE HEAT & THE GLOBAL ENERGY BALANCE -----	3
2.2 NET RADIATION -----	4
2.3 FACTORS CONTROLLING THE RELEASE OF LATENT AND SENSIBLE HEAT -----	5
2.4 TRANSPORTATION PROCESSES OF LATENT AND SENSIBLE HEAT -----	5
2.5 BOWEN RATIO -----	6
2.6 TILE EQUATIONS FOR LATENT AND SENSIBLE HEAT -----	6
2.7 TILE EQUATIONS FOR NET RADIATION -----	8
2.8 SOIL TEXTURE CLASS, FIELD CAPACITY & WILTING POINT -----	8
2.9 SOIL WATER -----	9
2.10 SOIL TEMPERATURE -----	9
2.11 LEAF AREA INDEX -----	10
2.12 WATER FLOWS -----	10
2.13 INTERCEPTION -----	11
2.14 HEAT CAPACITY OF TREES -----	12
2.15 VAPOUR DEFICIT -----	12
2.16 DISPLACEMENT HEIGHT -----	12
2.17 ROUGHNESS LENGTH -----	13
3. DATA PREPARATION -----	15
3.1 DATA MEASUREMENTS -----	15
3.2 SITE DESCRIPTION -----	16
3.3 GAP FILLING -----	17
3.3.1 <i>GAPS IN GLOBAL RADIATION</i> -----	18
3.3.2 <i>GAPS IN LONG WAVE RADIATION</i> -----	19
3.3.2.1 <i>Gaps in net radiation</i> -----	19
3.3.2.2 <i>Gaps in short wave outgoing radiation & albedo</i> -----	21
3.3.3 <i>GAPS IN PRECIPITATION</i> -----	21
3.3.4 <i>EXAMPLES OF WHAT CAN GO WRONG</i> -----	23
3.4 FURTHER DATA PREPARATION -----	23
3.4.1 <i>CONVERSION OF RELATIVE HUMIDITY TO SPECIFIC HUMIDITY</i> -----	23
3.4.2 <i>DIVISION OF PRECIPITATION INTO RAIN OR SNOW</i> -----	24
3.4.3 <i>SOIL WATER IN NORUNDA</i> -----	24
4. METHODS -----	27

4.1 MODEL INPUT	27
4.2 CONTROL OF DRIVING- AND VERIFICATION DATA	28
4.3 SENSITIVITY TEST FOR NORUNDA	28
4.4 HOURLY DEVIATIONS BETWEEN OBSERVATIONS AND MODELLED VALUES	31
5. RESULTS	33
5.1 SENSITIVITY TEST FOR NORUNDA	33
5.2 DIURNAL VARIATION	37
6. DISCUSSION	39
6.1 GAP FILLING PROCESS	39
6.2 CONTROL OF DRIVING- AND VERIFICATION DATA	39
6.3 SENSITIVITY TEST	39
6.4 DIURNAL VARIATION	39
7. CONCLUSIONS & FUTURE WORK	41
7.1 CONCLUSIONS	41
7.2 FUTURE WORK	41
REFERENCES	43
APPENDIX	APPENDIX A-1
APPENDIX A: EQUATIONS	APPENDIX A-1
APPENDIX A: TABLES	APPENDIX A-2
APPENDIX B: SENSITIVITY TEST TABLES	APPENDIX B-1
APPENDIX C: FIGURES FOR NORUNDA AND CABAUW	APPENDIX C-1

Symbols & Abbreviations

In those cases where the nomenclature in Samuelsson *et al.* (2006) differs from that of Choudhury & Monteith (1988), the original name is also provided in the explanation.

A	[m]	altitude above sea level
a	[Pa]	constant in Tetens formula
B		Bowen ratio
b		constant in Tetens formula
C	[W/m ²]	total loss of sensible heat from the system (Choudhury & Monteith, 1988)
C_s	[W/m ²]	sensible heat component of R_s (sensible heat transfer from the soil to the reference level within the foliage)
C_v	[W/m ²]	sensible heat component of R_v (sensible heat flux transfer from the foliage surface to the canopy air)
c	[°C]	constant in Tetens formula
c_p	[J/KgK]	specific heat capacity of air at constant pressure
D	[Pa]	vapour deficit
DOY		day of year
d	[m]	displacement height
E	[W/m ²]	latent heat (Samuelsson <i>et al.</i> , 2006)
E_{for}	[W/m ²]	total loss of latent heat from the system (Samuelsson <i>et al.</i> , 2006); λE
E_{forc}	[W/m ²]	total latent heat flux from the forest canopy (total evapotranspiration from the forest canopy)
E_{forsn}	[W/m ²]	latent heat flux from the forest snow surface to the canopy air space
E_v	[W/m ²]	evaporation of intercepted water
e_a	[Pa]	vapour pressure at the reference height (Choudhury & Monteith, 1988)
e_b	[Pa]	vapour pressure in the canopy air (Choudhury & Monteith, 1988)
e_s	[Pa]	saturation vapour pressure
e_l^*	[Pa]	saturation vapour pressure at the top of wet soil layer (Choudhury & Monteith, 1988)
e_1^*	[Pa]	saturation vapour pressure inside stomata
e_2	[Pa]	vapour pressure at the soil surface
Fc	[cm ³ /cm ³]	field capacity
f	[μmol/J]	ratio between Q_{PPFD} and global radiation (broadband irradiance)
G	[W/m ²]	total heat exchange by conduction

G_0	[W/m ²]	conduction downwards from the soil surface
H	[W/m ²]	sensible heat
H_{for}	[W/m ²]	total loss of sensible heat flux from the system (Samuelsson <i>et al.</i> , 2006); C
H_{forsn}	[W/m ²]	sensible heat flux from the forest snow surface to the canopy air space
h	[m]	vegetation height
h_r		relative humidity
h_{vfor}		coefficient that includes the fraction of vegetation covered with water (δ)
LAI	[m ² /m ²]	leaf area index
LE	[W/m ²]	evapotranspiration (latent heat)
LSS		land surface scheme
L_{\downarrow}	[W/m ²]	incoming long wave radiation
L_{\uparrow}	[W/m ²]	outgoing long wave radiation
l	[m]	depth of the dry soil layer
P	[kg/m ² s]	rain intensity
Q_{PPFD}	[μ mol/m ² s]	photosynthetic photon flux density
q_{am}	[Kg _{water} /Kg _{air}]	specific humidity at z_{am}
q_{fora}	[Kg _{water} /Kg _{air}]	specific humidity in the canopy air space (Samuelsson <i>et al.</i> , 2006)
q_s	[Kg _{water} /Kg _{air}]	surface saturated specific humidity
RCA		Rosby Centre Regional Atmospheric Climate Model
R_g	[W/m ²]	global radiation
R_n	[W/m ²]	net radiation
R_s	[W/m ²]	net absorption of radiation at the soil surface
R_{solar}	[W/m ²]	solar broadband irradiance
R_v	[W/m ²]	net absorption of radiation at vegetation treated as a simple surface
R^2		mean square, root mean square $\sqrt{R^2}$
r_a	[s/m]	aerodynamic resistance (Choudhury & Monteith, 1988)
r_{afor}	[s/m]	aerodynamic resistance (Samuelsson <i>et al.</i> , 2006); r_a
r_b	[s/m]	aerodynamic resistance between the forest canopy and the canopy air (Samuelsson <i>et al.</i> , 2006); r_1
r_c	[s/m]	canopy equivalent of the physiological resistance to the diffusion of water vapour through the stomata (Choudhury & Monteith, 1988)
r_d	[s/m]	aerodynamic resistance between forest floor and canopy air (Samuelsson <i>et al.</i> , 2006); r_2

r_l	[s/m]	resistance proportional to the depth of the wet soil layer
r_s	[s/m]	resistance to the diffusion of water vapour through the dry layer of the soil (Choudhury & Monteith, 1988)
r_{sforc}	[s/m]	forest canopy surface resistance (Samuelsson <i>et al.</i> , 2006); r_c
r_{sfors}	[s/m]	forest floor soil surface resistance (Samuelsson <i>et al.</i> , 2006); r_s
r_u	[s/m]	resistance proportional to the depth of the dry layer
r_1	[s/m]	aerodynamic resistance between the foliage and the canopy air (Choudhury & Monteith, 1988)
r_2	[s/m]	resistance between the soil surface and the canopy air (Choudhury & Monteith, 1988)
S_{\downarrow}	[W/m ²]	incoming short wave radiation
S_{\uparrow}	[W/m ²]	reflected solar (short wave) radiation
T	[°C]	air temperature (Tetens, 1930)
T_a	[K]	air temperature at an arbitrary reference height (Choudhury & Monteith, 1988)
T_{am}	[K]	air temperature at an arbitrary reference height (Samuelsson <i>et al.</i> , 2006); T_a
T_b	[K]	canopy air temperature (Choudhury & Monteith, 1988)
T_{fora}	[K]	canopy air temperature (Samuelsson <i>et al.</i> , 2006); T_b
T_{forc}	[K]	forest canopy temperature (Samuelsson <i>et al.</i> , 2006); T_1
T_{fors}	[K]	temperature at the soil surface (Samuelsson <i>et al.</i> , 2006);
T_{forsn}	[K]	forest snow surface temperature (Samuelsson <i>et al.</i> , 2006)
T_l	[K]	temperature at the interface between wet and dry soil
T_m	[K]	temperature at the bottom of the wet layer
T_s	[K]	surface temperature
T_1	[K]	mean temperature of the foliage (Choudhury & Monteith, 1988)
T_2	[K]	temperature at the soil surface (Choudhury & Monteith, 1988)
thr	[kg/m ² s]	throughfall
u	[m/s]	wind speed as a function of height (z)
u^*	[m/s]	friction velocity
ν	[m ² /s]	kinematic viscosity
veg		vegetation cover parameter
Wp	[cm ³ /cm ³]	wilting point
$w_{veg\ max}$	[kg/m ²]	maximum amount of water allowed on the vegetation
w_{veg}^{τ}	[kg/m ²]	amount of intercepted water in the present time step
$w_{veg}^{\tau+1}$	[kg/m ²]	amount of intercepted water in the next time step
X	[m ⁴]	mean drag coefficient for individual leaves multiplied with LAI

z	[m]	height
z_{am}	[m]	atmospheric reference level
z_0	[m]	roughness length
<i>Greek</i>		
α		surface albedo
γ	[Pa/K]	psychrometric constant
Δt	[s]	length of time step
δ		fraction of vegetation covered with water
ε		emissivity
κ		Von Karman constant
λE	[W/m ²]	total loss of latent heat flux from the system
λE_s	[W/m ²]	latent heat of evaporation from the top of the wet soil layer (latent heat transfer from the soil to the reference level within the foliage)
λE_c	[W/m ²]	latent heat of transpiration through stomata
λ	[J/Kg]	latent heat of evaporation
ρ	[Kg/m ³]	air density
ρc_p	[J/m ³ K]	volumetric specific heat of air
σ	[W/m ² K ⁴]	Stephan-Boltzmann constant
τ		present time step
$\psi_m(\xi)$	[m/s]	function that describes the influence of atmospheric stability on turbulence

1. Introduction

There is an economic interest in the development of reliable climate models that can give us a good estimation of the present and future climate. Farmers, electricity- and insurance- companies are some of the clients that need long term (monthly) weather information from the Swedish Meteorological and Hydrological Institute (SMHI).

The climate modeling research unit, Rossby centre, at SMHI was built up during the Swedish Regional Climate Modelling Programme (SWECLIMP), during 1996-2003 (<http://www.smhi.se/>). The goal of the program was to provide regional estimates of future anthropogenic climate change for the Nordic region (Jones *et al.*, 2004).

To realize this effort a space limited area coupled regional model (RCA) was developed by the Rossby Centre. One of the advantages with a regional climate model compared to a global climate model is that less computational work is required.

Further, it is possible to include more regional forcing (mountain chains, larger lakes *etc.*) in a regional model since it has a higher spatial grid resolution (20-50 km) than a common global climate model (200-300 km). The high spatial resolution also makes it possible to explicitly resolve a greater number of atmospheric and oceanic processes. A more accurate climate representation is therefore expected with a regional model when it is compared to a global model for the same region (Jones *et al.*, 2004).

The RCA consists of an atmospheric model coupled to an ocean- sea ice model for the Baltic Sea. A land surface scheme is included in the atmospheric model part where it serves as a lower boundary condition for the atmosphere. The main purpose of the land surface scheme is to provide the atmosphere with radiation, heat and momentum fluxes in a representative manner (Samuelsson *et al.*, 2006).

Representation of realistic fluxes and radiation is important since *e.g.* latent heat release in the atmosphere provides energy that fuels storms and atmospheric circulation (Bonan, 2002).

Grid scale variables in the land surface scheme, which has been developed with focus on high- and middle latitudes (Samuelsson *et al.*, 2006), include the overall effect from sub grid scale processes (Persson, 2001).

Deviations between modelled and observed values are less clear to identify during coupled model runs since the atmosphere adjusts the results in the next time step (Samuelsson, pers. comm.). The easiest way to improve the RCA is to adjust the model to observed values based on the results of uncoupled simulations.

During the evaluation of the RCA atmospheric component Jones *et al.* (2004) used a three dimensional model domain with a horizontal resolution of 0.44° and 24 vertical levels. In this study a one dimensional (1D) model run is used to evaluate the land surface scheme. The surface coverage fraction of forest and/or open land for the grid cell, in which the studied site lies within, must therefore be determined manually.

Before the 1D model can be run with continuous meteorological input data, which have been measured at the site, additional site specific information must be defined.

Examples of such information is soil texture class and reference height. The latter is defined as the height where heat flux measurements at the site have been performed.

The modelled heat fluxes are therefore calculated for this height. As a final step output files from the model and verification data records (containing heat fluxes, temperatures soil water *etc.*) measured at the site, are compared.

The aim of this paper is to identify weaknesses in an uncoupled version of the RCA model's land surface scheme, using data and observations from different vegetation types. It can be summarized in a few questions:

- Which parameters and meteorological forcing data is the model sensitive to?
- Do variable/parameter output data differ from observed values during any special time of day and/or season?
- Can a deviation in one parameter/variable be connected to a deviation in another parameter/variable?

2. Theory

To give a detailed description of all parameters, variables and equations derived and used in the RCA land surface scheme (LSS) is far beyond the scope of this paper. This theory part will therefore account only for the parameters/variables that most affect sensible and latent heat fluxes and the main features of the LSS. Additionally, some of the concepts used in the sensitivity test will be explained. The interested reader can find information about parameterization equations in the paper written by Samuelsson *et al.* (2006).

2.1 Definition of latent and sensible heat & the global energy balance

Heat is either absorbed or released during phase changes of water. Since this heat does not affect the temperature of the water molecules, but only changes the energy state of them, it is called latent heat, LE , (Bonan, 2002).

Sensible heat, H , is a flow that arises due to a temperature gradient between two bodies (Campbell & Norman, 1998).

Both latent and sensible heat are included in the global energy balance, where the energy input from the sun on average equals the amount of radiation that goes back to space.

The energy density flux, known as the solar constant, from the sun has a present value of 1370 W/m^2 at the Earth's orbit. Each unit area of the Earth receives 342 W/m^2 of solar radiation, which corresponds to $\frac{1}{4}$ of the solar constant, since only a cross section of the Earth's entire area can intercept the radiation (Seinfeld & Pandis, 1998). To maintain the global energy balance, and thereby prevent a surface temperature change, a corresponding amount of energy needs to exit into space (Figure 1).

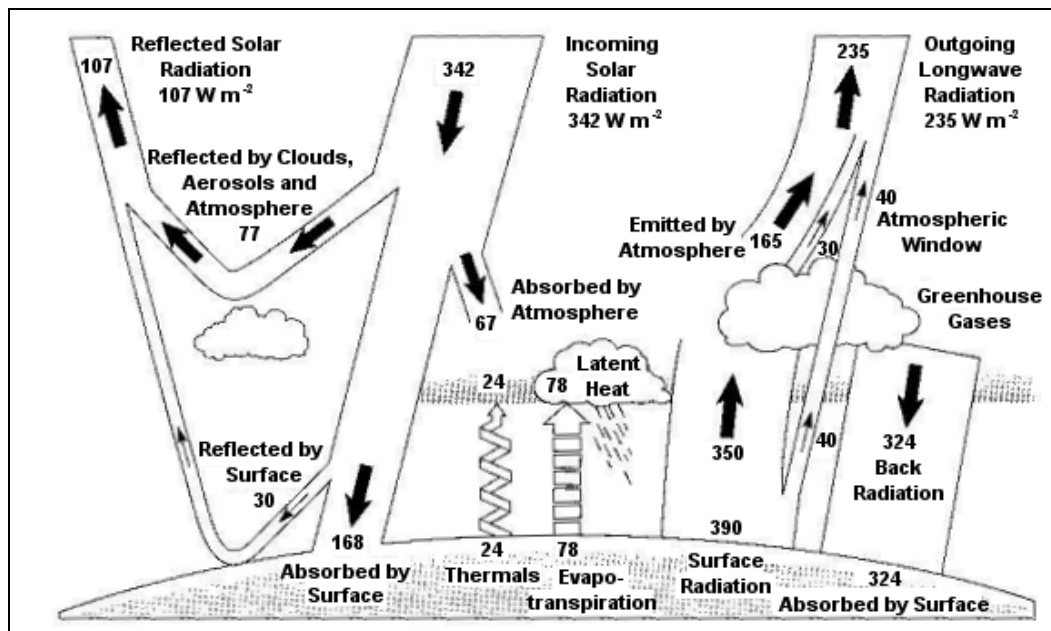


Figure 1. Global mean energy flows for the different paths and interactions in the Earth's energy balance (after Harvey, 2000).

Surface albedo and backscatter from clouds, aerosols and molecules constitute the mean planetary reflectance (Seinfeld & Pandis, 1998). As seen, (Figure 1), $\sim 31\%$ of the incident solar radiation is reflected back to space due to the global mean planetary

reflectance (albedo). About 67 W/m^2 ($\sim 20\%$) of the incoming solar radiation, which also is called global radiation or short wave radiation, is absorbed by the atmosphere. The remaining $\sim 49\%$ of the short wave radiation is absorbed at the surface, which it reaches by taking a direct- (not scattered) or diffuse- (downward scattered) path (Chapin *et al.*, 2002).

The amount of energy emitted from a body depends on its temperature and its inherent ability to emit which is called emissivity (Harvey, 2000). A hot body emits more radiation at shorter wavelengths than a cold body. Land, oceans, clouds and atmosphere emit long wave radiation instead of short wave radiation, since they are colder than the sun. Out of 390 W/m^2 of long wave radiation, that leaves the earth's surface, 40 W/m^2 is direct emitted to space. The remaining 350 W/m^2 is absorbed by the atmosphere. Clouds emit 30 W/m^2 of long wave radiation to space while the atmosphere emits 165 W/m^2 . The atmosphere also emits 324 W/m^2 of long wave radiation to the surface, which the surface then absorbs.

This means that the Earth's surface on average has a net surplus of 102 W/m^2 . About 23.5% of the surface net surplus, called thermals (Figure 1), enters the atmosphere as sensible heat (Bonan, 2002), while the remaining $\sim 76.5\%$ is used to evaporate water, instead of raising the surface temperature. The amount of energy consumed during the evaporation process is released in the atmosphere during condensation, which often occurs far away from where the evaporation took place (Chapin *et al.*, 2002).

This means that the 102 W/m^2 of excess energy at the surface reaches the atmosphere and balances the lost radiative energy.

Three balancing equations, balance at the top of the atmosphere (a), balance within the atmosphere (b) and balance at the surface (c) (Chapin *et al.*, 2002), can be used to describe Figure 1:

$$(a) \quad S_{\downarrow}(342) = L_{\uparrow}(235) + S_{\uparrow}(107)$$

$$(b) \quad S_{\downarrow}(67)_{\text{absorbed by the atmosphere}} + L_{\uparrow}(350)_{\text{from the surface, absorbed by the atmosphere}} + LE(78) + H(24) = L_{\uparrow}(195)_{\text{emitted to space by the atmosphere + clouds}} + L_{\downarrow}(324)_{\text{from the atmosphere, absorbed by the surface}}$$

$$(c) \quad S_{\downarrow}(168)_{\text{absorbed by the surface}} + L_{\downarrow}(324)_{\text{absorbed by the surface}} = LE(78) + H(24) + L_{\uparrow}(390)_{\text{emitted from the surface}}$$

2.2 Net radiation

A systems net radiation (R_n) is defined as the energy absorbed by the system. It can either be expressed in terms of shortwave and long wave radiation or as a sum of sensible and latent heat and ground heat flows (G).

The net radiation balance can be described by

$$R_n = S_{\downarrow} - S_{\uparrow} + L_{\downarrow} - L_{\uparrow} = H + LE + G \quad (\text{Bonan, 2002}) \quad \text{Eq. (1)}$$

under the assumption that the supply term of energy to the surface, by processes such as photosynthesis and metabolism (Campbell & Norman, 1998), is neglected.

R_n is positive when it is directed towards the surface, while the opposite is true for the terms on the right hand side of Equation 1 (Chapin *et al.*, 2002).

Latent and sensible heat is often approximated to constitute the entire amount of net radiation since most ecosystems have a small storage term and negligible daily averages of G . However, the relation is not valid for lakes, oceans and permafrost regions since they have significant ground heat flux (Chapin *et al.*, 2002).

2.3 Factors controlling the release of latent and sensible heat

Many factors affect the amount of latent and sensible heat release from the surface. Since latent heat flux is responsible both for energy and water transfers to the atmosphere from the ecosystem (Chapin *et al.*, 2002), factors controlling the system's water access also need to be accounted for.

Water can only evaporate from a surface in the presence of a vapour pressure gradient between the air immediately adjacent to the evaporating surface and the air with which it mixes (Chapin *et al.*, 2002). The evaporation efficiency is controlled by surface- and atmospheric- resistances, which varies depending on if the surface is vegetated or not. Air inside a leaf is always saturated with water vapour, because it is adjacent to moist cell surfaces (Chapin *et al.*, 2002). The water vapour is released from the leaf when small microscopic cavities, called stomata, in the leaf open. The plants water release, transpiration, is connected to its carbon uptake since stomata opening occur during photosynthesis. Vapour must therefore overcome a stomatal resistance, acting between the stomatal cavity and the leaf surface, before it can leave the leaf (Bonan, 2002). Stomatal resistance does not need to be accounted for during bare ground evaporation. However, the efficiency of the atmosphere to transport the water vapour away from the surface is a direct controlling factor in the process of latent heat release, regardless of whether it is vegetated or not, since the vapour pressure gradient would become weaker otherwise.

Sensible heat is controlled by the surface ability to conduct heat to the near surface atmosphere, in the presence of a temperature gradient, from where it is transferred to the bulk atmosphere by convection (Chapin *et al.*, 2002).

2.4 Transportation processes of latent and sensible heat

Thermal convection is a process in which air that is warmer than the adjacent air, starts to rise due to positive buoyancy, which is a vertical force that arises due to density differences (Dunlop, 2005). Convection that has arisen due to turbulence, driven by vertical wind shear, is called mechanical convection (McIlveen, 1998).

An eddy is a package of air or liquid, which moves in an almost circular motion within a fluid, without following the overall flow of the fluid (Dunlop, 2005). It is eddy motions that give rise to random fluctuations in wind speed and direction, which characterize turbulent flow (Campbell & Norman, 1998).

The eddies are either created by wind flowing over rough surfaces or by thermal convection. In the former case the received turbulence is called mechanical, while it is called convective or thermal in the latter case (Campbell & Norman, 1998).

Mechanical turbulence also depends on vegetation height, which means that a tall uneven forest canopy generates more mechanical turbulence than a low smooth canopy *e.g.* grass (Chapin *et al.*, 2002).

The entire atmosphere, with the exception of a thin layer next to the ground, is essentially almost always exposed to turbulence (Campbell & Norman, 1998). Due to turbulence, warm moist air near an evaporative surface is replaced with cold dry air from the bulk atmosphere. This air replacement makes it possible for the surface to continue its evaporation since the vapour pressure gradient has been maintained or even increased (Chapin *et al.*, 2002).

2.5 Bowen ratio

The ratio between sensible and latent heat is called Bowen ratio: $B = H/LE$.

Its value differ among different ecosystems, where it is less than 0.1 for tropical oceans and greater than 10 for deserts (Chapin *et al.*, 2002), but it should be close to 0.30 on a global scale (Figure 1).

The ratio is used as a measure of the connection strength between the energy- and water balances (Chapin *et al.*, 2002). A low B implies a strong connection since the ratio is inversely proportional to R_n (Equation 2) that drives the water loss from the system (Chapin *et al.*, 2002).

$$R_n \propto LE \text{ (Equation 1)} \Rightarrow R_n \propto \frac{H}{B} \Leftrightarrow B \propto \frac{H}{R_n} \quad \text{Eq. (2)}$$

B is reduced by turbulence since the temperature gradient that drives H will not be established during such conditions (Chapin *et al.*, 2002). The temperature gradient is also reduced during evaporation because of the surface cooling that takes place during the process (Chapin *et al.*, 2002).

Heating of the surface air, by sensible heat, does not only lead to convective turbulence but it also makes it possible for the air to hold more water vapour. This means that sensible heat facilitates latent heat release. The availability of moisture near the surface therefore has a strong effect on B (Chapin *et al.*, 2002).

2.6 Tile equations for latent and sensible heat

Each grid cell in the model is divided into different tiles instead of treating the entire grid as homogenous mixture with only one energy balance, one water balance and parameter values set to grid mean averages. The advantage with the tile approach is that each tile has its own parameters and a separate energy- and water balance.

Forest, open land- and snow- tiles constitute the main tiles. The open land tile has been further divided into bare soil- and vegetated- tiles, while the forest tile has been subdivided into canopy-, forest floor soil- and snow on the forest floor- tiles.

Motivations to the different divisions are found in Samuelsson *et al.* (2006). Snow- and soil freezing processes have been accounted for in the LSS which makes it possible to study high latitude areas such as the forest in Norunda.

Since the land surface scheme is run in a one dimensional mode the fraction of the forest- and open land tiles needs to be defined before the model can be run. As shown later (Section 4.1), the fraction of forest at Norunda is set to 0.9 which means that 10 % of the grid cell (in which Norunda is situated) is considered to be open land. Depending on the station's latitude and longitude, a division into coniferous and deciduous forest tiles is carried out for the forest fraction. Because the latitude for Norunda is larger than 60° the fraction of deciduous trees becomes 15 %. In the case of an open landed landscape, such as for the Cabauw site, the forest fraction is set to 0 (Section 4.1).

The RCA land surface scheme is based on a model scheme (Figure 2) developed by Choudhury and Monteith (1988).

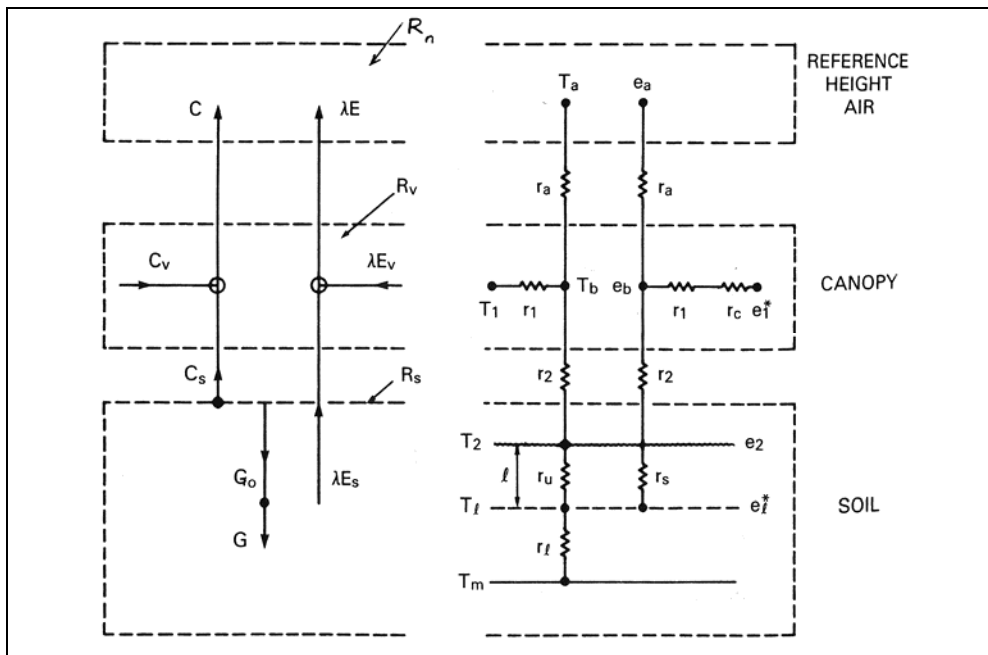


Figure 2. Model description derived by Choudhury & Monteith (1988). The left hand side of the figure shows the model in terms of main component fluxes, while the right hand side shows resistance network and potentials. Symbols for the different variables/parameters are found in the beginning of the paper (vii-x).

Their model system, which consisted of a uniform vegetation layer and a soil layer, was used to solve closed water and energy equations. The soil layer was divided into a dry layer, wherefrom evaporation were assumed negligible, on top of a wet layer. Furthermore, the vegetation layer was divided into two sub layers where the first extended from an atmospheric reference level to the canopy air and the second layer extended from the canopy air to the ground (Choudhury & Monteith, 1988). Forces that controlled the exchange of heat and vapour between the different components in the systems were described in analogy to electrical resistances (right side, Figure 2).

The work performed by Choudhury and Monteith (1988) resulted in latent and sensible heat equations (Table 1, next page) which are used in the RCA model's LSS. A complementary set of equations representing snow conditions have been derived by Samuelsson *et al.* (2006).

Table 1. Latent and sensible heat equations used in the land surface scheme. Explanations to the equations are given in the left column. Equation symbols are found in symbols & abbreviations (vii-x).

Explanation	Latent heat	Sensible heat
Total loss in the system (Choudhury & Monteith, 1988).	$\lambda E = \frac{(\rho c_p / \gamma)(e_b - e_a)}{r_a}$	$C = \rho c_p \frac{(T_b - T_a)}{r_a}$
Fluxes from the foliage to the canopy air (Choudhury & Monteith, 1988).	$\lambda E_c = \frac{(\rho c_p / \gamma)(e_1^* - e_b)}{r_1 + r_c}$	$C_v = \rho c_p \frac{(T_1 - T_b)}{r_1}$
Heat exchange from the soil to the reference level within the foliage (Choudhury & Monteith, 1988).	$\lambda E_s = \frac{(\rho c_p / \gamma)(e_l^* - e_b)}{r_s + r_2}$	$C_s = \rho c_p \frac{(T_2 - T_b)}{r_2}$
Forest floor snow (Samuelsson <i>et al.</i> , 2006)	$E_{forsn} = \rho \lambda \frac{q_s(T_{forsn}) - q_{fora}}{r_d}$	$H_{forsn} = \rho c_p \frac{(T_{forsn} - T_{fora})}{r_d}$

If the equation for latent heat is expressed using specific humidity (Equation 3) instead of vapour pressure, it is easier to notice that the system's temperature only needs to increase with a small amount to release latent energy between the canopy air and the atmosphere. However, a large temperature increase is needed, in order for the system to release sensible heat (Equation 4) (Samuelsson, pers. comm.). The difference between the system's ability to release latent and sensible heat is due to the large difference ($\sim 10^3$) between latent heat of vaporization of water, λ , and specific heat capacity of air, c_p .

$$E_{for} = \rho \lambda \frac{q_s(T_{fora}) - q_{am}}{r_{afor}} \quad (\text{Samuelsson } et al., 2006). \quad \text{Eq. (3)}$$

$$H_{for} = \rho c_p \frac{(T_{fora} - T_{am})}{r_{afor}} \quad (\text{Samuelsson } et al., 2006). \quad \text{Eq. (4)}$$

2.7 Tile equations for net radiation

Total net radiation for a tile of the forest type is given by:

$$R_{n, \text{forest}} = R_{n, \text{forest canopy}} + R_{n, \text{forest floor (no snow)}} * (1 - \text{snow fraction for forest}) + R_{n, \text{forest floor (snow)}} * (\text{snow fraction}) \quad \text{Eq. (5)}$$

Total net radiation for the open land tile is given by:

$$R_{n, \text{open land}} = R_{n, \text{(no snow)}} * (1 - \text{fractional area of open land snow}) + R_{n, \text{(snow)}} * (\text{fractional area of open land snow}) \quad \text{Eq. (6)}$$

2.8 Soil texture class, field capacity & wilting point

“Soil is the interface in the cycling of water between the atmosphere and land. It is the location of large transformations of energy, as radiation absorbed by the surface is transformed to sensible heat, latent heat or stored in the ground” (Bonan, 2002).

Organic material, minerals, water and air are the components that build up a soil. It is the type, abundance and arrangement of mineral and organic particles that determine heat flow, water flow and nutrient availability in the soil (Bonan, 2002). The abundance of the three mineral fractions: clay (<0.002 mm), silt (0.002-0.05 mm) and sand (0.05-2 mm), in a soil determine its texture class (Bonan, 2002) (Figure 3).

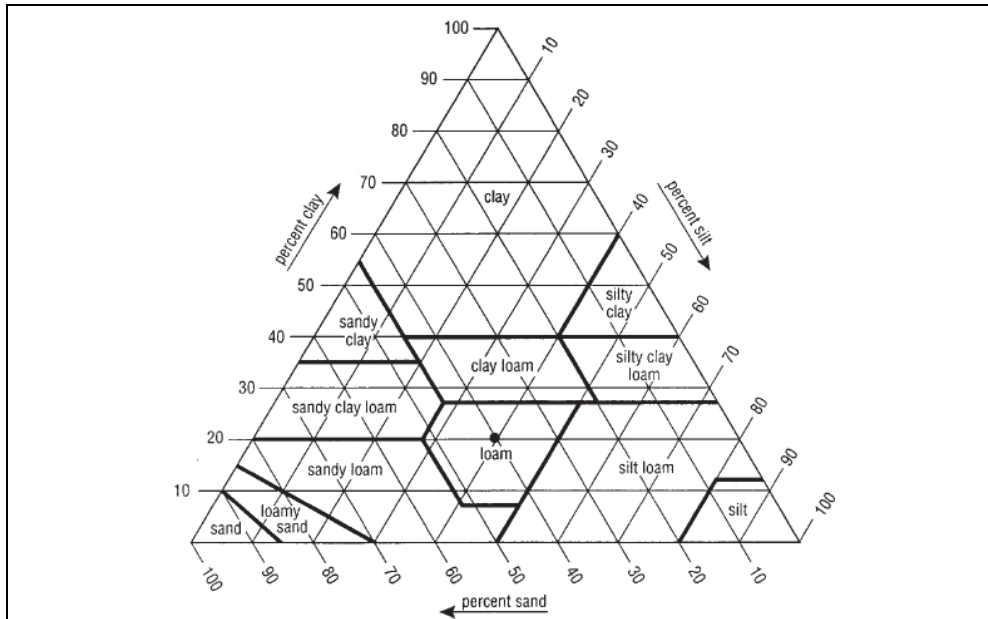


Figure 3. Definition of soil texture classes with respect to mineral abundance. The six different soil texture classes defined in the program are: sand, loam, clay, sandy loam, silt loam and peat.

A soil is saturated when all air pockets, between the grains of organic- and inorganic material, are filled with water. Field capacity is the remaining amount of water held in the soil, when its saturated state has been exposed to gravitational drainage.

The entire amount of field capacity water is not available for plant extraction since some of the water molecules are too tightly bound to the soil particles. A soil is said to have reached its wilting point when only unavailable water is left in the soil (Bonan, 2002). The difference between field capacity and wilting point is the amount of water that is available for the plants (Bonan, 2002).

Each soil texture class has its characteristic values of field capacity and wilting point in the RCA model's LSS (Table 2).

Table 2. Values of wilting point and field capacity, derived by Clapp *et al.* (1978), for the different soil texture classes defined in the model (Samuelsson *et al.*, 2006).

Soil texture class	Sand	Loam	Clay	Sandy loam	Silt Loam	Loam	Peat
Wilting point [cm ³ /cm ³]	0.068	0.155	0.286	0.114	0.179	0.155	0.395
Field capacity [cm ³ /cm ³]	0.174	0.314	0.400	0.249	0.369	0.314	0.629

2.9 Soil water

The storage of soil moisture is defined at two depths only, 0.072 m and 2.2 m, since it is assumed that soil moisture does not depend on surface coverage (Samuelsson *et al.*, 2006).

2.10 Soil temperature

A division of the soil into five different layers, with thicknesses of 0.01, 0.062, 0.21, 0.72, and 1.89 m, respectively, has been carried out with respect to temperature. The temperatures of each layer are calculated for the mid point in each layer, which corresponds to depths of 0.005, 0.041, 0.141, 0.501 and 1.446 m, respectively.

The effect of snow cover isolation has led to a definition of two temperature classes, depending on if snow is present or not, for both the forest tile and the open land tile. Each temperature class is defined at the five different depths mentioned above.

2.11 Leaf area index

Leaf area index is defined as the total one-sided projected area of leaves per unit ground area (Bonan, 2002). More latent heat is exchanged with the atmosphere with an increased *LAI* since the total area from which moisture is lost increases (Bonan, 2002). A greater *LAI* also increases the sensible heat exchange with the atmosphere (Bonan, 2002). This is consistent with the reasoning that a complex canopy has a smaller albedo than a sparse canopy (individual leaves), since much of the light transmitted by one leaf is absorbed by other leaves and stems (Chapin *et al.*, 2002). A study performed by Asner *et al.* (2003) showed that boreal and temperate forest's mean *LAI* vary between $2.6 \text{ m}^2/\text{m}^2$ and $6.7 \text{ m}^2/\text{m}^2$ when both deciduous and evergreen species are considered.

The RCA model's LSS applies a *LAI* value of $4 \text{ m}^2/\text{m}^2$ all year round for coniferous forest. Vegetation types, such as open land and deciduous forest, that have non permanent *LAI* values, are represented with *LAI* values calculated as functions of soil temperature and soil moisture (Samuelsson *et al.*, 2006).

2.12 Water flows

Figure 4 shows the different ways that water enters and leaves ecosystems. Averaged over longer times, precipitation input equals the amount of runoff and evapotranspiration, which are the ecosystems main outputs (Chapin *et al.*, 2002). Most water reaches the soil as throughfall (Chapin *et al.*, 2002), which is the amount of water that reach the ground through openings in the canopy foliage or by dripping down from leaves, twigs and branches (Bonan, 2002). Interception is important to consider in the LSS and is therefore explained more in detail below.

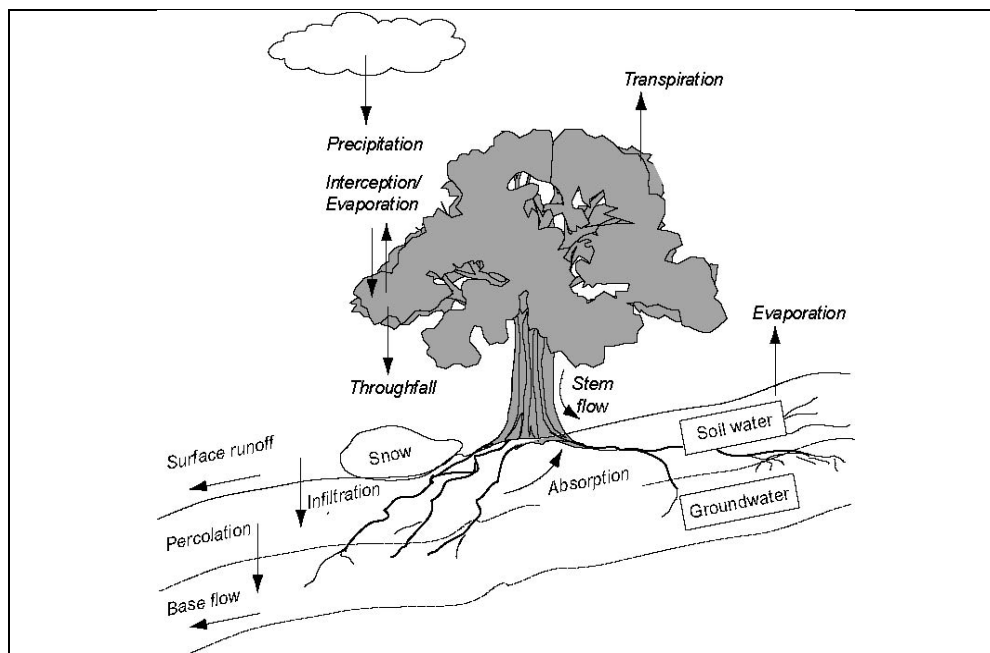


Figure 4. Water paths in the ecosystem (Chapin *et al.*, 2002)

2.13 Interception

Intercepted water and snow is precipitation that has been caught by leaves, twigs and branches of plants from where it evaporates or undergoes sublimation before it reaches the ground. The intercepted fraction of the precipitation is therefore only temporarily stored in the system (Bonan, 2002).

Latent heat release due to evaporation of intercepted water (Equation 7) is described by the same equation as latent heat release due to transpiration (Equation 8) with the only exception that a stomatal resistance (r_c) also is included in the latter case.

$$E_v = \rho\lambda \frac{q_s(T_s) - q_{am}}{r_a} \quad (\text{Samuelsson } et al., 2006) \quad \text{Eq. (7)}$$

$$E_v = \rho\lambda \frac{q_s(T_s) - q_{am}}{r_a + r_c} \quad (\text{Samuelsson } et al., 2006) \quad \text{Eq. (8)}$$

Evaporation of intercepted water is therefore a faster process than transpiration. The rate of transpiration, for a pine forest, was found to be three times slower than the rate of evaporation of intercepted water during the same radiation conditions (Stewart, 1977).

Leaf area index, canopy surface area, season, leaf type, rainfall intensity, duration and frequency are some of the factors that influence the amount of intercepted precipitation (Bonan, 2002, Chapin *et al.*, 2002).

Conifer forest, which has needle shaped leaves that makes it difficult for water droplets to run together and drip off the leaf, store on average about 15 % of precipitation while deciduous forest, which has broad leaves that facilitates dripping intercept about 5-10 % (Bonan, 2002, Chapin *et al.*, 2002). The greater interception of conifer forests compared to deciduous forests also depends on their permanent foliage and less stemflow due to rougher stems and horizontal branches (Bonan, 2002).

Grasses annually intercept less than trees, since the absence of twigs and branches does not enable interception during the resting period, but they have the same storage capacity when they are in full leaf (Bonan, 2002).

About twice as much water equivalent can be stored in canopies that intercept snow and hale. The amount of snow interception is increased with an increased *LAI* (Chapin *et al.*, 2002).

Snow interception is not included in the land surface scheme. Interception is forbidden if the canopy temperature is below freezing ($T_{forc} \leq 0^\circ\text{C}$). However, already stored water is assumed to stay until it evaporates as super cooled water (Samuelsson *et al.*, 2006). The model's interception rate (Equation 9) is given by the difference between the interception in the following time step, $w_{veg}^{\tau+1}$, and the present time step, w_{veg}^{τ} , divided by the length of the time step, Δt . It can also be expressed in terms of a vegetation cover parameter, *veg*, rain intensity, P , the fraction of the vegetation that is covered by water, δ , evaporation of intercepted water, E_v , and the latent heat of evaporation, λ .

$$\frac{w_{veg}^{\tau+1} - w_{veg}^{\tau}}{\Delta t} = \text{veg} \left(P - \frac{\delta}{\lambda} E_v \right) \quad (\text{Samuelsson } et al., 2006) \quad \text{Eq. (9)}$$

Equation 10 describes the maximum amount of precipitation that is allowed to intercept.

$$w_{veg\ max} = 0.2 * veg * LAI \quad \text{Eq. (10)}$$

If maximum interception rate is exceeded, which occurs when the difference between the interception in the following time step, and the maximum amount of water that is allowed to intercept, divided by the time step length becomes positive, the surplus leaves the system as throughfall, thr (Equation 11).

$$thr = \max\left(0.0, \frac{(w_{veg}^{\tau+1} - w_{veg\ max})}{\Delta t}\right) \quad \text{(Samuelsson et al., 2006)} \quad \text{Eq. (11)}$$

2.14 Heat Capacity of trees

The energy required to warm 1 g of a substance by 1°C is called specific heat (Chapin *et al.*, 2002). A large heat capacity indicates that the temperature of a body changes more slowly for a given energy input than the temperature would do for a body with a lower heat capacity (Chapin *et al.*, 2002).

Air temperatures near large water bodies, fluctuate less because of the high heat capacity of water (Chapin *et al.*, 2002). In analogy to this a greater heat capacity of trees should reduce the fluctuations in the canopy temperature. The canopy temperature may also be delayed due to a bigger storage-flux (Lagergren, pers. comm.).

2.15 Vapour deficit

Vapour deficit, D , is the difference in vapour pressure between saturated and ambient air (Campbell & Norman, 1998): $D = e_s(T_a) - e_a$

Even though relative humidity, h_r , defined as the ratio of ambient vapour pressure to saturation vapour pressure at air temperature (Campbell & Norman, 1998), is directly measured at sites, vapour deficit is a better indicator of the evaporative demand of the atmosphere. The reason for this is that the same relative humidity can occur at a lot of different temperatures and vapour pressures (Chapin *et al.*, 2002).

As seen in Table 1, all of the latent heat expressions are directly proportional to the vapour pressure expression.

2.16 Displacement height

If wind speed is plotted as a function of height above ground on a logarithmic scale, a linear relationship becomes evident, with a small offset due to the properties off the underlying surface (Campbell & Norman, 1998). The relationship can be expressed as:

$$u(z) = \left[\frac{u^*}{\kappa} \ln\left(\frac{z-d}{z_0}\right) - \psi_m(\xi) \right], \text{ where } d \text{ is the displacement height, } \kappa = 0.4 \text{ is the Von}$$

Karman constant, z_0 is the roughness length, u^* is the friction velocity and $\psi_m(\xi)$ is a function that describes the influence of atmospheric stability on turbulence (Bonan, 2002). The latter is zero during neutral atmospheric conditions, which may occur over

forests and grasslands (Bonan, 2002). The above given relationship, which is used for the atmospheric surface layer, is only valid if $z \geq d + z_0$ (Campbell & Norman, 1998). The displacement height is zero for bare ground and greater than zero for vegetation (Bonan, 2002). Based on an equation, derived in Choudhury and Monteith (1988), the displacement height, d , is given by:

$$d = 1.1h \ln(1 + X^{1/4}), \quad \text{Eq. (12)}$$

where h is the vegetation height X is the mean drag coefficient for individual leaves multiplied with LAI .

The displacement height has a minimum value that equals the difference between the vegetation height and vegetation momentum roughness (z_0) subtracted by 0.3 if the calculated displacement height is larger than this difference:

$$d = \min(d, h - z_0 - 0.3) \quad \text{Eq. (13)}$$

2.17 Roughness length

The theoretical height where the wind speed extrapolates to zero in the linear relationship given above is called roughness length, z_0 , (Bonan, 2002). It is known as a momentum sink and is approximately given by: $z_0 \approx h/30$ (Seinfeld & Pandis, 1998). A smooth flow is when $u^* z_0/v < 0.13$ while a rough flow is when $u^* z_0/v > 2.5$. The kinematic viscosity of the fluid, ν , is typically $10^{-6} \text{ m}^2/\text{s}$ for the atmosphere while the friction velocity, u^* , typically is 0.1 m/s (Seinfeld & Pandis, 1998). Table 3 shows a few roughness lengths for different surfaces.

Table 3. Roughness lengths for different surfaces (Campbell & Norman, 1998).

Surface	[cm]
Thick grass, 50 height	9
Bare soil, tilled	0.2-0.6
Farmland, snow covered	0.2
Coniferous forest	110
Grass, closely mowed	0.1
Potatoes, 60 cm high	4
Ice	0.001
Urban buildings, business district	175-320
Calm open sea	0.003
Villages, towns	40-50

The roughness length for forest is not fixed in the model, instead it is varying with the forests annual cycle. Open land surface roughness length is set to 0.2.

3. Data preparation

3.1 Data measurements

During land surface scheme modelling it is necessary to have access to high quality continuously measured meteorological data (pressure, air temperature, wind, specific humidity, rain, snow, global radiation and long wave radiation), which is used as input to the model, as well as verification data (latent heat, sensible heat, air temperatures, soil temperatures, friction velocity, soil water *etc*), which is used to compare the model's output to. Data from three stations (Figure 5), Cabauw, Hyytiälä and Norunda situated in the Netherlands, Finland and Sweden, respectively have been used in this project.

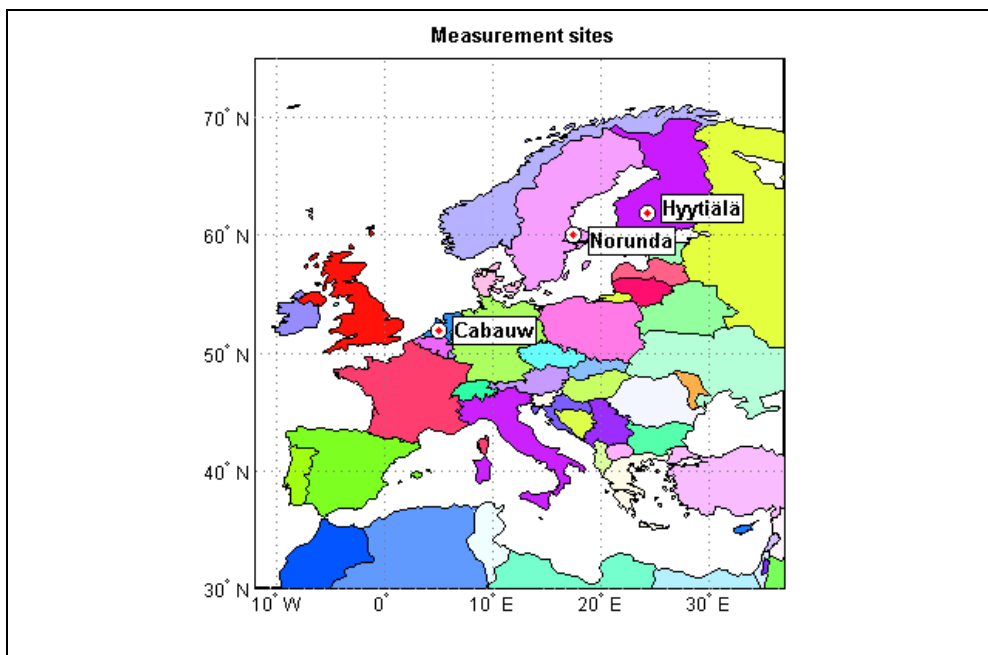


Figure 5. Locations of Cabauw (the Netherlands), Hyytiälä (Finland) and Norunda (Sweden), where from the data have been measured. Map produced by Margareta Hellström.

The first long term record of flux measurements was registered in the beginning of 1970s at Cabauw, where instrumentation had been placed in a 203 m high mast. The measurements were performed in purpose to study air pollution in the lower part of the atmospheric boundary layer. Continuous measurements have been performed since 1986 and the instrumentation has been complemented in a way so that important biologically and hydrologically influences on a soil –vegetation atmosphere system are accounted for (Lundin *et al.*, 1999). Heat flux measurements at the two forest sites, Norunda and Hyytiälä, have been performed since 1994 and 1996, respectively. The heat fluxes are registered by eddy flux systems which are monitored at different heights on a 102 m high mast in Norunda (Lundin *et al.*, 1999) and a 73 m high mast in Hyytiälä (<http://www.bgcjena.mpg.de/public/carboeur/sites/hyyti.html>). Meteorological measurements are also performed at several heights in the towers. The instrumentation accuracy at Norunda was investigated thoroughly during a climate monitoring programme lasting from May-June 1994, April-July 1995 and March-April 1997. It was concluded that most of the instrumentation components

were working 90 % of the time during the five first operation years of the station and that 97 % of the registered eddy flux data was valid.

Further on, sensible and latent heat fluxes, temperature and specific humidity had operational errors of 1.8 % and 7.3 %, 0.03 K and 0.015 g/Kg, respectively while the maximum error for the rain gauges were 20 % and the wind measuring devices (anemometers) reached an accuracy of 2 % during wind tunnel test (Lundin *et al.*, 1999). The radiation measurement sensors had problem when wet snow covered its surface.

Even though the system worked 90 % of the time it was considered not to be accurate enough for registering rarely occurring phenomenon since it is possible that they occur during equipment malfunction (Lundin *et al.*, 1999).

3.2 Site description

The Cabauw mast is placed in an open pasture area 0.7 m below mean sea level, which has a soil that consist of river-clay (0.6 m) overlaying a thick peat layer. The soil texture class is sandy loam (Samuelsson, pers. comm.).

Surrounding areas are agricultural and are situated at a minimum distance of 400 m from the mast (<http://www.knmi.nl/onderzk/atmoond/cabauw/cabauw.html>).

The surface coverage around the tower site consists of grass. During 1997 the leaf area varied between 0.8-1.8 m²/m² where the maximum value was reached during June-July (Chen *et al.*, 1997).

Data from 1986-1988 will be used in this project. Temperature, wind and specific humidity are measured at 20 m above ground. The annual mean temperature and precipitation were 8.85°C and 776 mm, respectively during 1987, which corresponded to 0.5°C and 10 % above the climatological mean (Chen *et al.*, 1997).

Measurements at Hyytiälä have been carried out in a 16 m high forest at an elevation of 180 m above sea level. Scots pine is the main tree specie while *Vaccinium* (low, ground-covering shrubs) and mosses dominate the ground vegetation. The time of bud burst is approximately in beginning of May. A leaf area index minimum of 1.7 is reached in April while the maximum value of 2.2 is reached between July and September. The forest has a roughness length of 1 m, a displacement height of 11 m, a main rooting zone at 0.3 m depth and a 7.89 kgm⁻² stem (stem+branches) mass. The soil texture class is sandy loam. Field capacity/wilting points for 0-10 cm, 10-20 cm and 20-40 cm are respectively found at 33.5/10 %, 30/8 % and 29/7 % (Kolari, pers. comm.). Data from 2002-2004 were prepared in the project. Mean annual temperature and precipitation are 3.5°C and 640 mm, respectively (<http://www.bgcjena.mpg.de/public/carboeur/sites/hyyti.html>).

Norunda is a 26.5 m high mixed forest situated at an altitude of 45 m (Widén & Majdi, 2001). The vegetation composition is typical for a boreal forest with a mixture of evergreen and deciduous trees (Bonan, 2002) where pine and spruce are the dominating species. Blue berries (*Vaccinium myrtillus*) and grasses dominate the ground vegetation. The time of bud burst occurs during the first half of May. Seasonal variations of leaf area index, which has a maximum value of 4.5, can be described as:

$$LAI_{DOY} = 4.29 + 0.42 * EXP\left(-0.5 * \left(\frac{DOY - 224.8}{48.76}\right)^2\right), \text{ where } DOY \text{ is day of year.}$$

The forest has a roughness length of 1.75 m, a displacement height of 21.1 m, a main rooting zone at 0.7 m depth and a 20.1 kgm⁻² above ground biomass. Also this site has a sandy loam soil texture class. The water content at field capacity/wilting point is 17/5 % when it has been corrected for stone contents (Lagergren, pers. comm.). Mean air temperature and precipitation were 5.5°C (1961-1990) and 527 mm, respectively at Uppsala 30 km south of Norunda (Lundin *et al.*, 1999).

There are different tree stands, in the closest vicinity (1 km) of the mast, that differ in specie composition, age, *LAI* and soil characteristics (Table 4). Data used in this paper (1994-1996) originates from the 100-year-old stand and the 70-year-old stand, where the latter also is referred to as the 50-year-old stand (Lundin *et al.*, 1999).

Table 4. Soil characteristics of the top most soil layer in the 100-year-old and 70-year-old tree stands at Norunda (Lundin *et al.*, 1999). Wilting point and field capacity are not corrected due to stone contents in this table.

Stand age [years]	Depth [cm]	Clay content [%] (Kg/Kg)	Silt content [%] (Kg/Kg)	Sand content [%] (Kg/Kg)	Porosity [%] (m ³ /m ³)	Wilting Point [%] (m ³ /m ³)	Field capacity [%] (m ³ /m ³)
100	0-25	5-9	26-43	45-63	44.1	6.4	0.29
70	0-25	6-8	23-25	61-65	48.7	6.9	0.26

3.3 Gap filling

As mentioned above, pressure, air temperature, wind, specific humidity, rain, snow, global radiation and long wave radiation are the model meteorological forcing variables that need to be continuous with, preferable, half hourly time resolution. Replacing missing data in non continuous data sets is therefore the first thing that has to be done before the model can be used.

Linear interpolation is a method often applied if 2-3 half hourly meteorological variables, such as temperature or relative humidity, are missing (Falge *et al.*, 2001). In this paper, linear interpolation has been used as a primary approach to fill the gaps in temperature, wind, relative humidity, pressure, short wave outgoing radiation and net radiation. The gap size tolerance has been extended to 4h for the latter two and 12h for the remaining variables. Gaps in global radiation have also been filled with “4h tolerance linear interpolation”, but in this case it has only been used as a secondary option following regression, which is explained more in detail below (Section 3.3.1). Regression has also been used as a secondary method in filling the gaps in net radiation (Section 3.3.2.1). Remaining gaps, with the exception of albedo and precipitation which are explained in (3.3.2.2) and (3.3.3) respectively, have been filled with mean values or being replaced as the last option. Following example shows how a mean value for a specific gap is calculated.

A gap, present at 2004/02/05 13:30 (yyyy/mm/dd), is replaced by:
 $gap = \text{value at } (2004/02/04 \text{ 13:30} + 2004/02/06 \text{ 13:30})/2$

This “mean value method” was used for gaps smaller than 24h. Gaps larger than this were filled by replacement using values from a nearby day. Finally, gaps larger than 1 week were replaced by values from the previous or following year.

Gaps in the hourly data set, measured at 00:30, 01:30 *etc*, from Norunda had already been filled, with the exception of pressure, which had a half hourly time resolution. Pressure readings did not start at Norunda before June 1994. A standard pressure would in normal case have been good enough to use for all the gaps before the summer of 1994, but since pressure readings are important in the division of precipitation into snow or rain, all data before the summer of 1994 were excluded. Finally, all times taken at full hours were excluded before the gap filling process of Norunda pressure was carried out.

The percentages of missing data at the different sites are represented in Table 5. As seen, Cabauw is not represented in the table since this data set had already been filled.

Table 5. The missing data is represented as a percentage of the number of values for each variable at respectively site and year. All data from Cabauw and Norunda, with the exception for pressure readings at Norunda, had already been prepared.

Variable	Hyytiälä 2002	Hyytiälä 2003	Hyytiälä 2004	Norunda
Global radiation	4.75 %	4.45 %	0.29 %	-----
Global outgoing	3.76 %	4.90 %	0.66 %	-----
Long wave radiation	Not measured	Not measured	Not measured	-----
Net radiation	8.18 %	9.92 %	5.73 %	-----
Relative humidity	4.93 %	8.87 %	9.46 %	-----
Wind speed	5.36 %	19.8 %	0.64 %	-----
Temperature at 16.8 m	3.66 %	4.87 %	0.87 %	-----
Temperature at 8.4 m	3.66 %	4.87 %	0.64 %	-----
Temperature at 4.2 m	100 %	32.17 %	9.82 %	-----
Precipitation	3.88 %	1.47 %	0.68 %	-----
Pressure	3.66 %	3.62 %	0.64 %	2.81 %

A detailed description of how the gaps in the Hyytiälä data set were replaced is given below (Section 3.3.1-3.3.3) as well as examples of how bad estimations of the meteorological data can affect the model result (Section 3.3.4). Excel (Windows 2000 XP) was used during the entire gap filling process, with the exception of precipitation data visualisation and construction of figures which was carried out in MATLAB 7.0.

3.3.1 Gaps in global radiation

Photosynthetic photon flux density, Q_{PPFD} , is related to solar broadband irradiance, R_{solar} , through the equation:

$$Q_{PPFD} = fR_{solar} \quad \text{Eq. (14)}$$

which can be applied to either global, direct or diffuse radiation. The ratio f is near $2 \mu\text{mol/J}$ and it is given as a product between two different ratios:

(i) the fraction of the broadband energy flux that lies in the PAR wave-band (400–700 nm) and (ii) the photon or quantum efficiency of this band (Gonzalez & Calbó, 2002). The method of filling gaps in meteorological variables using redundant measures was mentioned in an article by Falge *et al.* (2001) who used the site specific ratio between Q_{PPFD} and global radiation (broadband irradiance) to fill gaps in Q_{PPFD} when the global radiation was known.

Using the same method as Falge *et al.* (2001), but with Q_{PPFD} as redundant data and an average ratio of $2.1 \mu\text{mol/J}$, about half of the global radiation gaps in the Hyytiälä data set are filled. Figure 6 displays times where data of the two variables were available before the gap filling procedure. It verifies that the used ratio is a good choice.

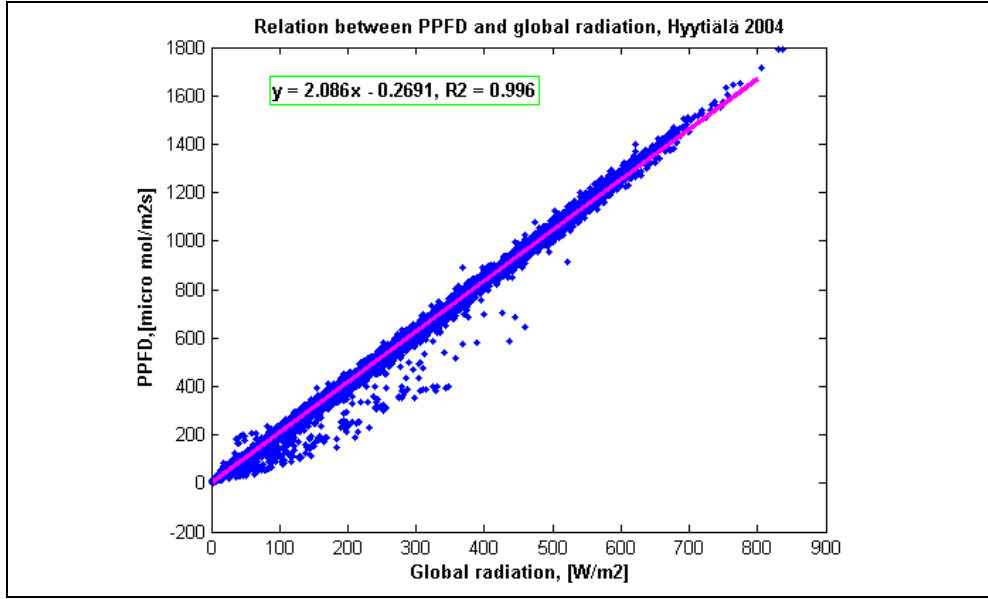


Figure 6. Relation between photon flux density and global radiation. The site specific ratio between the two variables is close to 2.1 $\mu\text{mol}/\text{J}$.

3.3.2 Gaps in long wave radiation

Long wave radiation needs to be calculated since it was not measured in Hyttiälä. All components included in the long wave radiation equation (Equation 15) therefore needs to be gap filled before the calculation can be carried out.

$$R_n = (1 - \alpha)R_g + \varepsilon L_{\downarrow} - \varepsilon \sigma T_s^4 \Leftrightarrow$$

$$L_{\downarrow} = \frac{R_n - (1 - \alpha)R_g}{\varepsilon} + \sigma T_s^4 \quad (\text{Baldocchi, 2005}) \quad \text{Eq. (15)}$$

The temperature, T_s (K), is calculated as a mean value of the temperature readings at 16.8 m and 8.4 m since this height is representative for the forest canopy. A constant value of 0.985 is used for the emissivity, ε , during the forest calculations in the model. The same value is therefore used in the gap filling procedure. Gaps in net- and global radiation, R_g , are filled as described in Section 3.3.2.1 and Section 3.3.2.2, respectively. The latter section also contain information about albedo, α , calculations.

3.3.2.1 Gaps in net radiation

A linear relationship between net- and global radiation is seen in Figure 7, where all original gap free data for the two variables are included. The relationship, which is used to fill gaps in net radiation, is valid during day- time only (global radiation > 0), since all night values of net radiation would be the same ($-28.65 \text{ W}/\text{m}^2$) otherwise.

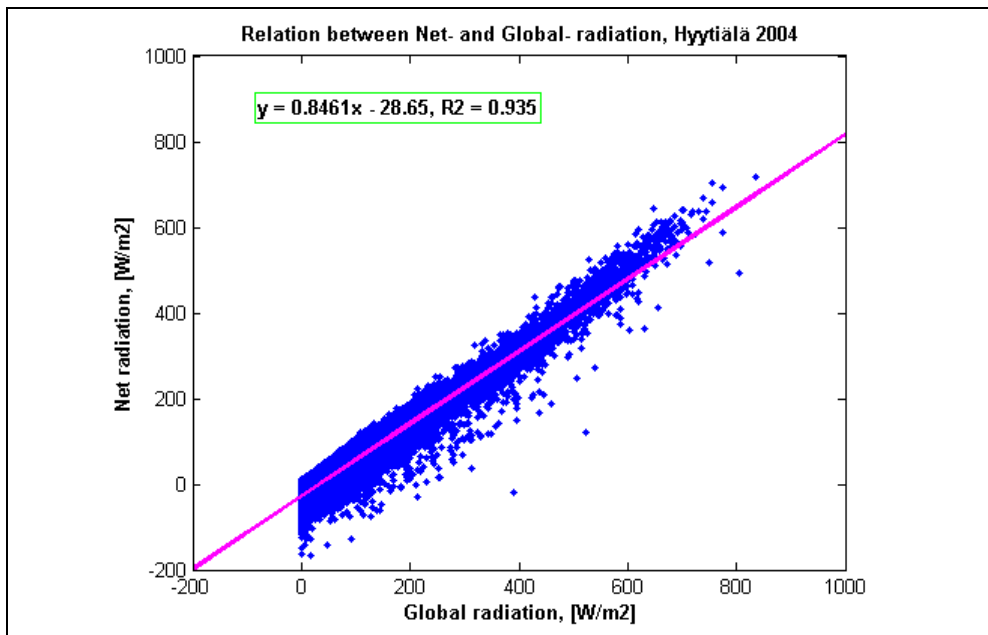


Figure 7. Relation between net- and global- radiation when only original gap free data is used. The received linear equation, seen in the green box, is used to fill gaps in net radiation.

Plots of daily global radiation, e.g. Figure 8, which displays January 1:st 2004, made it possible to estimate the sun hours at Hyttiälä. In this case the sun hours would be estimated to 10:00 -16:00. A plot like Figure 8 was made for every 14:th day of the year 2004. If it was difficult to estimate the first or the last sun hour of a specific day the prior day or the following day was used instead. If the last day in the interval did not fit the chosen sun hours, the time for the entire interval was changed with half an hour. This is why January 1:st 2004 has sun hours only between 10:00 and 15:30 in Table A1 (Appendix A), which displays the estimated sun hours and periods that were used.

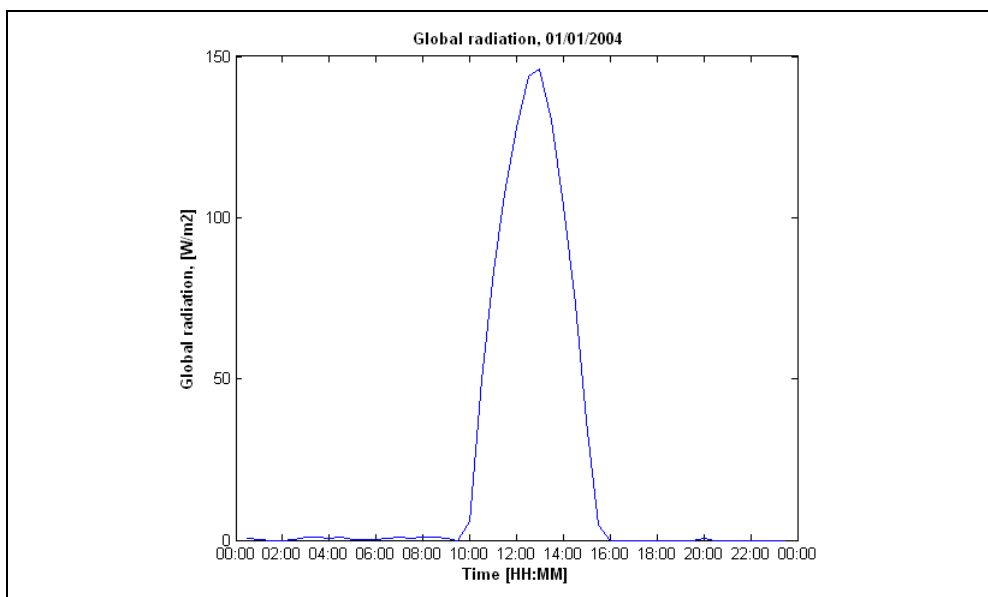


Figure 8. Sun hours at Hyttiälä on 1 January, 2004. In this case the sun hours would be estimated to 10:00 -16:00.

3.3.2.2 Gaps in short wave outgoing radiation & albedo

Global reflected radiation is used to calculate the albedo, but before this can be done gaps in the data set was filled using the priority order mentioned above.

The albedo was calculated as the sum of reflected global radiation divided by the sum of incoming global radiation, during a time step of 3 days. Received values were put in the middle of each interval, which means that the same method could not be used for the first 1.5 days of 2002 and the last 1.5 days of 2004.

Calculated albedo values from 1/3/2002 00:30-1/4/2002 11:30 were used to replace the gaps during 1/1/2002 00:30-1/2/2002 11:30, while calculated albedo values from 12/28/2004 12:30-12/29/2004 23:30 were used to replace gaps during 12/30/2004/12:30-12/31/2004 23:30.

3.3.3 Gaps in precipitation

The original data sets from Hyytiälä did not include snow measurements. A supplementary set of daily precipitation measurements, registered by the Finnish Meteorological Institute, was therefore used during the gap filling process of precipitation. The nearby station, where the daily totals were measured is situated a few hundreds of meters away from the place where the original data was measured. Days when precipitation had been observed at the nearby station but no value reported, as the amount was too small to be registered, were arbitrarily given a value of 0.05 mm.

The precipitation measurements from both Hyytiälä and the near by station were implemented in MATLAB 7.0. Gaps in the original data sets were replaced by MATLAB's nomenclature of missing values, NaN (not a number). Figures, illustrated by Figure 9a-c, were then used in the judgement of how the missing data should be replaced.

If the daily sum of precipitation were 0 mm at both the nearby station and at Hyytiälä, then the gaps (NaN) were set to 0 mm.

The gaps were also set to 0 mm if the daily sum of the nearby station was less than the daily sum at Hyytiälä. An example of this can be seen in Figure 9a.

Two possibilities were used to replace NaN if the daily sum of precipitation at Hyytiälä was smaller than the daily sum at the nearby station.

- 1) The precipitation difference is evenly distributed over all current-period time steps with missing values.
- 2) All current-period time steps with missing values are set to 0 mm if the Hyytiälä daily sum is 0 mm. This implies that possible precipitation events occurring at Hyytiälä during periods of *e.g.* equipment malfunction are ignored. The reason for this is that gap free days at Hyytiälä in some cases have been precipitation free while precipitation has been registered at the nearby station.

Figure 9b is an example of where the former alternative has been used, while Figure 9c is an example of where the latter alternative has been used.

Table A2 in Appendix A presents the final values that were used to replace the missing precipitation measurements with.

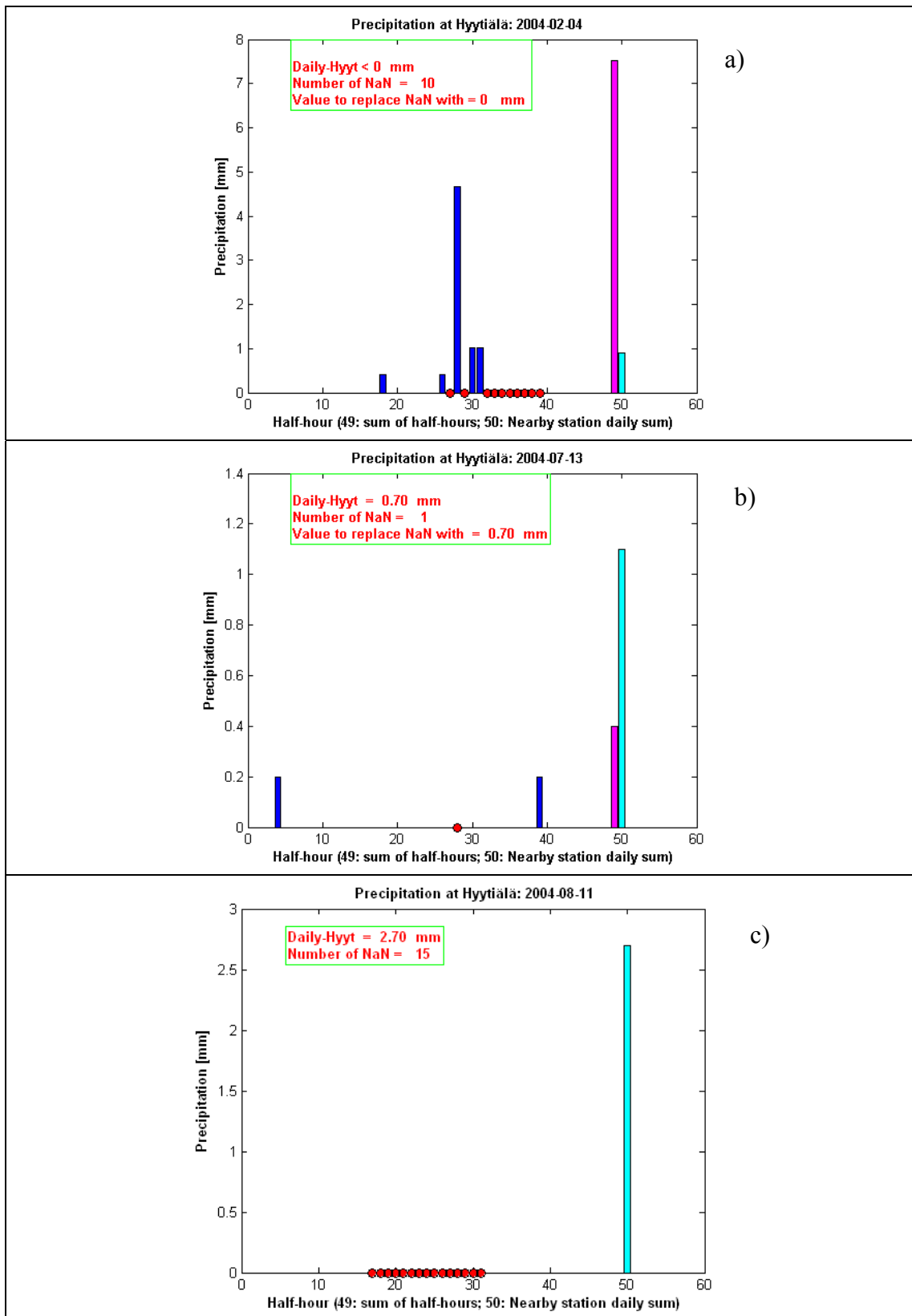


Figure 9. Half hourly precipitation values at Hyttiälä, total precipitation amount at Hyttiälä and daily mean precipitation value at the nearby station are represented as blue bars (half hour No. 1-48), magenta coloured bar (No. 49) and cyan coloured bar (No. 50), respectively. The number of gaps (NaN) and the difference between bar No. 50 and bar No. 49 are given in the green textbox. **a)** All 10 NaN are replaced by 0 mm (green textbox). **b)** The NaN value is replaced by 0.70 mm (green textbox). **c)** Each of the 15 NaN values is replaced by 0 mm because bar No. 49 = 0 mm.

3.3.4 Examples of what can go wrong

With the intention that periods in which larger gaps had appeared would not be included in the final evaluation, and therefore not affect the result, the gap filling process was carried out as described above.

However, bad estimations of variable values for a given period may affect the model calculations over long time intervals, sometimes months, since slow-changing soil water processes are involved (Samuelsson, pers. comm.). It is therefore not possible to simply overlook longer gaps in the model driver data, since their effect on the outcome is not an isolated event (Examples 1-2).

Example 1

Too low wind estimation → too high aerodynamic resistance, r_a → lower sum of latent and sensible heat.

More water is held in the ground if latent heat is underestimated → the soil water contents becomes overestimated → stomatal resistance becomes too low → latent heat becomes overestimated → The canopy temperature is too cold in proportion to the amount of latent heat that is released.

Some equations that show the connections between the different steps are given in Appendix A (Equation A1-A5)

Example 2

If the incoming long wave radiation is too small → lower net radiation (see net radiation section in the theory part) → lower sum of latent and sensible heat → ... see Example 1.

Comment: A combination of huge gaps, filled by replacement, missing supplementary precipitation information and lack of time made it impossible to continue the work with Hyytiälä data during the years 2002-2003. However, gap filling was successfully carried out on Hyytiälä data starting from 2004. Here, the “average value method” needed to be applied a few times only, and data replacement was required for a single, one-month period (for which relative humidity data from 2002 was substituted).

3.4 Further data preparation

Following sections describes how some of the gap filled data was recalculated in the process to reshape it to a model “friendly” format. Excel was used during the specific humidity calculations in Section 3.4.1 while MATLAB 7.0 was used during the treatment of soil water data from Norunda (Section 3.4.3). The wet bulb code (Section 3.4.2) was originally written in FORTRAN 77 but it was translated to MATLAB 7.0 since it was easier to create the final input data file to the model in this program.

3.4.1 Conversion of relative humidity to specific humidity

Atmospheric water vapour content is expressed as relative humidity in the original data set from Hyytiälä. It was calculated using dew point temperature at 23 m and an average value of the air temperatures at 16.8 m and 33.6 m.

$$\left(T_a = \frac{T_{a,16.8m} + T_{a,33.6m}}{2} \right)$$

Since the RCA model uses specific humidity (q_a) instead of relative humidity a conversion is made using the equation:

$$q_a = \frac{0.622e_a}{P - 0.378e_a} \quad (\text{Bonan, 2002})$$

The pressure is calculated using:

$$P_a = 101.3 \text{ kPa} \exp\left(\frac{-A}{8200}\right) \quad (\text{Campbell \& Norman, 1998})$$

To obtain a more accurate value the measured ground level pressure is used instead of 101.3 kPa, which is the sea level pressure. The elevation, A , is set to 16.8 m since the air temperature that will be used in Tetens (1930) formula (see below) is measured at this height. Another reason to why A is set to 16.8 m is that the model requires specific humidity, wind speed and temperature from the same height.

Rearranging the formula for relative humidity, $h_r = \frac{e_a}{e_s(T_a)}$ (Campbell & Norman, 1998), and replacing the saturation vapour pressure at air temperature with Tetens formula,

$$e_s(T) = a \exp\left(\frac{bT}{T+c}\right) \quad (\text{Campbell \& Norman, 1998}),$$

gives following expression for the air vapour:

$$e_a = h_r a \exp\left(\frac{bT_a}{T_a+c}\right)$$

The constants in Tetens formula are set to $a = 0.611 \text{ kPa}$, $b = 17.502$ and $c = 240.97^\circ\text{C}$ since these values are typical for biophysics applications (Campbell & Norman, 1998).

Rearranging the formulas above makes it possible to convert specific humidity, used as driving data in the Cabauw data set, to vapour pressure deficit (which is used in driving and verification plots (Section 4.2)). However, in this case P_a was calculated using the Cabauw driving pressure as standard pressure and an elevation of 20 m.

3.4.2 Division of precipitation into rain or snow

By calculating wet bulb temperatures, using a program developed by Stefan Gollvik (pers. comm.) it was possible to estimate whether the precipitation should be divided into snow or rain. If the values of pressure, specific humidity and temperature contributed to a wet bulb temperature greater than 273.15 K, the entire amount of precipitation should be accounted for as rain, otherwise it should be accounted for as snow.

3.4.3 Soil water in Norunda

The soil water data at 10 cm depth have been measured from June 1994-October 1995 at the 100-year-old stand and in the 70-year-old stand during June-September 1994 at Norunda. Measurements have also been performed in the latter stand since June 1995 (Lundin *et al.*, 1999). Data from the 100-year-old stand would have been preferable since the mast is placed in this stand (Lundin *et al.*, 1999), yet it is only used as supplementary information. The reason for this is that it is better to use as much data from one location as possible and soil water is not measured any longer at the 100-year stand. In Figure 10 which was used to judge what data to use, time series of soil water from the 100- and 70-years stands are shown.

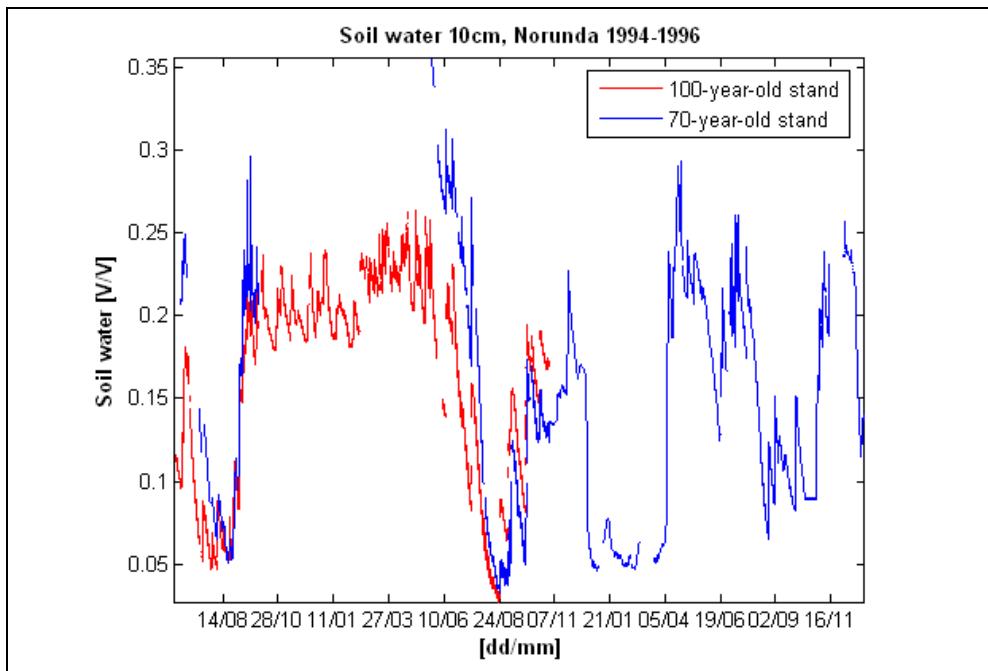


Figure 10. Soil water at 10 cm depth in the 100-year and 70-year-old tree stands at Norunda.

Since the two different stands seems to be close to each other during 1994/08/14 and 1995/08/25 (yyyy/mm/dd) following periods were chosen:
 Data from the supplementary stand (100 years) was used during 1994/08/15-1995/08/24, while data from the 70-year old stand was used during the remaining time (1994/06/05-1994/08/14 and 1995/08/25-1996/12/31).

4. Methods

4.1 Model input

Site specific input data and parameters need to be defined in the model's main program before the model can be run. Some of the parameter values are assumed to be the same for all stations; snow albedo (0.7), orography ($1 \cdot 10^{-5}$) and the thickness of the top (0.072 m) – and deep (2.2 m) soil layers with respect to soil moisture can be given as examples.

Parameter values and other input data, which I have changed, that differ among the three stations are given in Table 6. The fraction of forest varies between 0-1 where 0 represents open land. Time step describes the time difference between two observations.

All site specific data necessary for Cabauw were set together by Patrick Samuelsson. When the input data for Hyytiälä was put together some new problems were found. The reference level was situated only 0.8 m above the forest, which is far too close. Further, the coordinates for the station were not defined in the program. Unfortunately the model did not work after implementation of the new code (the program is written in FORTRAN 77 and LINUX was used for running the model). The work with Hyytiälä will therefore include only the production of a gap filled data set for 2004. However, as soon as the model works again this data set can be used. Missing site specific information about Norunda was treated as seen below.

Table 6. The ECMWF (European Centre for Medium- Range Weather Forecasts) Re- Analysis ERA 40 project consists of a number of climate data sets from 1957-2002 which has been used in a consistent model to describe the climate (<http://www.ecmwf.int/research/era/>). The test run values for Norunda are based on the values used for the station during ERA-40, with the exception for snow, which is set to 0 m. The final input values used for Cabauw and Norunda are seen in column two and four, respectively. The left column describes the site specific parameters, their program names and input units.

Site name	Cabauw	Norunda ERA-40 test run	Norunda
Latitude, alat, [°]	51.971	60.0833	60.0833
Longitude, along, [°]	4.927	17.4667	17.4667
Modelled period, [yy/mm/dd]	86/10/01-89/01/01	94/06/05-96/12/31	94/06/05-96/12/31
Time step, dtime, [s]	900	3600	3600
Soil type number	4 (sandy loam)	4 (sandy loam)	4 (sandy loam)
Fraction of forest, frfor	0	0.9	0.9
Reference level, zhnlev, [m]	20	35	35
Top soil temperature, ts, [K]	283.6	271.5	289.92
Deep soil temperature, tsd, [K]	285.4	273.5	274.535
Snow, sn, [m]	0.0	0.0000	0.0000
Top soil moisture, sw, [m]	0.23	0.3036	0.0154
Deep soil moisture, swd, [m]	0.23	0.3046	0.49305

The original data from Norunda did not contain information about top soil temperature, deep soil temperature, top soil water or deep soil water, that could be used to initialize the model with.

Input values used during an ERA 40 (see table text above), for Norunda with the start date 1993/12/31 23:30, were used in the model test run. However, snow was put to 0 m instead of the original value of 0.0071 m.

A mean value of the output values for forest soil surface temperature (tsc) during 1995/06/05 13:30 and 1996/06/05 13:30 was calculated. This value was then used, as

top soil temperature, in the real simulation. The same method was used to receive values of forest soil surface temperature at layer five (tsc5), which then were used to represent deep soil temperature, top soil water and deep soil water. Output values at 1994/06/05 13:30 from the model test run were excluded in the mean calculations, so the effects of the “ERA 40- winter initialization” would be excluded. Table 7 displays values from the test run, calculated mean values and observed values for top soil temperature and soil water during 1996. Note that the observed soil water values have the unit [V/V] while the model output is given as both [m of water] and [V/V].

Table 7. The output values from the model 1995/06/05 and 1996/06/05 at 13:30 are given in column two and three, respectively. The calculated RCA mean values are seen in column four while observed data from 1996 are given in column five for comparison. The first column contains information of the depths where the top soil moisture (sw), the deep soil moisture (swd) and the first (tsc) and fifth (tsc5) forest soil surface temperatures have been measured.

	RCA 1995	RCA 1996	RCA mean	Observed values 1996
tsc at 0.5 cm	289.24 K	290.60 K	289.92 K	282.52 K at 10 cm
tsc5 at 1.446 m	275.34 K	273.73 K	274.535 K	----
sw at 7.2 cm	0.0169 m	0.0139 m	0.0154 m	----
			0.214 V/V	0.182 V/V at 10 cm
swd at 2.2 m	0.5181 m	0.4680 m	0.49305 m	----
			0.224 V/V	----

4.2 Control of driving- and verification data

To be able to identify periods where driving data and/or verification data seemed to be untrue, daily averages of global radiation, long wave radiation, net radiation, rain, snow, soil water, soil temperature, wind, vapour pressure deficit (VPD) and air temperature were calculated and plotted one year at the time. Appendix C Figures C1-C3 shows the result for Norunda 1994-1996 while Figures C19-C21 displays the Cabauw years 1986-1988.

Using the same type of figures (C4-C10 for Norunda and C22-C27 for Cabauw), but for different RCA model output variables such as, global radiation, long wave radiation, net radiation, friction velocity and soil temperatures, makes it possible to estimate whether the model is working overall or not.

4.3 Sensitivity test for Norunda

Meteorological variables and land surface scheme typical parameters have been used during the model sensitivity test. The test was performed on Norunda data, changing one parameter at the time. Multiparameter and multiresponse interactions will therefore not be accounted for (Bastidas *et al.*, 1999) in this study. However, different studies where non multiresponse methods were used, have in general reported that latent and sensible heat fluxes are sensitive to the same parameters, where stomatal resistance of the vegetation is universally important for different land surface schemes (Bastidas *et al.*, 1999). It is therefore reasonable to use “one parameter at the time method” as a first approach trying to reveal for which forcing variables or parameters extra care needs to be attended to in gap filling and/or calibration procedures.

All original parameter and variable values, except leaf area index and air temperature, have been exposed to both a percentage increase and a percentage decrease.

Used parameter rates, recommended by Anders Lindroth and Fredrik Lagergren are given in Table 8. The same table also displays the meteorological rates, based on the values used in a sensitivity test of a land data assimilation system (Chen *et al.*,

unpublished). The used precipitation rates, 30 % for snow and 20 % for rain, are based on measurements uncertainties.

Table 8. Sensitivity test changes in meteorological variables and parameters for the land surface scheme (LSS). The abbreviated variables and parameters names are seen in parenthesis in column one and three, respectively.

Meteorological Variables	Change	LSS parameters	Change
Global radiation (Global)	±10 %	Heat Capacity of trees (C2)	±50 %
Wind speed (Wind)	±20 %	Change in available water content (WpFc)	+20 % -17 %
Specific Humidity (q)	±20 %	Displacement height at reference level (d)	±25 %
Air temperature (T)	±2°C	Roughness length for forest (z0)	±25 %
Precipitation (Precip.)		Forest Canopy surface resistance (zrsforc)	±25 %
rain	±20 %	Amount of water allowed to intercept (zvegmax)	±25 %
snow	±30 %	Leaf area index (LAI_4.5) (LAI_5.0)	+12.5 % +25 %

The original model run values for sandy loam has field capacity, F_c , and wilting point, W_p , values derived by Clapp *et al.* (Table 9). The difference between these to parameters is $0.135 \text{ cm}^3/\text{cm}^3$. A $\pm 20 \%$ change of $0.135 \text{ cm}^3/\text{cm}^3$ corresponds to $0.162 \text{ cm}^3/\text{cm}^3$ and $0.108 \text{ cm}^3/\text{cm}^3$, respectively. To receive realistic F_c and W_p values during the decrease in available water content, values derived by Rawls *et al.* (1982) were used (Table 9), even though these values only corresponds to a 17 % decrease in the original amount of available water content.

The linear relation (Figure 11) between W_p and F_c values derived from Clapp *et al.* (1978), Rawls *et al.* (1982) and Cosby *et al.* (1982) were used to extrapolate new W_p and F_c values for the 20 % increase of available water content.

Table 9. Wilting point and field capacity values derived by Clapp *et al.* (1978), Cosby *et al.* (1984) and Rawls *et al.* (1982).

	Wilting point [cm^3/cm^3]	Field Capacity [cm^3/cm^3]
Clapp <i>et al.</i> (1978)	0.114	0.249
Cosby <i>et al.</i> (1984)	0.099	0.222
Rawls <i>et al.</i> (1982)	0.095	0.207

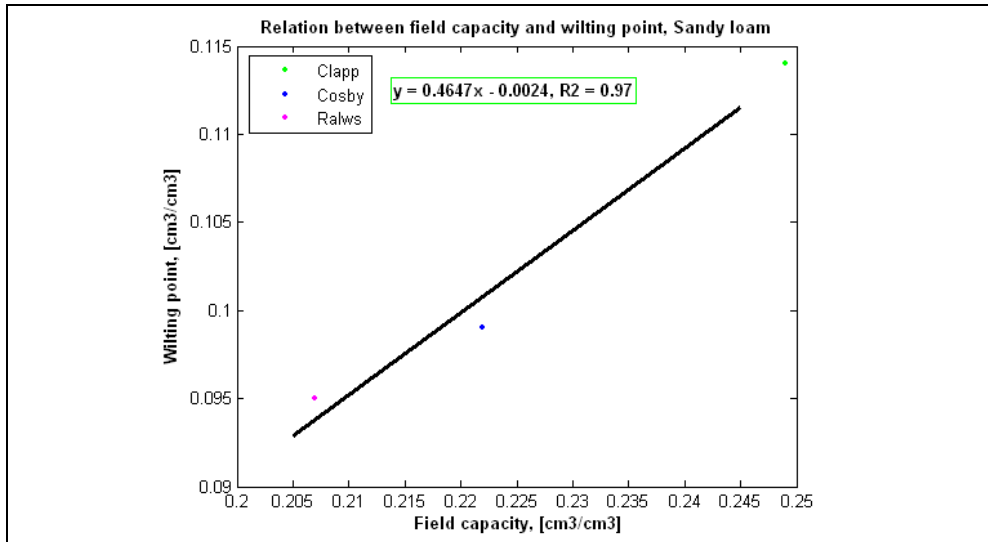


Figure 11. Relation between the wilting point and field capacity values from Table 9. The received linear equation is used to derive the new values of Wp and Fc after an increase by 20 % in the available water content.

As a result of the calculation field capacity were set to 0.298 cm³/cm³ and wilting point to 0.136 cm³/cm³ (Appendix A, Equation A6-A9).

On the contrary, to the remaining sensitivity test participants, temperature values have been exposed to the same absolute change, $\pm 2^{\circ}\text{C}$, instead of a relative change. To avoid vapour pressure deficit effects when the temperature was increased/decreased during the test, a corresponding +15 % respectively -13 % change (rates derived by Fredrik Lagergren) in specific humidity was carried out at the same time. Wet bulb temperatures were recalculated whenever q or T where changed, thereby accounting for a new precipitation division.

Each of the different model runs were plotted against observed values for latent and sensible heat. To be able to discern if the land surface scheme is extra sensitive to some of the parameters or variables during a special season all data (1994-1996) is divided into the four meteorological seasons: December-February (DJF), March-May (MAM), June-August (JJA) and September-November (SON). All data points are also evaluated for each parameter and variable. Finally, one plot containing all data was made for each model run.

Latent heat values that did not fit into the interval -200 W/m^2 to 1000 W/m^2 were cut off while the corresponding sensible heat values were cut off if they did not fit into the interval -300 W/m^2 to 1000 W/m^2 . Mean square values, R^2 , for the remaining points were then calculated, using a first degree polynomial fit function with a 95 % coefficient confidence bound: $fit(x) = x \cdot p1 - p2$, where $p1$ is the slope of the fit and $p2$ denotes the offset. These high intervals for the accepted data were chosen since they are defined well above (almost ten times) typical heat flow intervals for a boreal forest in North America (Bonan, 2002) and because values can not be excluded without a motivation. However, values higher or lower than the chosen interval limits would be too unrealistic and it would be meaningless to fit the data with a first degree polynomial function.

4.4 Hourly deviations between observations and modelled values

To be able to see if the model is deviating during special hours, *e.g.* during night time or during day time, a mean daily variation with an one hour time step was calculated for the four meteorological periods. This means that a mean value for all points beginning with 01, which are 01:00, 01:15, 01:30 and 01:45 for Cabauw, during DJF 1986-1989 represents the time 01.

Figure 12 shows how the diurnal variation for the modelled latent heat mean values relates to the diurnal variation of observations during JJA at Cabauw.

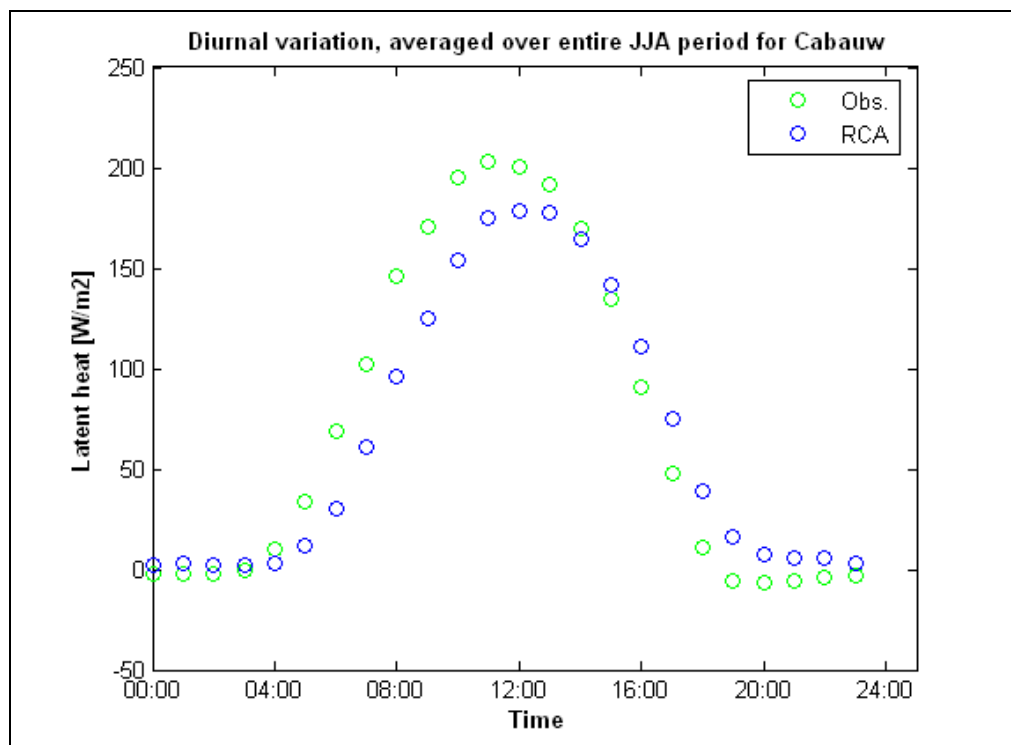


Figure 12. Diurnal variation for latent heat at Cabauw during JJA 1986-88. Modelled values are blue while the observations are green.

Soil temperatures at Cabauw, registered at 0 cm and 2 cm, are plotted against the first (tsns) and the second (tsns2) open land surface temperatures, which correspond to 0.5 cm and 4.1 cm depths, respectively. The same observations are also plotted against the calculated temperatures at same depths (tssn and tssn2) but under open land snow.

Soil water and soil temperature, both observed at 10 cm depth at Norunda, were evaluated against the models top soil moisture (7.2 cm) and the third layers forest soil surface temperature at 14.1 cm (tsc3). The same soil temperature observations were also used to compare the third layers soil temperature under forest snow (tscsn3). Mean temperature values from observations at 31.69 m and 36.91 m, corresponding to a height of 34.3 m, were used to evaluate the models air temperature at Norunda's reference level. Finally, the observed canopy temperature was calculated as a mean value of air temperatures observed at 24.47 m and 28.01 m since the forest height is 26.5 m.

All diurnal variation figures are found in Appendix C (Figure C11-C18 for Norunda and C28-C35 for Cabauw).

5. Results

5.1 Sensitivity test for Norunda

Examples of how the different sensitivity plots for Norunda looks like are shown in Figure (13-16).

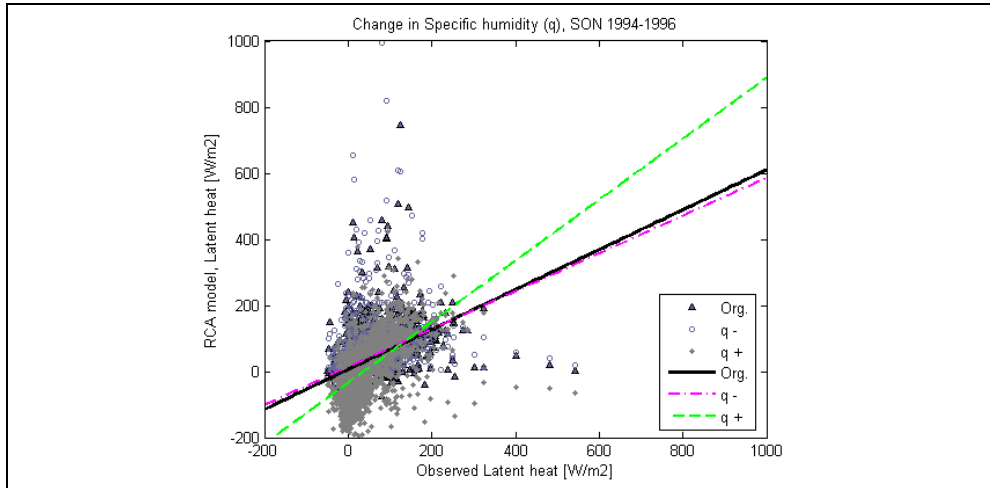


Figure 13. Modelled latent heat as a function of observed latent heat during September-November (SON). Data points obtained with original driving data are labelled as 'Org.', while 'q +' and 'q -' represent model output when specific humidity has been changed in the driving data with $\pm 20\%$, respectively. The lines represent linear regression fits for the three data sets.

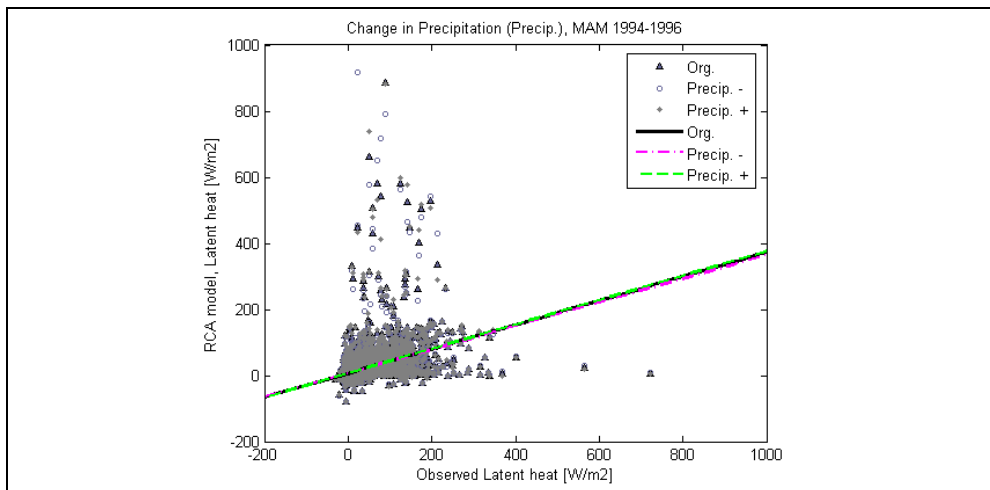


Figure 14. Modelled latent heat as a function of observed latent heat during March-April (MAM). Data points obtained with original driving data are labelled as 'org.', while 'Precip. +' and 'Precip. -' represent model output when precipitation has been changed in the driving data with $\pm 20\%$ and $\pm 30\%$ for rain and snow, respectively. The lines represent linear regression fits for the three data sets.

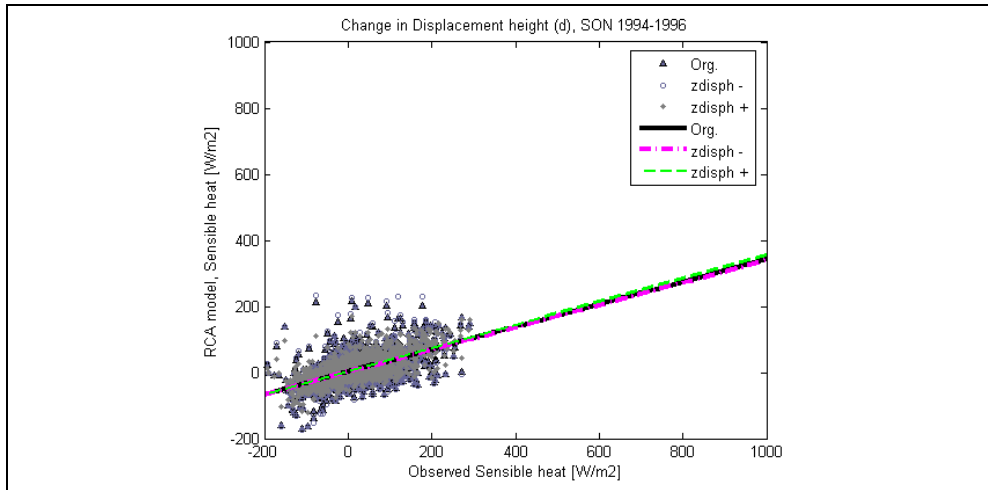


Figure 15. Modelled sensible heat as a function of observed sensible heat during September–November (SON). Data points obtained with original driving data are labelled as ‘Org.’, while ‘zdisph +’ and ‘zdisph -’ represent model output when displacement height has been changed in the driving data with $\pm 25\%$. The lines represent linear regression fits for the three data sets.

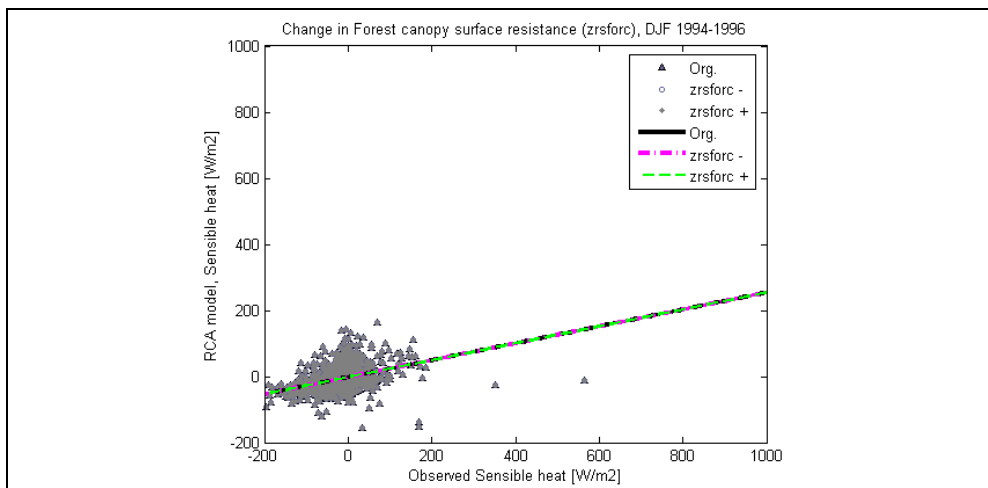


Figure 16. Modelled sensible heat as a function of observed sensible heat during December–February (DJF). Data points obtained with original driving data are labelled as ‘Org.’, while ‘zrsforc +’ and ‘zrsforc -’ represent model output when forest canopy surface resistance has been changed in the driving data with $\pm 25\%$. The lines represent linear regression fits for the three data sets.

The resulting tables for the different model runs are shown in Appendix B (Table B1–B4). Table B1 and B2 contain information about latent respectively sensible heat correlations when meteorological forcing variables have been changed. Corresponding tables that contain information about latent and sensible heat correlations when different parameters have been changed are given in Table B3 and B4, respectively. Since the four tables (B1–B4) are quite long, two new tables are put together (Table 10–11). Table 10 lists the periods where the maximum and minimum amounts of data have been rejected due to their inability to fit into chosen latent and sensible heat intervals. The same table also shows the maximum amount of rejected points when the entire period (1994–1996) is considered.

Table 10. Maximum and minimum number of excluded points, due to their inability to fit into chosen intervals, are given as a percentage. Also shown is the percentage of points that have been excluded when all values are considered.

	Latent heat meteorological variables	Sensible heat meteorological variables	Latent heat parameters	Sensible heat parameters
Max. number of excluded points	MAM 0.063 %	MAM 0.061 %	MAM 0.063 %	MAM 0.061 %
Min. number of excluded points	SON 0.038 %	SON 0.038 %	SON 0.038 %	SON 0.038 %
Number of excluded points when the entire period is considered	----- 0.053 %	----- 0.049 %	----- 0.052 - 0.053 %	----- 0.049 %

The maximum number of excluded points occurs for latent heat during MAM and corresponds to 0.063 % of the data measured in this period. A peak value for rejected data is also reached for sensible heat during the same period, but the percentage is a bit lower in this case. September-November (SON) is the period where the minimum amount of values (247-249 values) is excluded. In this case, all variable and parameter changes have the same minimum percentage of missing values.

When all values are taken into account 0.053 % of the values are rejected for all variables and parameters, except for displacement height increase for which only 0.052 % are excluded, when latent heat is studied. 0.049 % of the data is excluded when sensible heat is studied and all periods are taken into account.

For regressions between observed and modelled latent heat the R^2 values varies between 0.04-0.49 and 0.13-0.54 when meteorological variables respectively land surface scheme parameters are studied. The intervals are a bit higher, 0.13-0.69 and 0.16-0.78 for variables respectively parameters, when sensible heat is studied.

The linear regression fitting slopes varies between 0.31-0.97 and 0.30-0.79 for meteorological variables respectively parameters when latent heat is studied. The corresponding intervals are 0.13-0.69 and 0.24-0.63 for sensible heat.

Changes that have the largest deviation from the confidential bounds of the original runs slope are listed in Table 11.

As seen in the table, the largest positive (+0.27) and negative (-0.13) deviation are given when latent heat respectively sensible heat are studied after an increase in specific humidity during SON.

The land surface scheme is less sensitive to changes in parameters compared to changes in meteorological variables. Table 11 also shows that sensible heat is more frequently affected by variable and parameter changes compared to latent heat.

Table 11. Variables/parameters (abbreviations in Table 8) that have a slope (p1-value) that does not lie within the 95 % slope confidential bounds of the original model run are listed, as well as the period (e.g. DJF). It is also given whether the deviations occurred due to an increase (Inc.) or decrease (Dec.) of the original model run. Deviations from to the original runs are seen within parenthesis.

Latent heat meteorological variables	Sensible heat meteorological variables	Latent heat parameters	Sensible heat parameters
q Inc.	q Inc.	LAI_5.0 inc.	C2 Dec.
SON (+0.27)	SON (-0.13)	ALL (+0.04)	SON (+0.03)
q Inc.	q Inc.	d Inc.	WpFc Inc.
DJF (+0.22)	JJA (-0.12)	DJF (-0.03)	JJA (-0.03)
q Inc.	q Inc.	LAI_5.0 inc.	C2 Dec.
ALL (+0.20)	MAM (-0.11)	JJA (+0.03)	JJA (+0.02)
q Dec.	q Inc.	d Dec.	C2 Inc.
DJF (-0.17)	ALL (-0.11)	ALL (+0.02)	JJA (-0.02)
T Inc.	Global Dec.	d Inc.	C2 Inc.
MAM (+0.17)	JJA (-0.11)	ALL (-0.01)	SON (-0.02)
q Inc.	Global Inc.	LAI_4.5 Inc.	C2 Inc.
JJA (+0.16)	JJA (+0.11)	ALL (+0.01)	MAM (-0.02)
q Inc.	Global Inc.		C2 Dec.
MAM (+0.12)	ALL (+0.11)		ALL (+0.02)
T Inc.	Global Dec.		WpFc Dec.
ALL (+0.09)	ALL (-0.10)		JJA (+0.02)
T Inc.	Global Dec.		WpFc Dec.
JJA (+0.06)	MAM (-0.09)		ALL (+0.02)
T Dec.	Global Inc.		WpFc Inc.
MAM (-0.06)	MAM (+0.09)		ALL (-0.02)
T Inc.	T Inc.		C2 Inc.
SON (+0.04)	MAM (-0.09)		ALL (-0.01)
T Dec.	Global Dec.		d Dec.
ALL (-0.03)	SON (-0.07)		MAM (-0.01)
Wind Dec.	Global Inc.		LAI_5.0 Inc.
DJF (-0.02)	SON (-0.07)		JJA (-0.01)
q Dec.	T Inc.		LAI_5.0 Inc.
MAM (-0.02)	ALL (-0.06)		MAM (+0.01)
q Dec.	T Inc.		
ALL (-0.02)	SON (-0.05)		
T Dec.	T Inc.		
JJA (-0.02)	JJA (-0.04)		
Global Dec.	Wind Dec.		
ALL (-0.01)	DJF (-0.04)		
q Dec.	q Dec.		
JJA (-0.01)	SON (+0.03)		
Precip. Dec.	T Dec.		
ALL(-0.01)	SON (+0.03)		
	Wind Dec.		
	SON (-0.02)		
	Wind Inc.		
	SON (+0.01)		
	Wind Dec.		
	DJF (+0.01)		
	q Dec.		
	JJA (+0.01)		
	q Dec.		
	ALL (+0.01)		
	T Dec.		
	JJA (+0.01)		
	T Dec.		
	ALL (+0.01)		

5.2 Diurnal variation

Table 12 displays the largest difference between modelled and observed values during the average diurnal variation for different variables. However, it should be kept in mind that the large differences in latent and sensible heat during summer months are due to larger heat fluxes during these months compared to the winter month.

Differences in heat fluxes during the different periods can therefore not be mutually compared just looking at the table. The purpose with the table is to get an estimation of whether the deviations lie within an accepted range or not. Some of the soil temperatures beneath snow are referred to corresponding temperatures without snow when their figures were identical *e.g.* Figure C16 in Appendix C.

Table 12. Maximum daily deviations between observations and modelled values (Appendix C, Figure C11-C18 and C28-C35) for: Net radiation (R_n), Friction velocity (u^*), Sensible heat (H), Latent heat (LE), Forest soil temperature at layer 3 without- ($tsc3$) and with ($tscsn3$) snow, Soil water (top), Atmospheric temperature at the reference level (z_{tam}), Canopy air temperature (Canopy air T.), open land soil surface temperature at layer 1 and layer 2 without ($tsns$ respectively $tsns2$) and with snow ($tssn$ respectively $tssn2$).

Norunda	R_n	u^*	H	LE	$tsc3$	$tscsn3$	Soil water V/V	z_{tam}	Canopy air T.
	W/m^2	m/s	W/m^2	W/m^2	$^{\circ}C$	$^{\circ}C$		$^{\circ}C$	$^{\circ}C$
DJF	25.4	0.24	19.9	7.1	3.05	1.79	0.0811	0.39	1.11
MAM	74.0	0.29	43.1	47.3	0.53	0.65	0.0540	0.69	1.90
JJA	88.8	0.27	84.4	53.9	2.46	$tsc3$	0.0868	1.19	1.96
SON	41.1	0.29	31.2	10.6	0.30	0.22	0.0746	0.68	0.65

Cabauw	R_n	u^*	H	LE	$tsns$	$tssn$	$tsns2$	$tssn2$
	W/m^2	m/s	W/m^2	W/m^2	$^{\circ}C$	$^{\circ}C$	$^{\circ}C$	$^{\circ}C$
DJF	12.1	0.15	14.1	25.5	0.61	0.46	0.56	0.41
MAM	33.7	0.13	17.6	60.9	0.71	0.58	0.80	0.64
JJA	32.3	0.10	35.9	50.0	2.37	$tsns$	1.55	$tsns2$
SON	14.6	0.11	16.9	33.2	0.87	$tsns$	1.00	$tsns2$

As seen in some of the figures, *e.g.* C11 (Appendix C) for friction velocity and sensible heat during the midnight hour, it is obvious that some observations can not be accurate.

The trend for sensible heat discrepancy at Norunda is positive (modelled values > observed values) during the evening, night and early morning while it is negative (modelled values < observed values) during the morning. The discrepancy varies during the afternoon depending on season. DJF differs from the rest of the periods since the modelled values are higher during all hours compared to observations. The sensible heat flux trend at Cabauw consists of a negative discrepancy during the early evening until a couple of hours before midday and a positive discrepancy, of various lengths, during the afternoon.

Latent heat release during the winter months, DJF, at Norunda is underestimated at almost all hours. The model values for latent heat are irregular and do not follow the smooth observation curve during MAM. Observations and modelled values coincide during morning hours in JJA but the remaining model values are overestimated. Finally, all values from midnight until 04 are negative during SON, while the rest are positive. The model has the same mutual latent heat pattern at Cabauw during the different periods. Most times are overestimated from a couple of hours past midday until early morning (around 04 and 08 for DJF) from where it pass to a negative trend that lasts until the transitional period a couple of hours past midday.

Friction velocity is under estimated during all hours, with the exception of 23-00 where the observations seems inaccurate, and every season at Norunda. At Cabauw, the opposite relationship exists.

6. Discussion

6.1 Gap filling process

Instead of just using one linear relationship between net- and global radiation it would have been better to use one equation for each season during the gap filling process of net radiation (Lagergren, pers. comm.).

It was judged that the method used for estimating the sun hours at Hyytiälä was good enough for this purpose. However, a more accurate value can be received by calculating the time for the sunset, but since this approach would demand more programming time it was not used.

6.2 Control of driving- and verification data

Soil water measurements performed with TDR system have problem during winter time at small depths (Lundin *et al.*, 1999). Figure C2-C3 confirms that the soil water readings at Norunda during the end of 1995 and beginning of 1996 did not work since there is no reason why a sudden drop in soil water below a snow covered surface takes place (Figure C2).

6.3 Sensitivity test

The slope ($p1$ -values) of the linear equations are used instead of mean square values since most of these values were very low in both the original model runs and during the runs denoted by Inc. and Dec., during the evaluation of the sensitivity test (Appendix B, Table B1-B4). The low R^2 values are due to a narrow spread of the data, which was lumped instead of having a typical “cigar”- looked shape suitable for a first degree polynomial fit.

Table 10 shows that the maximum and minimum number of rejected points was low during all model runs and that the model were consistent for both latent and sensible heat regardless of whether parameters or variables had been changed. Since the numbers of rejected values have the same order of magnitude in all cases, just looking at Table 10, it cannot be generally said that MAM is more difficult to model than SON.

It is shown in Table 11 that the model is most sensitive to changes in the meteorological forcing data. An overestimation in specific humidity especially affects the latent heat results, which becomes positively biased. Sensible heat is also affected by changes in meteorological variables, especially specific humidity and global radiation, but to a less extent than latent heat.

Compared to meteorological variables, small biases in latent and sensible heat are given as a result of changes in different parameters. However, in both cases most biases occurred when sensible heat was studied. Parameter values that the model is most sensitive to are overestimations of LAI , displacement height, available water content and under estimations of tree heat capacity.

It is very surprising that both precipitation and canopy surface resistance have a negligible roll in the sensitivity test, especially since the latter have had an important roll in earlier land surface scheme sensitivity tests.

6.4 Diurnal variation

The diurnal variation comparison between observations and model output were generally good for both the forested site, Norunda, and the open landed site, Cabauw, when heat fluxes were considered (Appendix C, Figure C11, 13, 15, 17 for Norunda and Figure C28, 30, 32 and 34 for Cabauw). Since it was difficult for me to decide if

the deviations between observations and modelled heat fluxes were within a satisfying interval for what is reasonable, Stefan Gollvik was consulted for comments. The model reproduced the fluxes in a better way at Cabauw, which was expected since it is generally easier to both model and perform measurements in an open pasture landscape than in a forest. The modelled net radiation was satisfying all around the year for both stations but it had a remarkable high diurnal variation during the winter months at Norunda (Figure C11, top left). The diurnal variation for sensible heat (Figure C11, bottom left) flow seemed to be quite low compared to the observations for the same station and period (DJF).

A surplus of radiation must be conducted to the ground during MAM at the forest site (Figure C13) since the modelled net radiation (top left) is underestimated with $\sim 40 \text{ W/m}^2$ while the sum of modelled sensible (bottom left) and latent heat (bottom right) is underestimated with $\sim 70 \text{ W/m}^2$.

The summer months at Norunda (Figure C15) are characterised by a small overestimation of modelled latent heat (bottom right) and a small underestimation of modelled sensible heat (bottom left), but these deviations are not very dramatic. The modelled net radiation during the summer months at Cabauw (Figure C32) is a bit overestimated (bottom right) while the sum of modelled sensible heat (top right) and latent heat (bottom left) is underestimated, which must be a result of too large heat conduction to the ground.

When comparing modelled and observed values for soil water and soil temperatures it must be kept in mind that the measurements have not been performed at the model's simulation depths.

Diurnal variations for soil temperatures have an almost sinusoidal pattern and the amplitudes decrease rapidly with a greater depth. Maximum temperature is reached a couple of hours past midday for the surface temperature but it lags noon more at deeper depths (Campbell, 1998).

The pattern described above is not apparent in any of the diurnal variation figures for neither Norunda nor Cabauw (Appendix C). At both stations, modelled soil temperatures generally have higher amplitudes than the observations even though they are modelled for deeper depths than the observations are measured at. The time for maximum temperatures also occurs at the same hour for both the model and the observations even though a lag between the two of them should be recognizable at Norunda where 4.1 cm differs between the different soil depths.

It is also notable that the modelled temperature is higher than the observations at all hours during JJA at Norunda (Figure C16) and that the opposite relationship yields during MAM (Figure C14) and SON (Figure C18).

Soil water content close to the surface should be lower than the water content at deeper depths due to strong gravitational drainage. The modelled diurnal variation figures for soil water therefore seems inaccurate since all of them have a higher value than the observed values, even though the modelled depth is closer to the surface than the depth of the measurements (Appendix C, Figure C12, 14, 16 and 18).

7. Conclusions & Future work

7.1 Conclusions

The RCA land surface scheme seems to be highly sensitive to specific humidity, global radiation and temperature. Extra care must therefore be attended to these variables during gap filling processes. It has also been shown that *LAI*, displacement height and heat capacity of trees are the parameters that affect latent and sensible heat the most. Surprisingly both precipitation and canopy surface resistance have a negligible effect on the latent and sensible heat outcome.

The land surface scheme seems to reproduce heat flows, net radiation, and temperatures well for both forest and open land sites, but especially for open land. In the middle of the day, a net surplus of radiation is conducted to the ground during March-May at the forest site. The modelled net radiation is a bit overestimated at the open land site, which contributes to small overestimations of latent and sensible heat fluxes.

7.2 Future work

It would be a good idea to carry on the work with the assignment that I did not have the time to begin, namely looking for relationships among the different variables. This could be done, by plotting different variables against each other in scatter plots, tinting data points with large deviations and implement these deviating data points in other scatter figures with different variables.

It would also be interesting to see if the model is sensitive to the same variables/parameters when multi response interactions are considered.

Since the sensitivity test performed in this paper showed that the land surface scheme is sensitive to leaf area index, the model would probably be improved by using *LAI* values that vary with latitude for coniferous forest.

Snow free soil temperatures are identical to corresponding snow soil temperatures during the summer months while they are less accurate than these during the winter months. According to my opinion, snow free soil temperatures therefore seem to be superfluous and could be removed in the purpose to save computational time.

Both Cabauw and Norunda have the same soil texture class, so it is therefore also a suggestion to evaluate the model with data from an area with another soil texture class. Finally, it would be interesting to see how much the Hyytiälä data for 2004 would deviate. If it had turned out that the result were good, it would be appropriate to recommend the used gap filling method for this kind of investigation.

The model could also be calibrated, changing one parameter at the time to see if the model result is closing in on the observations.

References

- Asner, G. P., Scurlock, J.M.O., Hicke, J.A., 2003. Global synthesis of leaf area index observations: implications for ecological and remote sensing studies
Global Ecology & Biogeography, **12**, 191–205
- Baldocchi, D., 2005. Lecture on Integrating and Scaling Information from Leaves to Canopy Scales: Big Leaf Models: ESPM 228
- Bastidas, L.A., Gupta, H .V., Sorooshian, S., Shuttleworth, W. J., Yang, Z. L.,1999. Sensitivity analysis of a land surface scheme using multicriteria methods.
Journal of geophysical research, **104**, 19,481-19,490
- Bonan, G., 2002. Ecological Climatology concepts and applications.
Cambridge university press, Cambridge, UK, 678 p
- Campbell, G.S, Norman J.M., 1998. An introduction to Environmental Biophysics (2nd edition). *Springer-Verlag New York, Inc.*, New York, USA, 286 p
- Chapin, F.S. III, Matson, P.A, Chapin, M.C., Mooney, H.A., 2002. Principles of Terrestrial Ecosystem Ecology. *Springer-Verlag New York, Inc.*, New York, USA, 436 p
- Chen, F., Manning, K.W, LeMone, M.A., Trier, S.B., Alfien, J.G, Roberts, R., Tewari, M., Niyogi, D., Horst, T.W., Oncley, S.P., Basara, J.B, Blanken, P.D. Evaluation of the characteristics of the NCAR High- Resolution Land Data Assimilation System. Submitted to *Journal of Applied Meteorology*
- Chen, T. H., Henderson-Sellers A., Milly, P. C. D., Pitman A. J., Beljaars, A. C. M., Polcher J., Abramopoulos, F., Boone, A., Chang, S., Chen, F., Dai, Y., Desborough, C. E., Dickinson, R. E., Dümenil, L., Ek, M., Garratt, J. R., Gedney, N., Gusev, Y., Kim, J., Koster, R., Kowalczyk, E. A., Laval, K., Lean, J., Lettenmaier, D., Liang, X., Mahfouf, J.-F., Mengelkamp, H.-T., Mitchell, K., Nasonova, O. N., Noilhan, J., Robock, A., Rosenzweig, C., Schaake, J., Schlosser, C. A., Schulz, J.-P., Shao, Y., Shmakin, A. B., Verseghy, D. L., Wetzell, P., Wood, E. F., Xue, Y., Yang, Z.-L., Zeng, Q., 1997. Cabauw Experimental Results from the Project for Intercomparison of Land-Surface Parameterization Schemes.
Journal of Climate, **10**, 1194–1215
- Clapp, R.B., Hornberger, G.M., 1978. Empirical equations for some soil hydraulic-properties. *Water Resources Research*, **14**, 601-604
- Cosby, B.J., Hornberger, G.M., Clapp, R.B., Ginn, T.R., 1984. A statistical exploration of the relationships of soil moisture characteristics to the physical properties of soils. *Water Resources Research*, **20**, 682-690
- Dunlop, S., 2005. A Dictionary of Weather. *Oxford University Press Inc.*, New York, USA, 268 p

Falge, E., Baldocchi, D., Olson, R., Anthoni, P., Aubinet, M., Bernhofer, C., Burba, G., Ceulemans, R., Clement, R., Dolman, H., Granier, A., Gross, P., Grünwald, T., Hollinger, D., Jensen, N.L., Katul, G., Keronen, P., Kowalski, A., Ta Lai, C, Law, B.E, Meyers, T., Moncrieff, J., Moors, E., Munger, J.W., Pilegaard, K., Rannik, U., Rebmann, C., Suyker, A., Tenhunen, J., Tu, K., Verma, S., Vesala, T., Wilson, K., Wofsy, S., 2001. Gap filling strategies for defensible annual sums of net ecosystem exchange. *Agricultural and Forest Meteorology*, **107**, 43–69

González, J.A., Calbó, J., 2002. Modelled and measured ratio of PAR to global radiation under cloudless skies. *Agricultural and Forest Meteorology*, **110**, 319–325

Harvey, D., 2000. Global Warming. *Pearson Education Limited*, Essex, UK, 336 p

Jones, C., Willén, U., Ullerstig, A., Hansson, U., 2004. The Rossby Centre Regional Atmospheric Climate Model Part I: Model Climatology and Performance for the Present Climate over Europe. *Ambio*, **33**, 211-220

Lundin, L- C., Halldin, S., Lindroth, A., Cienciala, E., Grelle, A., Hjelm, P., Kellner, E., Lundberg, A., Mölder, M., Morén, A.-S., Nord, T., Seibert, J., Stähli, M. 1999. Continuous long-term measurements of soil-plant-atmosphere variables at a forest site. *Agricultural and Forest Meteorology*, **98-99**, 53-73

McIlveen, R., 1998. Fundamentals of weather and climate. *Stanley Thornes (Publishers) Ltd.* Cheltenham, UK, 496 p

Persson A., 2001. User guide to ECMWF forecast products. *European Centre for Medium-Range Weather Forecasts*, Reading, UK, 115 p

Rawls, W.J., Brakensiek, D.L., Saxton, K.E., 1982. Estimation of soil water properties. *Transactions of the ASAE*, **25**, 1316-1328

Samuelsson. P., Gollvik., S, Ullerstig, A., 2006. The land-surface scheme of the Rossby Centre regional atmospheric climate model (RCA3). *Report in Meteorology*, 122, SMHI, SE-601 76 Norrköping, Sweden

Seinfeld, J., Pandis, N. 1998, Atmospheric chemistry and physics. *John Wiley & Sons, Inc.*, New York, USA, 1326 p

Stewart, J.B., 1977. Evaporation from the wet canopy of a pine forest. *Water Resources Research*, **13**, 915-921

Tetens, O., 1930. Uber einige meteorologische Begriffe. *Zeitschrift für Geophysik*, **6**, 297-309

Widén, B., Majdi, H., 2001. Soil CO₂ efflux and root respiration at three sites in a mixed pine and spruce forest: seasonal and diurnal variation. *Canadian Journal of Forest Research*, **31**, 786–796

Appendix

Appendix A: Equations

The vegetation (canopy) surface resistance, r_{sc} , is given by

$$r_{sc} = \frac{r_{sc,\min}}{LAI} * F_1 F_2^{-1} F_3 F_4^{-1} F_5^{-1} \quad \text{Eq. (A1)}$$

(Samuelsson *et al.*, 2006) where F_2 depends on soil moisture availability. The value of F_2 becomes close to 1 when the soil moisture, θ , availability increases, implying a lower value of the canopy resistance.

F_2 varies between 0 and 1 depending on the relationship between wilting point, θ_{wi} , and θ_{cr} which is 90 % of the field capacity.

$$F_2 = 1 \text{ if } \theta > \theta_{cr} \quad \text{Eq. (A2)}$$

$$F_2 = (\theta - \theta_{wi}) / (\theta_{cr} - \theta_{wi}) \text{ if } \theta_{wi} \leq \theta \leq \theta_{cr} \quad \text{Eq. (A3)}$$

$$F_2 = 0 \text{ if } \theta < \theta_{wi} \quad \text{Eq. (A4)}$$

(Samuelsson *et al.*, 2006)

The forest canopy latent heat flux, E_{forc} , becomes higher with a decreased canopy surface resistance because of following relationship:

$$E_{forc} = \rho \lambda h_{vfor} \frac{q_s(T_{forc}) - q_{fora}}{r_b + r_{sforc}}, \quad \text{Eq. (A5)}$$

where r_{sforc} is the canopy surface resistance (Samuelsson *et al.*, 2006).

$$\text{Linear relationship between Wp and Fc: } y = 0.4647x - 0.0024 \quad \text{Eq. (A6)}$$

The available water content is $0.162 \text{ cm}^3/\text{cm}^3$ after a 20 % increase in the original amount of available water.

$$x - y = 0.162 \text{ cm}^3/\text{cm}^3 \quad \text{Eq. (A7)}$$

$$\text{Combining Equation A6 and Equation A7 } \Rightarrow x - 0.4647x + 0.0024 = 0.162 \text{ cm}^3/\text{cm}^3$$

\Rightarrow

$$x = 0.298 \text{ cm}^3/\text{cm}^3 \quad \text{Eq. (A8)}$$

$$\text{Replacing the value of x in Equation A7 } \Rightarrow y = 0.13615 \quad \text{Eq. (A9)}$$

Appendix A: Tables

Table A1. Approximated sun hours at Hyytiälä.

Date	First sun	Last sun	Date	First sun	Last sun
1/1	10:00	15:30	2/7	03:30	21:30
15/1	09:30	16:00	15/7	04:30	21:00
29/1	09:30	16:30	29/7	05:00	20:30
12/2	08:30	17:00	12/8	05:30	20:00
26/2	08:00	17:30	26/8	06:00	19:00
12/3	07:30	18:00	23/9	07:30	17:30
27/3	07:00	18:30	8/10	07:30	17:00
8/4	06:00	19:00	22/10	08:30	16:00
22/4	05:30	19:30	4/11	09:00	15:30
6/5	05:00	20:00	18/11	09:30	15:30
20/5	04:30	20:30	2/12	10:00	15:00
2/6	04:00	21:00	16/12	10:00	15:00
17/6	03:30	21:30			

Table A2. Values used to replace precipitation gaps at Hyytiälä. The third and fourth column represent whether it has been precipitation during gap free hours at Hyytiälä and the nearby station, respectively. The rightmost column shows the final value that each missing value were replaced with.

dd/mm/yyyy	Number of missing values	Precipitation at Hyytiälä	Precipitation at nearby station	Value to replace with (mm)
10/1/2004	2	0	+	0
21/1/2004	1	0	+	0
4/2/2004	10	+	+	0
10/2/2004	1	0	0	0
12/2/2004	2	0	+	0
14/2/2004	1	+	+	0.50
20/2/2004	7	0	0	0
1/3/2004	2	0	+	0
7/3/2004	2	0	+	0
11/3/2004	1	0	0	0
16/3/2004	1	+	0	0
21/3/2004	2	0	+	0
8/4/2004	1	0	0	0
10/4/2004	5	0	0	0
11/4/2004	1	0	+	0
12/4/2004	2	0	0	0
5/7/2004	9	+	+	0.40
6/7/2004	2	0	+	0
11/7/2004	6	+	+	0
13/7/2004	1	+	+	0.70
14/7/2004	2	+	+	0.25
26/7/2004	1	0	0	0
11/8/2004	15	0	+	0
12/9/2004	1	+	+	3.66
13/10/2004	1	0	0	0
21/10/2004	5	0	+	0
26/11/2004	3	0	0	0
1/12/2004	1	+	+	0
5/12/2004	3	+	+	2.63
7/12/2004	6	0	+	0
8/12/2004	1	0	+	0
16/12/2004	2	0	+	0
30/12/2004	7	+	+	0.19
31/12/2004	1	0	0	0

Appendix B: Sensitivity test tables

Column header information for Table B1-B4.

Id is the abbreviation for the variable/parameter that is studied. Each of the abbreviated names is found in Table 8, which also contains an explanation to each abbreviation. **Change** indicates whether the variable/parameter belongs to the original model run (Org.) where latent/sensible heat has been plotted against observed latent/sensible heat, or if it has been increased (Inc) or decreased (Dec) before it was plotted against observed values. **Period** indicated whether the data has been divided into the meteorological periods, December + January + February (DJF), March + April + May (MAM), June + July + August (JJA) and September + October + November (SON), or if all data, January-December 1994-1996 (ALL) is considered at the same time. The columns containing **p1(+ -)** respectively **p2(+ -)** represent the slope and intercept and their upper and lower limits within 95 % -accuracy.

Mean square values from the different runs are given in the **R²** column, while the number of points that did not fit into the limit intervals (-200 W/m² to 1000 W/m² for latent heat and -300 W/m² to 1000 W/m² for sensible heat) are given in **No** which also is expressed as a percentage of all values in the column with **%** as header.

Table B1. The effect on latent heat after changes in different meteorological variables. See column header information above.

Id	Change	Period	p1(+ -)	p2(+ -)	R²	No	%
Global	Org.	JJA	0.74(+0.02 -0.02)	29.58(+2.14 -2.14)	0.44	385	0.059
Global	Dec.	JJA	0.72(+0.02 -0.02)	26.32(+2.10 -2.10)	0.44	383	0.059
Global	Inc.	JJA	0.75(+0.02 -0.02)	32.13(+2.19 -2.19)	0.43	386	0.059
Global	Org.	SON	0.60(+0.02 -0.02)	4.58(+0.86 -0.86)	0.35	249	0.038
Global	Dec.	SON	0.59(+0.02 -0.02)	3.71(+0.81 -0.81)	0.36	249	0.038
Global	Inc.	SON	0.63(+0.02 -0.02)	5.34(+0.91 -0.91)	0.34	249	0.038
Global	Org.	DJF	0.38(+0.03 -0.03)	-0.47(+0.31 -0.31)	0.14	279	0.055
Global	Dec.	DJF	0.36(+0.03 -0.03)	-0.62(+0.31 -0.31)	0.13	279	0.055
Global	Inc.	DJF	0.40(+0.03 -0.03)	-0.31(+0.31 -0.31)	0.15	279	0.055
Global	Org.	MAM	0.37(+0.02 -0.02)	6.47(+1.44 -1.44)	0.18	277	0.063
Global	Dec.	MAM	0.34(+0.02 -0.02)	5.49(+1.36 -1.36)	0.17	277	0.063
Global	Inc.	MAM	0.39(+0.03 -0.03)	7.53(+1.52 -1.52)	0.18	277	0.063
Global	Org.	ALL	0.75(+0.01 -0.01)	7.38(+0.70 -0.70)	0.46	1190	0.053
Global	Dec.	ALL	0.72(+0.01 -0.01)	6.19(+0.68 -0.68)	0.46	1188	0.053
Global	Inc.	ALL	0.77(+0.01 -0.01)	8.41(+0.73 -0.73)	0.46	1191	0.053
Wind	Org.	JJA	0.74(+0.02 -0.02)	29.58(+2.14 -2.14)	0.44	385	0.059
Wind	Dec.	JJA	0.74(+0.02 -0.02)	27.25(+2.15 -2.15)	0.44	381	0.058
Wind	Inc.	JJA	0.74(+0.02 -0.02)	31.59(+2.23 -2.23)	0.42	386	0.059
Wind	Org.	SON	0.60(+0.02 -0.02)	4.58(+0.86 -0.86)	0.35	249	0.038
Wind	Dec.	SON	0.59(+0.02 -0.02)	4.01(+0.80 -0.80)	0.37	249	0.038
Wind	Inc.	SON	0.61(+0.02 -0.02)	5.27(+0.93 -0.93)	0.32	249	0.038
Wind	Org.	DJF	0.38(+0.03 -0.03)	-0.47(+0.31 -0.31)	0.14	279	0.055
Wind	Dec.	DJF	0.31(+0.02 -0.02)	-0.18(+0.27 -0.27)	0.13	279	0.055
Wind	Inc.	DJF	0.42(+0.03 -0.03)	-0.21(+0.36 -0.36)	0.13	279	0.055
Wind	Org.	MAM	0.37(+0.02 -0.02)	6.47(+1.44 -1.44)	0.18	277	0.063
Wind	Dec.	MAM	0.34(+0.02 -0.02)	6.06(+1.48 -1.48)	0.15	276	0.063
Wind	Inc.	MAM	0.38(+0.03 -0.03)	7.45(+1.53 -1.53)	0.17	277	0.063
Wind	Org.	ALL	0.75(+0.01 -0.01)	7.38(+0.70 -0.70)	0.46	1190	0.053
Wind	Dec.	ALL	0.74(+0.01 -0.01)	6.61(+0.70 -0.70)	0.46	1185	0.053
Wind	Inc.	ALL	0.76(+0.01 -0.01)	8.31(+0.74 -0.74)	0.45	1191	0.053
q	Org.	JJA	0.74(+0.02 -0.02)	29.58(+2.14 -2.14)	0.44	385	0.059
q	Dec.	JJA	0.69(+0.02 -0.02)	38.47(+2.42 -2.42)	0.35	389	0.06
q	Inc.	JJA	0.94(+0.02 -0.02)	1.51(+2.54 -2.54)	0.47	377	0.058
q	Org.	SON	0.60(+0.02 -0.02)	4.58(+0.86 -0.86)	0.35	249	0.038

Id	Change	Period	p1(+ -)	p2(+ -)	R^2	No	%
q	Dec.	SON	0.57(+0.03 -0.03)	13.21(+1.07 -1.07)	0.24	250	0.038
q	Inc.	SON	0.92(+0.03 -0.03)	-35.38(+1.35 -1.35)	0.34	255	0.039
q	Org.	DJF	0.38(+0.03 -0.03)	-0.47(+0.31 -0.31)	0.14	279	0.055
q	Dec.	DJF	0.16(+0.02 -0.02)	4.16(+0.24 -0.24)	0.04	279	0.055
q	Inc.	DJF	0.69(+0.06 -0.06)	-24.96(+0.75 -0.75)	0.08	279	0.055
q	Org.	MAM	0.37(+0.02 -0.02)	6.47(+1.44 -1.44)	0.18	277	0.063
q	Dec.	MAM	0.30(+0.03 -0.03)	9.58(+1.51 -1.51)	0.12	277	0.063
q	Inc.	MAM	0.54(+0.03 -0.03)	-8.75(+1.72 -1.72)	0.25	276	0.063
q	Org.	ALL	0.75(+0.01 -0.01)	7.38(+0.70 -0.70)	0.46	1190	0.053
q	Dec.	ALL	0.71(+0.01 -0.01)	13.76(+0.79 -0.79)	0.38	1195	0.053
q	Inc.	ALL	0.97(+0.01 -0.01)	-20.89(+0.88 -0.88)	0.48	1187	0.053
T	Org.	JJA	0.74(+0.02 -0.02)	29.58(+2.14 -2.14)	0.44	385	0.059
T	Dec.	JJA	0.68(+0.02 -0.02)	33.74(+2.22 -2.22)	0.38	389	0.06
T	Inc.	JJA	0.84(+0.02 -0.02)	25.57(+2.41 -2.41)	0.44	385	0.059
T	Org.	SON	0.60(+0.02 -0.02)	4.58(+0.86 -0.86)	0.35	249	0.038
T	Dec.	SON	0.57(+0.02 -0.02)	6.99(+0.91 -0.91)	0.3	249	0.038
T	Inc.	SON	0.68(+0.02 -0.02)	1.42(+0.96 -0.96)	0.35	249	0.038
T	Org.	DJF	0.38(+0.03 -0.03)	-0.47(+0.31 -0.31)	0.14	279	0.055
T	Dec.	DJF	0.35(+0.03 -0.03)	0.19(+0.30 -0.30)	0.13	279	0.055
T	Inc.	DJF	0.39(+0.03 -0.03)	-1.87(+0.35 -0.35)	0.12	279	0.055
T	Org.	MAM	0.37(+0.02 -0.02)	6.47(+1.44 -1.44)	0.18	277	0.063
T	Dec.	MAM	0.27(+0.02 -0.02)	7.42(+1.30 -1.30)	0.13	277	0.063
T	Inc.	MAM	0.59(+0.03 -0.03)	7.38(+1.62 -1.62)	0.31	278	0.063
T	Org.	ALL	0.75(+0.01 -0.01)	7.38(+0.70 -0.70)	0.46	1190	0.053
T	Dec.	ALL	0.70(+0.01 -0.01)	9.33(+0.72 -0.72)	0.41	1194	0.053
T	Inc.	ALL	0.86(+0.01 -0.01)	5.39(+0.77 -0.77)	0.49	1191	0.053
Precip.	Org.	JJA	0.74(+0.02 -0.02)	29.58(+2.14 -2.14)	0.44	385	0.059
Precip.	Dec.	JJA	0.70(+0.02 -0.02)	28.37(+2.06 -2.06)	0.43	385	0.059
Precip.	Inc.	JJA	0.76(+0.02 -0.02)	30.15(+2.19 -2.19)	0.44	385	0.059
Precip.	Org.	SON	0.60(+0.02 -0.02)	4.58(+0.86 -0.86)	0.35	249	0.038
Precip.	Dec.	SON	0.57(+0.02 -0.02)	4.29(+0.83 -0.83)	0.34	249	0.038
Precip.	Inc.	SON	0.63(+0.02 -0.02)	4.79(+0.89 -0.89)	0.36	249	0.038
Precip.	Org.	DJF	0.38(+0.03 -0.03)	-0.47(+0.31 -0.31)	0.14	279	0.055
Precip.	Dec.	DJF	0.38(+0.03 -0.03)	-0.53(+0.31 -0.31)	0.14	279	0.055
Precip.	Inc.	DJF	0.38(+0.03 -0.03)	-0.47(+0.31 -0.31)	0.14	279	0.055
Precip.	Org.	MAM	0.37(+0.02 -0.02)	6.47(+1.44 -1.44)	0.18	277	0.063
Precip.	Dec.	MAM	0.36(+0.02 -0.02)	6.76(+1.48 -1.48)	0.16	276	0.063
Precip.	Inc.	MAM	0.37(+0.02 -0.02)	6.42(+1.48 -1.48)	0.17	277	0.063
Precip.	Org.	ALL	0.75(+0.01 -0.01)	7.38(+0.70 -0.70)	0.46	1190	0.053
Precip.	Dec.	ALL	0.72(+0.01 -0.01)	7.14(+0.68 -0.68)	0.45	1189	0.053
Precip.	Inc.	ALL	0.77(+0.01 -0.01)	7.51(+0.72 -0.72)	0.46	1190	0.053

Table B2. The effect on sensible heat after changes in different meteorological variables. The column header information is given on page: *Appendix B-1*.

Id	Change	Period	p1(+ -)	p2(+ -)	R²	No	%
Global	Org.	JJA	0.46(+0.01 -0.01)	7.54(+1.11 -1.11)	0.63	369	0.057
Global	Dec.	JJA	0.33(+0.01 -0.01)	2.20(+0.99 -0.99)	0.53	369	0.057
Global	Inc.	JJA	0.59(+0.01 -0.01)	13.62(+1.27 -1.27)	0.69	369	0.057
Global	Org.	SON	0.34(+0.01 -0.01)	0.90(+0.53 -0.53)	0.37	247	0.038
Global	Dec.	SON	0.25(+0.01 -0.01)	-2.69(+0.49 -0.49)	0.28	247	0.038
Global	Inc.	SON	0.43(+0.01 -0.01)	4.73(+0.58 -0.58)	0.44	247	0.038
Global	Org.	DJF	0.26(+0.02 -0.02)	-2.40(+0.62 -0.62)	0.18	226	0.044
Global	Dec.	DJF	0.23(+0.01 -0.01)	-3.64(+0.60 -0.60)	0.17	226	0.044
Global	Inc.	DJF	0.28(+0.02 -0.02)	-1.12(+0.64 -0.64)	0.2	226	0.044
Global	Org.	MAM	0.60(+0.01 -0.01)	12.60(+1.45 -1.45)	0.65	269	0.061
Global	Dec.	MAM	0.49(+0.01 -0.01)	7.92(+1.32 -1.32)	0.6	269	0.061
Global	Inc.	MAM	0.71(+0.01 -0.01)	17.68(+1.59 -1.59)	0.69	269	0.061
Global	Org.	ALL	0.49(+0.01 -0.01)	6.20(+0.45 -0.45)	0.63	1111	0.049
Global	Dec.	ALL	0.38(+0.00 -0.00)	1.77(+0.41 -0.41)	0.54	1111	0.049
Global	Inc.	ALL	0.62(+0.01 -0.01)	11.01(+0.50 -0.50)	0.68	1111	0.049
Wind	Org.	JJA	0.46(+0.01 -0.01)	7.54(+1.11 -1.11)	0.63	369	0.057
Wind	Dec.	JJA	0.45(+0.01 -0.01)	10.26(+1.11 -1.11)	0.63	369	0.057
Wind	Inc.	JJA	0.46(+0.01 -0.01)	5.52(+1.15 -1.15)	0.62	369	0.057
Wind	Org.	SON	0.34(+0.01 -0.01)	0.90(+0.53 -0.53)	0.37	247	0.038
Wind	Dec.	SON	0.30(+0.01 -0.01)	3.75(+0.47 -0.47)	0.36	247	0.038
Wind	Inc.	SON	0.37(+0.01 -0.01)	-1.46(+0.60 -0.60)	0.35	247	0.038
Wind	Org.	DJF	0.26(+0.02 -0.02)	-2.40(+0.62 -0.62)	0.18	226	0.044
Wind	Dec.	DJF	0.19(+0.01 -0.01)	-0.48(+0.51 -0.51)	0.15	226	0.044
Wind	Inc.	DJF	0.31(+0.02 -0.02)	-3.78(+0.72 -0.72)	0.2	226	0.044
Wind	Org.	MAM	0.60(+0.01 -0.01)	12.60(+1.45 -1.45)	0.65	269	0.061
Wind	Dec.	MAM	0.59(+0.01 -0.01)	14.95(+1.43 -1.43)	0.65	269	0.061
Wind	Inc.	MAM	0.60(+0.01 -0.01)	10.78(+1.50 -1.50)	0.63	269	0.061
Wind	Org.	ALL	0.49(+0.01 -0.01)	6.20(+0.45 -0.45)	0.63	1111	0.049
Wind	Dec.	ALL	0.48(+0.00 -0.00)	9.34(+0.44 -0.44)	0.63	1111	0.049
Wind	Inc.	ALL	0.50(+0.01 -0.01)	3.79(+0.48 -0.48)	0.61	1111	0.049
q	Org.	JJA	0.46(+0.01 -0.01)	7.54(+1.11 -1.11)	0.63	369	0.057
q	Dec.	JJA	0.49(+0.01 -0.01)	3.78(+1.17 -1.17)	0.64	369	0.057
q	Inc.	JJA	0.33(+0.01 -0.01)	25.29(+1.34 -1.34)	0.38	369	0.057
q	Org.	SON	0.34(+0.01 -0.01)	0.90(+0.53 -0.53)	0.37	247	0.038
q	Dec.	SON	0.39(+0.01 -0.01)	-3.07(+0.52 -0.52)	0.44	247	0.038
q	Inc.	SON	0.18(+0.02 -0.02)	28.05(+0.98 -0.98)	0.05	247	0.038
q	Org.	DJF	0.26(+0.02 -0.02)	-2.40(+0.62 -0.62)	0.18	226	0.044
q	Dec.	DJF	0.26(+0.02 -0.02)	-4.40(+0.63 -0.63)	0.19	226	0.044
q	Inc.	DJF	0.30(+0.02 -0.02)	18.74(+0.89 -0.89)	0.13	226	0.044
q	Org.	MAM	0.60(+0.01 -0.01)	12.60(+1.45 -1.45)	0.65	269	0.061
q	Dec.	MAM	0.62(+0.01 -0.01)	11.59(+1.46 -1.46)	0.66	269	0.061
q	Inc.	MAM	0.47(+0.01 -0.01)	25.10(+1.61 -1.61)	0.49	269	0.061
q	Org.	ALL	0.49(+0.01 -0.01)	6.20(+0.45 -0.45)	0.63	1111	0.049
q	Dec.	ALL	0.52(+0.01 -0.01)	3.35(+0.47 -0.47)	0.64	1111	0.049
q	Inc.	ALL	0.36(+0.01 -0.01)	25.87(+0.57 -0.57)	0.36	1111	0.049
T	Org.	JJA	0.46(+0.01 -0.01)	7.54(+1.11 -1.11)	0.63	369	0.057
T	Dec.	JJA	0.49(+0.01 -0.01)	15.06(+1.26 -1.26)	0.61	369	0.057
T	Inc.	JJA	0.40(+0.01 -0.01)	1.54(+1.16 -1.16)	0.56	369	0.057

Id	Change	Period	p1(+ -)	p2(+ -)	R^2	No	%
T	Org.	SON	0.34(+0.01 -0.01)	0.90(+0.53 -0.53)	0.37	247	0.038
T	Dec.	SON	0.39(+0.01 -0.01)	7.82(+0.61 -0.61)	0.37	247	0.038
T	Inc.	SON	0.27(+0.01 -0.01)	-4.85(+0.51 -0.51)	0.28	247	0.038
T	Org.	DJF	0.26(+0.02 -0.02)	-2.40(+0.62 -0.62)	0.18	226	0.044
T	Dec.	DJF	0.30(+0.02 -0.02)	4.75(+0.70 -0.70)	0.19	226	0.044
T	Inc.	DJF	0.23(+0.02 -0.02)	-7.08(+0.65 -0.65)	0.14	226	0.044
T	Org.	MAM	0.60(+0.01 -0.01)	12.60(+1.45 -1.45)	0.65	269	0.061
T	Dec.	MAM	0.61(+0.01 -0.01)	19.32(+1.55 -1.55)	0.63	269	0.061
T	Inc.	MAM	0.49(+0.01 -0.01)	5.49(+1.38 -1.38)	0.58	269	0.061
T	Org.	ALL	0.49(+0.01 -0.01)	6.20(+0.45 -0.45)	0.63	1111	0.049
T	Dec.	ALL	0.52(+0.01 -0.01)	13.11(+0.50 -0.50)	0.61	1111	0.049
T	Inc.	ALL	0.42(+0.00 -0.00)	0.16(+0.45 -0.45)	0.56	1111	0.049
Precip.	Org.	JJA	0.46(+0.01 -0.01)	7.54(+1.11 -1.11)	0.63	369	0.057
Precip.	Dec.	JJA	0.48(+0.01 -0.01)	9.54(+1.15 -1.15)	0.64	369	0.057
Precip.	Inc.	JJA	0.44(+0.01 -0.01)	6.43(+1.10 -1.10)	0.62	369	0.057
Precip.	Org.	SON	0.34(+0.01 -0.01)	0.90(+0.53 -0.53)	0.37	247	0.038
Precip.	Dec.	SON	0.36(+0.01 -0.01)	1.76(+0.54 -0.54)	0.39	247	0.038
Precip.	Inc.	SON	0.33(+0.01 -0.01)	0.28(+0.52 -0.52)	0.36	247	0.038
Precip.	Org.	DJF	0.26(+0.02 -0.02)	-2.40(+0.62 -0.62)	0.18	226	0.044
Precip.	Dec.	DJF	0.26(+0.02 -0.02)	-2.22(+0.63 -0.63)	0.18	226	0.044
Precip.	Inc.	DJF	0.26(+0.01 -0.01)	-2.66(+0.61 -0.61)	0.19	226	0.044
Precip.	Org.	MAM	0.60(+0.01 -0.01)	12.60(+1.45 -1.45)	0.65	269	0.061
Precip.	Dec.	MAM	0.61(+0.01 -0.01)	13.78(+1.47 -1.47)	0.65	269	0.061
Precip.	Inc.	MAM	0.59(+0.01 -0.01)	11.91(+1.46 -1.46)	0.64	269	0.061
Precip.	Org.	ALL	0.49(+0.01 -0.01)	6.20(+0.45 -0.45)	0.63	1111	0.049
Precip.	Dec.	ALL	0.51(+0.01 -0.01)	7.35(+0.46 -0.46)	0.64	1111	0.049
Precip.	Inc.	ALL	0.48(+0.01 -0.01)	5.47(+0.45 -0.45)	0.62	1111	0.049

Table B3. The effect on latent heat after changes in different land surface scheme parameters. The column header information is given on page: *Appendix B-1*.

Id	Change	Period	p1(+ -)	p2(+ -)	R²	No	%
C2	Org.	JJA	0.74(+0.02 -0.02)	29.58(+2.14 -2.14)	0.44	385	0.059
C2	Dec.	JJA	0.76(+0.02 -0.02)	28.02(+2.20 -2.20)	0.43	385	0.059
C2	Inc.	JJA	0.72(+0.02 -0.02)	31.27(+2.10 -2.10)	0.43	386	0.059
C2	Org.	SON	0.60(+0.02 -0.02)	4.58(+0.86 -0.86)	0.35	249	0.038
C2	Dec.	SON	0.62(+0.02 -0.02)	4.22(+0.87 -0.87)	0.36	249	0.038
C2	Inc.	SON	0.59(+0.02 -0.02)	4.98(+0.85 -0.85)	0.34	249	0.038
C2	Org.	DJF	0.38(+0.03 -0.03)	-0.47(+0.31 -0.31)	0.14	279	0.055
C2	Dec.	DJF	0.40(+0.03 -0.03)	-0.52(+0.31 -0.31)	0.15	279	0.055
C2	Inc.	DJF	0.36(+0.03 -0.03)	-0.40(+0.31 -0.31)	0.13	279	0.055
C2	Org.	MAM	0.37(+0.02 -0.02)	6.47(+1.44 -1.44)	0.18	277	0.063
C2	Dec.	MAM	0.36(+0.02 -0.02)	6.31(+1.44 -1.44)	0.17	277	0.063
C2	Inc.	MAM	0.36(+0.02 -0.02)	6.88(+1.45 -1.45)	0.17	277	0.063
C2	Org.	ALL	0.75(+0.01 -0.01)	7.38(+0.70 -0.70)	0.46	1190	0.053
C2	Dec.	ALL	0.76(+0.01 -0.01)	6.87(+0.72 -0.72)	0.46	1190	0.053
C2	Inc.	ALL	0.74(+0.01 -0.01)	7.96(+0.70 -0.70)	0.46	1191	0.053
WpFc	Org.	JJA	0.74(+0.02 -0.02)	29.58(+2.14 -2.14)	0.44	385	0.059
WpFc	Dec.	JJA	0.73(+0.02 -0.02)	26.86(+2.14 -2.14)	0.43	385	0.059
WpFc	Inc.	JJA	0.74(+0.02 -0.02)	30.93(+2.12 -2.12)	0.44	385	0.059
WpFc	Org.	SON	0.60(+0.02 -0.02)	4.58(+0.86 -0.86)	0.35	249	0.038
WpFc	Dec.	SON	0.61(+0.02 -0.02)	4.02(+0.87 -0.87)	0.35	249	0.038
WpFc	Inc.	SON	0.61(+0.02 -0.02)	5.42(+0.87 -0.87)	0.35	249	0.038
WpFc	Org.	DJF	0.38(+0.03 -0.03)	-0.47(+0.31 -0.31)	0.14	279	0.055
WpFc	Dec.	DJF	0.38(+0.03 -0.03)	-0.79(+0.30 -0.30)	0.14	279	0.055
WpFc	Inc.	DJF	0.38(+0.03 -0.03)	-0.08(+0.31 -0.31)	0.14	279	0.055
WpFc	Org.	MAM	0.37(+0.02 -0.02)	6.47(+1.44 -1.44)	0.18	277	0.063
WpFc	Dec.	MAM	0.38(+0.02 -0.02)	6.56(+1.45 -1.45)	0.18	277	0.063
WpFc	Inc.	MAM	0.36(+0.02 -0.02)	6.18(+1.43 -1.43)	0.17	277	0.063
WpFc	Org.	ALL	0.75(+0.01 -0.01)	7.38(+0.70 -0.70)	0.46	1190	0.053
WpFc	Dec.	ALL	0.74(+0.01 -0.01)	6.63(+0.70 -0.70)	0.46	1190	0.053
WpFc	Inc.	ALL	0.75(+0.01 -0.01)	7.94(+0.70 -0.70)	0.47	1190	0.053
d	Org.	JJA	0.74(+0.02 -0.02)	29.58(+2.14 -2.14)	0.44	385	0.059
d	Dec.	JJA	0.78(+0.02 -0.02)	29.90(+2.34 -2.34)	0.42	386	0.059
d	Inc.	JJA	0.73(+0.02 -0.02)	19.70(+1.77 -1.77)	0.53	370	0.057
d	Org.	SON	0.60(+0.02 -0.02)	4.58(+0.86 -0.86)	0.35	249	0.038
d	Dec.	SON	0.62(+0.02 -0.02)	4.77(+0.94 -0.94)	0.32	249	0.038
d	Inc.	SON	0.58(+0.01 -0.01)	1.79(+0.61 -0.61)	0.49	249	0.038
d	Org.	DJF	0.38(+0.03 -0.03)	-0.47(+0.31 -0.31)	0.14	279	0.055
d	Dec.	DJF	0.40(+0.03 -0.03)	-0.46(+0.32 -0.32)	0.14	279	0.055
d	Inc.	DJF	0.30(+0.02 -0.02)	-1.18(+0.23 -0.23)	0.16	282	0.055
d	Org.	MAM	0.37(+0.02 -0.02)	6.47(+1.44 -1.44)	0.18	277	0.063
d	Dec.	MAM	0.40(+0.02 -0.02)	7.87(+1.45 -1.45)	0.2	278	0.063
d	Inc.	MAM	0.36(+0.02 -0.02)	2.01(+1.15 -1.15)	0.25	274	0.062
d	Org.	ALL	0.75(+0.01 -0.01)	7.38(+0.70 -0.70)	0.46	1190	0.053
d	Dec.	ALL	0.79(+0.01 -0.01)	7.72(+0.75 -0.75)	0.45	1192	0.053
d	Inc.	ALL	0.72(+0.01 -0.01)	3.39(+0.57 -0.57)	0.54	1175	0.052
z0	Org.	JJA	0.74(+0.02 -0.02)	29.58(+2.14 -2.14)	0.44	385	0.059
z0	Dec.	JJA	0.74(+0.02 -0.02)	27.91(+2.11 -2.11)	0.44	386	0.059

Id	Change	Period	p1(+ -)	p2(+ -)	R^2	No	%
z0	Inc.	JJA	0.74(+0.02 -0.02)	30.96(+2.13 -2.13)	0.44	385	0.059
z0	Org.	SON	0.60(+0.02 -0.02)	4.58(+0.86 -0.86)	0.35	249	0.038
z0	Dec.	SON	0.60(+0.02 -0.02)	4.15(+0.84 -0.84)	0.36	249	0.038
z0	Inc.	SON	0.61(+0.02 -0.02)	4.99(+0.88 -0.88)	0.34	249	0.038
z0	Org.	DJF	0.38(+0.03 -0.03)	-0.47(+0.31 -0.31)	0.14	279	0.055
z0	Dec.	DJF	0.37(+0.03 -0.03)	-0.53(+0.29 -0.29)	0.15	279	0.055
z0	Inc.	DJF	0.39(+0.03 -0.03)	-0.37(+0.33 -0.33)	0.14	279	0.055
z0	Org.	MAM	0.37(+0.02 -0.02)	6.47(+1.44 -1.44)	0.18	277	0.063
z0	Dec.	MAM	0.36(+0.02 -0.02)	5.87(+1.43 -1.43)	0.18	277	0.063
z0	Inc.	MAM	0.37(+0.02 -0.02)	7.11(+1.44 -1.44)	0.18	277	0.063
z0	Org.	ALL	0.75(+0.01 -0.01)	7.38(+0.70 -0.70)	0.46	1190	0.053
z0	Dec.	ALL	0.75(+0.01 -0.01)	6.74(+0.69 -0.69)	0.47	1191	0.053
z0	Inc.	ALL	0.75(+0.01 -0.01)	7.95(+0.71 -0.71)	0.46	1190	0.053
zrsforc	Org.	JJA	0.74(+0.02 -0.02)	29.58(+2.14 -2.14)	0.44	385	0.059
zrsforc	Dec.	JJA	0.74(+0.02 -0.02)	29.58(+2.14 -2.14)	0.44	385	0.059
zrsforc	Inc.	JJA	0.74(+0.02 -0.02)	29.58(+2.14 -2.14)	0.44	385	0.059
zrsforc	Org.	SON	0.60(+0.02 -0.02)	4.58(+0.86 -0.86)	0.35	249	0.038
zrsforc	Dec.	SON	0.60(+0.02 -0.02)	4.58(+0.86 -0.86)	0.35	249	0.038
zrsforc	Inc.	SON	0.60(+0.02 -0.02)	4.58(+0.86 -0.86)	0.35	249	0.038
zrsforc	Org.	DJF	0.38(+0.03 -0.03)	-0.47(+0.31 -0.31)	0.14	279	0.055
zrsforc	Dec.	DJF	0.38(+0.03 -0.03)	-0.47(+0.31 -0.31)	0.14	279	0.055
zrsforc	Inc.	DJF	0.38(+0.03 -0.03)	-0.47(+0.31 -0.31)	0.14	279	0.055
zrsforc	Org.	MAM	0.37(+0.02 -0.02)	6.47(+1.44 -1.44)	0.18	277	0.063
zrsforc	Dec.	MAM	0.37(+0.02 -0.02)	6.47(+1.44 -1.44)	0.18	277	0.063
zrsforc	Inc.	MAM	0.37(+0.02 -0.02)	6.47(+1.44 -1.44)	0.18	277	0.063
zrsforc	Org.	ALL	0.75(+0.01 -0.01)	7.38(+0.70 -0.70)	0.46	1190	0.053
zrsforc	Dec.	ALL	0.75(+0.01 -0.01)	7.38(+0.70 -0.70)	0.46	1190	0.053
zrsforc	Inc.	ALL	0.75(+0.01 -0.01)	7.38(+0.70 -0.70)	0.46	1190	0.053
zvegmax	Org.	JJA	0.74(+0.02 -0.02)	29.58(+2.14 -2.14)	0.44	385	0.059
zvegmax	Dec.	JJA	0.75(+0.02 -0.02)	29.78(+2.21 -2.21)	0.43	385	0.059
zvegmax	Inc.	JJA	0.73(+0.02 -0.02)	29.32(+2.12 -2.12)	0.44	384	0.059
zvegmax	Org.	SON	0.60(+0.02 -0.02)	4.58(+0.86 -0.86)	0.35	249	0.038
zvegmax	Dec.	SON	0.62(+0.02 -0.02)	4.80(+0.89 -0.89)	0.35	249	0.038
zvegmax	Inc.	SON	0.59(+0.02 -0.02)	4.39(+0.84 -0.84)	0.35	249	0.038
zvegmax	Org.	DJF	0.38(+0.03 -0.03)	-0.47(+0.31 -0.31)	0.14	279	0.055
zvegmax	Dec.	DJF	0.41(+0.03 -0.03)	-0.33(+0.32 -0.32)	0.15	279	0.055
zvegmax	Inc.	DJF	0.36(+0.03 -0.03)	-0.59(+0.30 -0.30)	0.14	279	0.055
zvegmax	Org.	MAM	0.37(+0.02 -0.02)	6.47(+1.44 -1.44)	0.18	277	0.063
zvegmax	Dec.	MAM	0.38(+0.02 -0.02)	6.76(+1.49 -1.49)	0.18	277	0.063
zvegmax	Inc.	MAM	0.35(+0.02 -0.02)	6.50(+1.49 -1.49)	0.16	276	0.063
zvegmax	Org.	ALL	0.75(+0.01 -0.01)	7.38(+0.70 -0.70)	0.46	1190	0.053
zvegmax	Dec.	ALL	0.76(+0.01 -0.01)	7.60(+0.72 -0.72)	0.46	1190	0.053
zvegmax	Inc.	ALL	0.74(+0.01 -0.01)	7.20(+0.70 -0.70)	0.46	1188	0.053
LAI	Org.	JJA	0.74(+0.02 -0.02)	29.58(+2.14 -2.14)	0.44	385	0.059
LAI_4.5	Inc.	JJA	0.77(+0.02 -0.02)	28.78(+2.14 -2.14)	0.46	385	0.059
LAI_5.0	Inc.	JJA	0.81(+0.02 -0.02)	28.18(+2.20 -2.20)	0.47	384	0.059
LAI	Org.	SON	0.60(+0.02 -0.02)	4.58(+0.86 -0.86)	0.35	249	0.038
LAI_4.5	Inc.	SON	0.62(+0.02 -0.02)	4.46(+0.85 -0.85)	0.37	249	0.038
LAI_5.0	Inc.	SON	0.64(+0.02 -0.02)	4.45(+0.85 -0.85)	0.38	249	0.038
LAI	Org.	DJF	0.38(+0.03 -0.03)	-0.47(+0.31 -0.31)	0.14	279	0.055

Id	Change	Period	p1(+ -)	p2(+ -)	R^2	No	%
LAI_4.5	Inc.	DJF	0.40(+0.03 -0.03)	-0.41(+0.32 -0.32)	0.14	279	0.055
LAI_5.0	Inc.	DJF	0.42(+0.03 -0.03)	-0.36(+0.33 -0.33)	0.15	279	0.055
LAI	Org.	MAM	0.37(+0.02 -0.02)	6.47(+1.44 -1.44)	0.18	277	0.063
LAI_4.5	Inc.	MAM	0.37(+0.02 -0.02)	5.93(+1.47 -1.47)	0.17	277	0.063
LAI_5.0	Inc.	MAM	0.38(+0.03 -0.03)	5.88(+1.58 -1.58)	0.16	276	0.063
LAI	Org.	ALL	0.75(+0.01 -0.01)	7.38(+0.70 -0.70)	0.46	1190	0.053
LAI_4.5	Inc.	ALL	0.78(+0.01 -0.01)	7.01(+0.71 -0.71)	0.48	1190	0.053
LAI_5.0	Inc.	ALL	0.81(+0.01 -0.01)	6.79(+0.73 -0.73)	0.48	1188	0.053

Table B4. The effect on sensible heat after changes in different land surface scheme parameters. The column header information is given on page: *Appendix B-1*.

Id	Change	Period	p1(+ -)	p2(+ -)	R²	No	%
C2	Org.	JJA	0.46(+0.01 -0.01)	7.54(+1.11 -1.11)	0.63	369	0.057
C2	Dec.	JJA	0.50(+0.01 -0.01)	8.08(+1.39 -1.39)	0.57	369	0.057
C2	Inc.	JJA	0.42(+0.01 -0.01)	9.02(+1.10 -1.10)	0.6	369	0.057
C2	Org.	SON	0.34(+0.01 -0.01)	0.90(+0.53 -0.53)	0.37	247	0.038
C2	Dec.	SON	0.39(+0.01 -0.01)	1.78(+0.58 -0.58)	0.39	247	0.038
C2	Inc.	SON	0.30(+0.01 -0.01)	0.62(+0.54 -0.54)	0.31	247	0.038
C2	Org.	DJF	0.26(+0.02 -0.02)	-2.40(+0.62 -0.62)	0.18	226	0.044
C2	Dec.	DJF	0.27(+0.02 -0.02)	-2.02(+0.62 -0.62)	0.2	226	0.044
C2	Inc.	DJF	0.24(+0.02 -0.02)	-2.55(+0.64 -0.64)	0.16	226	0.044
C2	Org.	MAM	0.60(+0.01 -0.01)	12.60(+1.45 -1.45)	0.65	269	0.061
C2	Dec.	MAM	0.63(+0.02 -0.02)	13.13(+1.67 -1.67)	0.61	269	0.061
C2	Inc.	MAM	0.56(+0.01 -0.01)	13.39(+1.47 -1.47)	0.62	269	0.061
C2	Org.	ALL	0.49(+0.01 -0.01)	6.20(+0.45 -0.45)	0.63	1111	0.049
C2	Dec.	ALL	0.53(+0.01 -0.01)	6.92(+0.53 -0.53)	0.59	1111	0.049
C2	Inc.	ALL	0.46(+0.01 -0.01)	6.47(+0.46 -0.46)	0.6	1111	0.049
WpFc	Org.	JJA	0.46(+0.01 -0.01)	7.54(+1.11 -1.11)	0.63	369	0.057
WpFc	Dec.	JJA	0.50(+0.01 -0.01)	9.37(+1.18 -1.18)	0.65	369	0.057
WpFc	Inc.	JJA	0.41(+0.01 -0.01)	6.09(+1.06 -1.06)	0.61	369	0.057
WpFc	Org.	SON	0.34(+0.01 -0.01)	0.90(+0.53 -0.53)	0.37	247	0.038
WpFc	Dec.	SON	0.34(+0.01 -0.01)	0.52(+0.53 -0.53)	0.38	247	0.038
WpFc	Inc.	SON	0.33(+0.01 -0.01)	1.22(+0.53 -0.53)	0.36	247	0.038
WpFc	Org.	DJF	0.26(+0.02 -0.02)	-2.40(+0.62 -0.62)	0.18	226	0.044
WpFc	Dec.	DJF	0.25(+0.01 -0.01)	-3.35(+0.60 -0.60)	0.19	226	0.044
WpFc	Inc.	DJF	0.26(+0.02 -0.02)	-1.18(+0.65 -0.65)	0.17	226	0.044
WpFc	Org.	MAM	0.60(+0.01 -0.01)	12.60(+1.45 -1.45)	0.65	269	0.061
WpFc	Dec.	MAM	0.61(+0.01 -0.01)	13.35(+1.49 -1.49)	0.65	269	0.061
WpFc	Inc.	MAM	0.58(+0.01 -0.01)	11.82(+1.42 -1.42)	0.64	269	0.061
WpFc	Org.	ALL	0.49(+0.01 -0.01)	6.20(+0.45 -0.45)	0.63	1111	0.049
WpFc	Dec.	ALL	0.53(+0.01 -0.01)	6.89(+0.47 -0.47)	0.65	1111	0.049
WpFc	Inc.	ALL	0.46(+0.00 -0.00)	5.74(+0.44 -0.44)	0.61	1111	0.049
d	Org.	JJA	0.46(+0.01 -0.01)	7.54(+1.11 -1.11)	0.63	369	0.057
d	Dec.	JJA	0.44(+0.01 -0.01)	6.80(+1.18 -1.18)	0.59	369	0.057
d	Inc.	JJA	0.45(+0.01 -0.01)	9.84(+0.90 -0.90)	0.72	369	0.057
d	Org.	SON	0.34(+0.01 -0.01)	0.90(+0.53 -0.53)	0.37	247	0.038
d	Dec.	SON	0.34(+0.01 -0.01)	0.54(+0.55 -0.55)	0.35	247	0.038
d	Inc.	SON	0.35(+0.01 -0.01)	2.49(+0.41 -0.41)	0.51	247	0.038
d	Org.	DJF	0.26(+0.02 -0.02)	-2.40(+0.62 -0.62)	0.18	226	0.044
d	Dec.	DJF	0.26(+0.02 -0.02)	-2.51(+0.65 -0.65)	0.17	226	0.044
d	Inc.	DJF	0.27(+0.02 -0.02)	-1.90(+0.64 -0.64)	0.18	227	0.045
d	Org.	MAM	0.60(+0.01 -0.01)	12.60(+1.45 -1.45)	0.65	269	0.061
d	Dec.	MAM	0.57(+0.01 -0.01)	11.47(+1.48 -1.48)	0.62	269	0.061
d	Inc.	MAM	0.58(+0.01 -0.01)	13.52(+1.14 -1.14)	0.74	269	0.061
d	Org.	ALL	0.49(+0.01 -0.01)	6.20(+0.45 -0.45)	0.63	1111	0.049
d	Dec.	ALL	0.48(+0.01 -0.01)	5.51(+0.47 -0.47)	0.6	1111	0.049
d	Inc.	ALL	0.49(+0.00 -0.00)	7.39(+0.37 -0.37)	0.71	1112	0.049
z0	Org.	JJA	0.46(+0.01 -0.01)	7.54(+1.11 -1.11)	0.63	369	0.057

Id	Change	Period	p1(+ -)	p2(+ -)	R^2	No	%
z0	Dec.	JJA	0.45(+0.01 -0.01)	8.03(+1.08 -1.08)	0.65	369	0.057
z0	Inc.	JJA	0.45(+0.01 -0.01)	6.96(+1.14 -1.14)	0.62	369	0.057
z0	Org.	SON	0.34(+0.01 -0.01)	0.90(+0.53 -0.53)	0.37	247	0.038
z0	Dec.	SON	0.33(+0.01 -0.01)	1.48(+0.49 -0.49)	0.39	247	0.038
z0	Inc.	SON	0.35(+0.01 -0.01)	0.32(+0.56 -0.56)	0.35	247	0.038
z0	Org.	DJF	0.26(+0.02 -0.02)	-2.40(+0.62 -0.62)	0.18	226	0.044
z0	Dec.	DJF	0.24(+0.01 -0.01)	-2.07(+0.57 -0.57)	0.19	226	0.044
z0	Inc.	DJF	0.27(+0.02 -0.02)	-2.68(+0.66 -0.66)	0.18	226	0.044
z0	Org.	MAM	0.60(+0.01 -0.01)	12.60(+1.45 -1.45)	0.65	269	0.061
z0	Dec.	MAM	0.59(+0.01 -0.01)	12.85(+1.40 -1.40)	0.66	269	0.061
z0	Inc.	MAM	0.60(+0.01 -0.01)	12.30(+1.49 -1.49)	0.64	269	0.061
z0	Org.	ALL	0.49(+0.01 -0.01)	6.20(+0.45 -0.45)	0.63	1111	0.049
z0	Dec.	ALL	0.49(+0.00 -0.00)	6.80(+0.44 -0.44)	0.64	1111	0.049
z0	Inc.	ALL	0.49(+0.01 -0.01)	5.60(+0.47 -0.47)	0.62	1111	0.049
zrsforc	Org.	JJA	0.46(+0.01 -0.01)	7.54(+1.11 -1.11)	0.63	369	0.057
zrsforc	Dec.	JJA	0.46(+0.01 -0.01)	7.54(+1.11 -1.11)	0.63	369	0.057
zrsforc	Inc.	JJA	0.46(+0.01 -0.01)	7.54(+1.11 -1.11)	0.63	369	0.057
zrsforc	Org.	SON	0.34(+0.01 -0.01)	0.90(+0.53 -0.53)	0.37	247	0.038
zrsforc	Dec.	SON	0.34(+0.01 -0.01)	0.90(+0.53 -0.53)	0.37	247	0.038
zrsforc	Inc.	SON	0.34(+0.01 -0.01)	0.90(+0.53 -0.53)	0.37	247	0.038
zrsforc	Org.	DJF	0.26(+0.02 -0.02)	-2.40(+0.62 -0.62)	0.18	226	0.044
zrsforc	Dec.	DJF	0.26(+0.02 -0.02)	-2.40(+0.62 -0.62)	0.18	226	0.044
zrsforc	Inc.	DJF	0.26(+0.02 -0.02)	-2.40(+0.62 -0.62)	0.18	226	0.044
zrsforc	Org.	MAM	0.60(+0.01 -0.01)	12.60(+1.45 -1.45)	0.65	269	0.061
zrsforc	Dec.	MAM	0.60(+0.01 -0.01)	12.60(+1.45 -1.45)	0.65	269	0.061
zrsforc	Inc.	MAM	0.60(+0.01 -0.01)	12.60(+1.45 -1.45)	0.65	269	0.061
zrsforc	Org.	ALL	0.49(+0.01 -0.01)	6.20(+0.45 -0.45)	0.63	1111	0.049
zrsforc	Dec.	ALL	0.49(+0.01 -0.01)	6.20(+0.45 -0.45)	0.63	1111	0.049
zrsforc	Inc.	ALL	0.49(+0.01 -0.01)	6.20(+0.45 -0.45)	0.63	1111	0.049
zvegmax	Org.	JJA	0.46(+0.01 -0.01)	7.54(+1.11 -1.11)	0.63	369	0.057
zvegmax	Dec.	JJA	0.45(+0.01 -0.01)	7.18(+1.13 -1.13)	0.62	369	0.057
zvegmax	Inc.	JJA	0.46(+0.01 -0.01)	7.92(+1.11 -1.11)	0.64	369	0.057
zvegmax	Org.	SON	0.34(+0.01 -0.01)	0.90(+0.53 -0.53)	0.37	247	0.038
zvegmax	Dec.	SON	0.33(+0.01 -0.01)	0.43(+0.53 -0.53)	0.36	247	0.038
zvegmax	Inc.	SON	0.35(+0.01 -0.01)	1.27(+0.53 -0.53)	0.39	247	0.038
zvegmax	Org.	DJF	0.26(+0.02 -0.02)	-2.40(+0.62 -0.62)	0.18	226	0.044
zvegmax	Dec.	DJF	0.26(+0.02 -0.02)	-2.53(+0.62 -0.62)	0.18	226	0.044
zvegmax	Inc.	DJF	0.26(+0.02 -0.02)	-2.28(+0.62 -0.62)	0.18	226	0.044
zvegmax	Org.	MAM	0.60(+0.01 -0.01)	12.60(+1.45 -1.45)	0.65	269	0.061
zvegmax	Dec.	MAM	0.59(+0.01 -0.01)	12.29(+1.47 -1.47)	0.64	269	0.061
zvegmax	Inc.	MAM	0.60(+0.01 -0.01)	12.88(+1.44 -1.44)	0.65	269	0.061
zvegmax	Org.	ALL	0.49(+0.01 -0.01)	6.20(+0.45 -0.45)	0.63	1111	0.049
zvegmax	Dec.	ALL	0.49(+0.01 -0.01)	5.90(+0.46 -0.46)	0.62	1111	0.049
zvegmax	Inc.	ALL	0.50(+0.01 -0.01)	6.48(+0.45 -0.45)	0.63	1111	0.049
LAI	Org.	JJA	0.46(+0.01 -0.01)	7.54(+1.11 -1.11)	0.63	369	0.057
LAI_4.5	Inc.	JJA	0.45(+0.01 -0.01)	6.58(+1.11 -1.11)	0.62	369	0.057
LAI_5.0	Inc.	JJA	0.43(+0.01 -0.01)	5.74(+1.13 -1.13)	0.6	369	0.057
LAI	Org.	SON	0.34(+0.01 -0.01)	0.90(+0.53 -0.53)	0.37	247	0.038
LAI_4.5	Inc.	SON	0.34(+0.01 -0.01)	0.54(+0.53 -0.53)	0.37	247	0.038
LAI_5.0	Inc.	SON	0.33(+0.01 -0.01)	0.14(+0.52 -0.52)	0.36	247	0.038

Id	Change	Period	p1(+ -)	p2(+ -)	R^2	No	%
LAI	Org.	DJF	0.26(+0.02 -0.02)	-2.40(+0.62 -0.62)	0.18	226	0.044
LAI_4.5	Inc.	DJF	0.26(+0.02 -0.02)	-2.41(+0.62 -0.62)	0.19	226	0.044
LAI_5.0	Inc.	DJF	0.26(+0.02 -0.02)	-2.47(+0.62 -0.62)	0.19	226	0.044
LAI	Org.	MAM	0.60(+0.01 -0.01)	12.60(+1.45 -1.45)	0.65	269	0.061
LAI_4.5	Inc.	MAM	0.62(+0.01 -0.01)	12.74(+1.50 -1.50)	0.65	269	0.061
LAI_5.0	Inc.	MAM	0.63(+0.01 -0.01)	12.68(+1.52 -1.52)	0.65	269	0.061
LAI	Org.	ALL	0.49(+0.01 -0.01)	6.20(+0.45 -0.45)	0.63	1111	0.049
LAI_4.5	Inc.	ALL	0.49(+0.01 -0.01)	5.86(+0.46 -0.46)	0.62	1111	0.049
LAI_5.0	Inc.	ALL	0.49(+0.01 -0.01)	5.46(+0.47 -0.47)	0.61	1111	0.049

Appendix C: Figures for Norunda and Cabauw

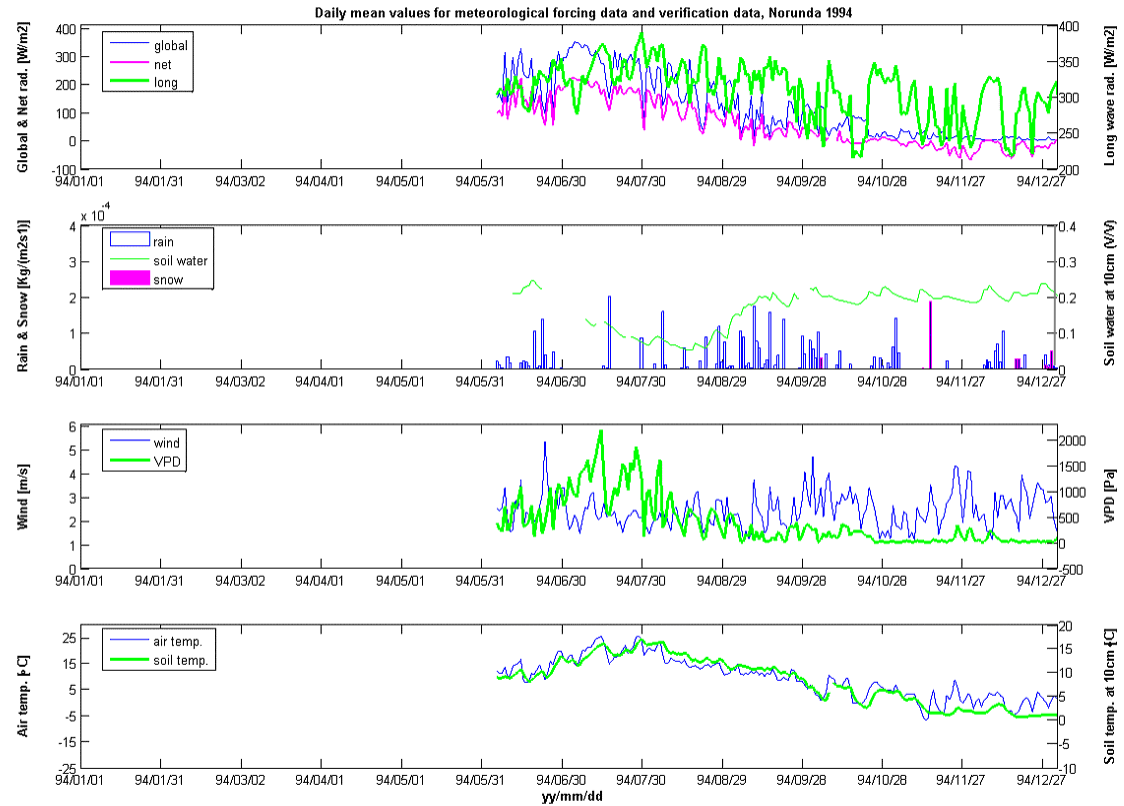


Figure C1. Daily averages of driving- and verification data at Norunda 1994. From top to bottom: global (blue)- net (magenta)- and long wave (green)- radiation, rain (blue)- and snow (magenta)- bars and soil water (green) at 10 cm depth, wind (blue) and VPD (green), air temperature (blue) and soil temperature (green) at 10 cm.

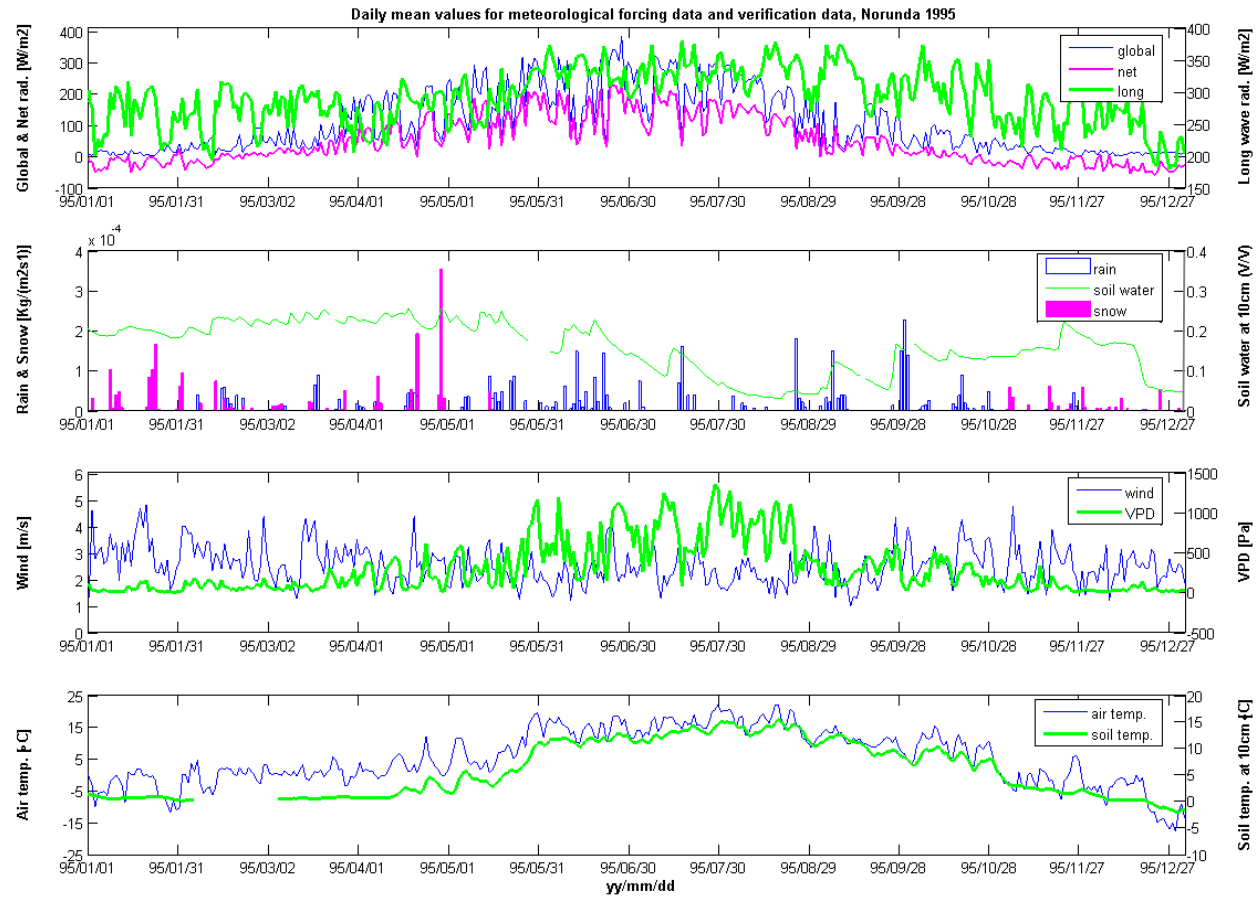


Figure C2. Daily averages of driving- and verification data at Norunda 1995. From top to bottom: global (blue)- net (magenta)- and long wave (green)- radiation, rain (blue)- and snow (magenta)- bars and soil water (green) at 10 cm depth, wind (blue) and VPD (green), air temperature (blue) and soil temperature (green) at 10 cm.

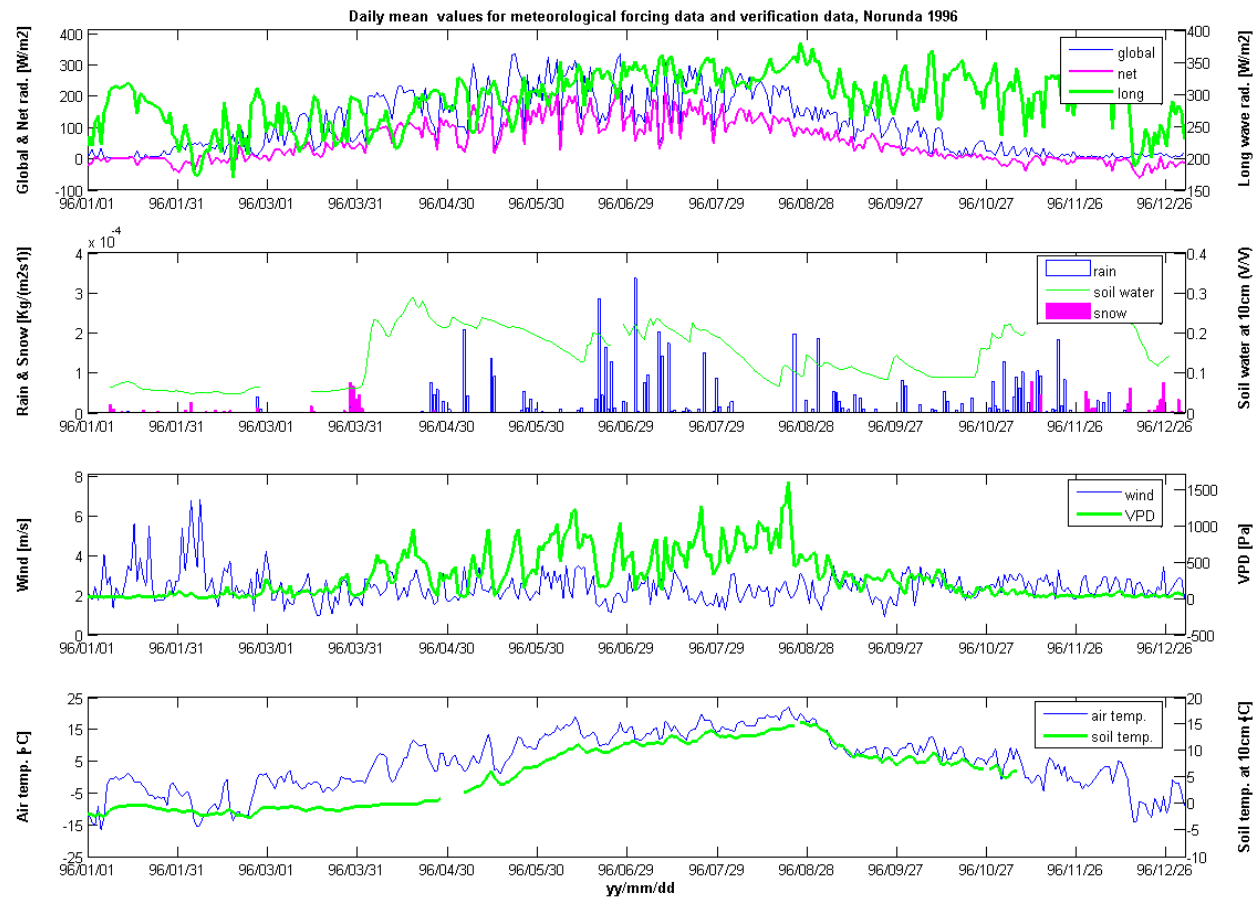


Figure C3. Daily averages of driving- and verification data at Norunda 1996. From top to bottom: global (blue)- net (magenta)- and long wave (green)- radiation, rain (blue)- and snow (magenta)- bars and soil water (green) at 10 cm depth, wind (blue) and VPD (green), air temperature (blue) and soil temperature (green) at 10 cm.

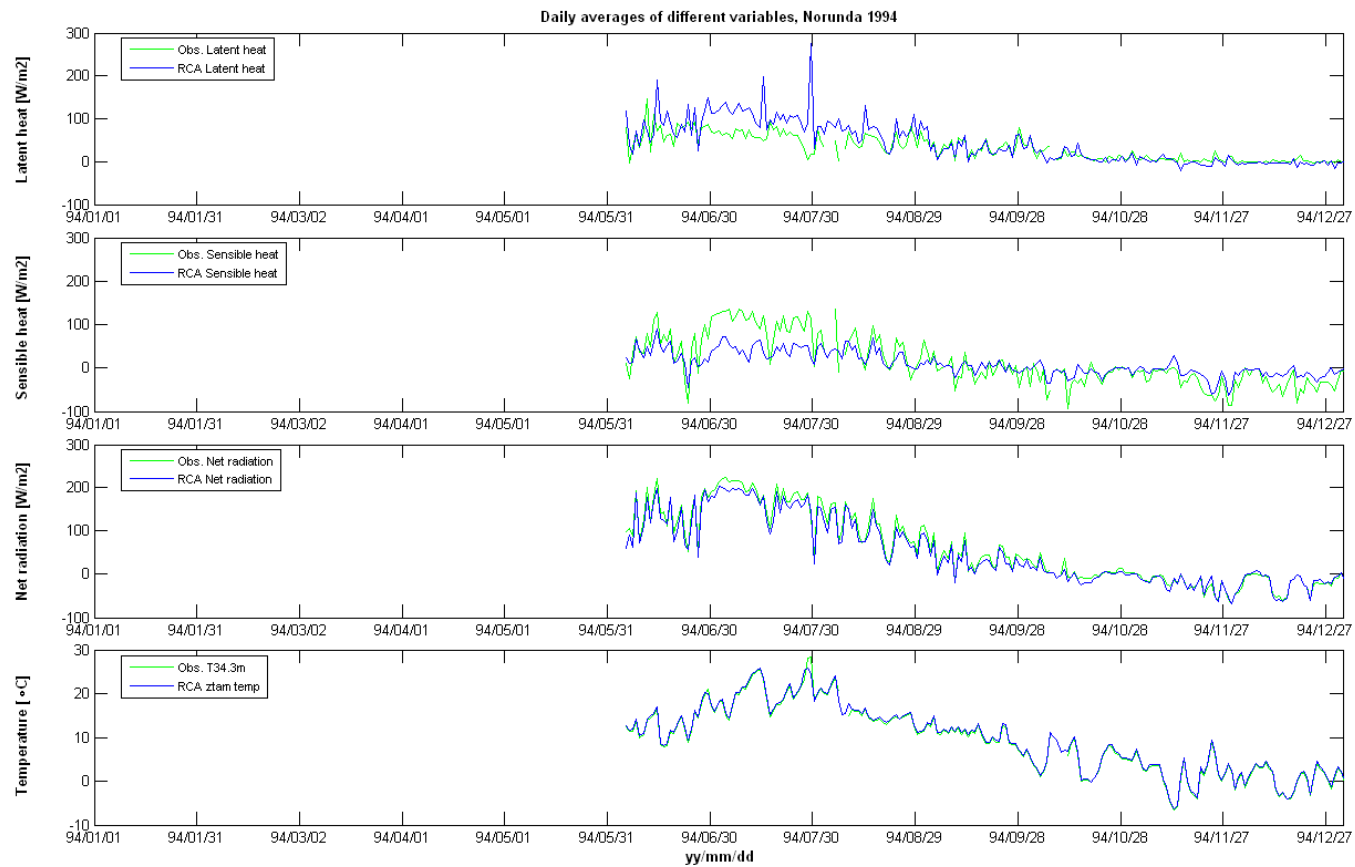


Figure C4. Daily averages for different variables at Norunda 1994. From top to bottom: Latent heat, Sensible heat, Net radiation and temperature at the reference level (ztam). Green lines are observations and blue lines are modelled values.

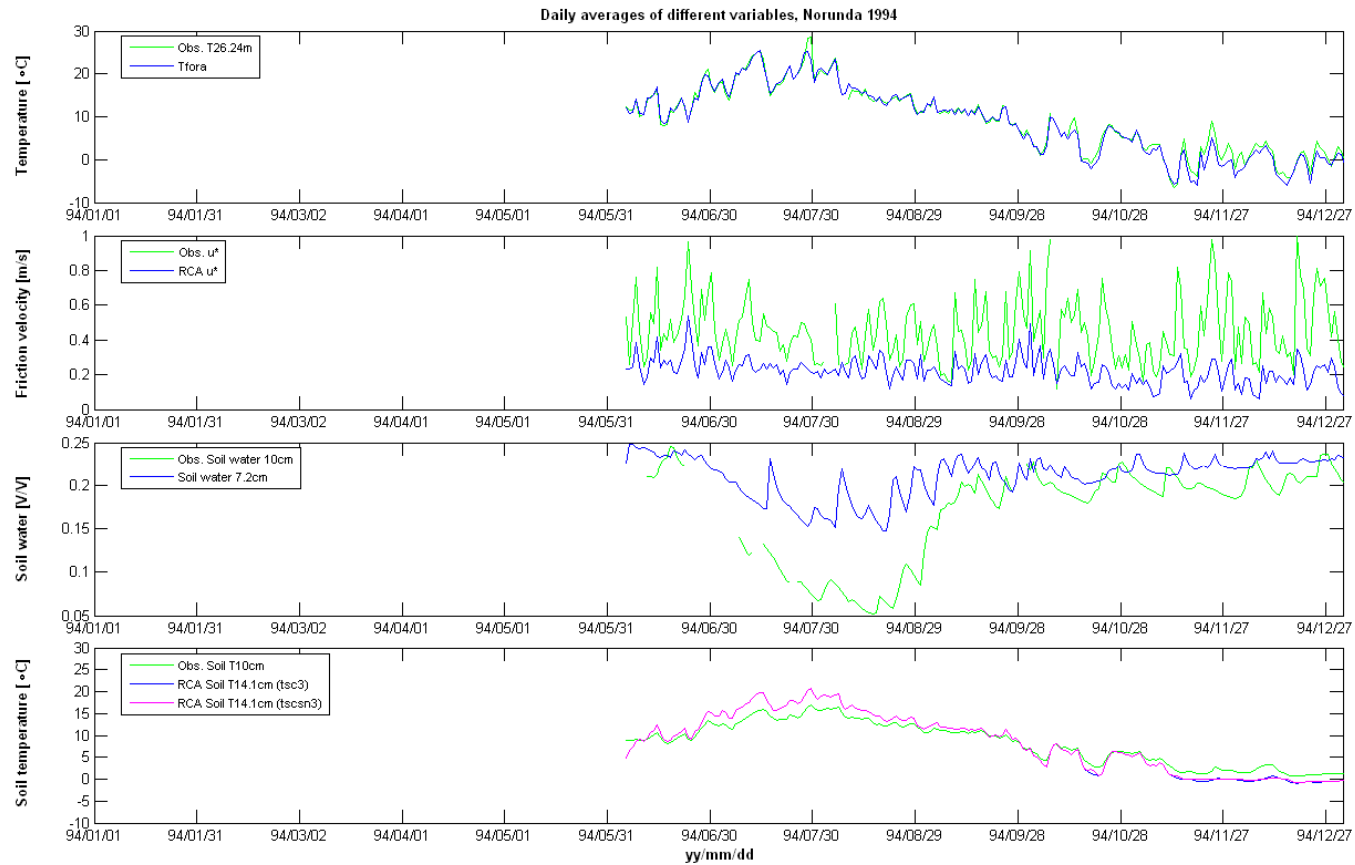


Figure C5. Daily averages for different variables at Norunda 1994. From top to bottom: canopy temperature (tfora), friction velocity, top soil water, third layer soil temperature without snow (blue) and with snow (magenta). All observations are green.

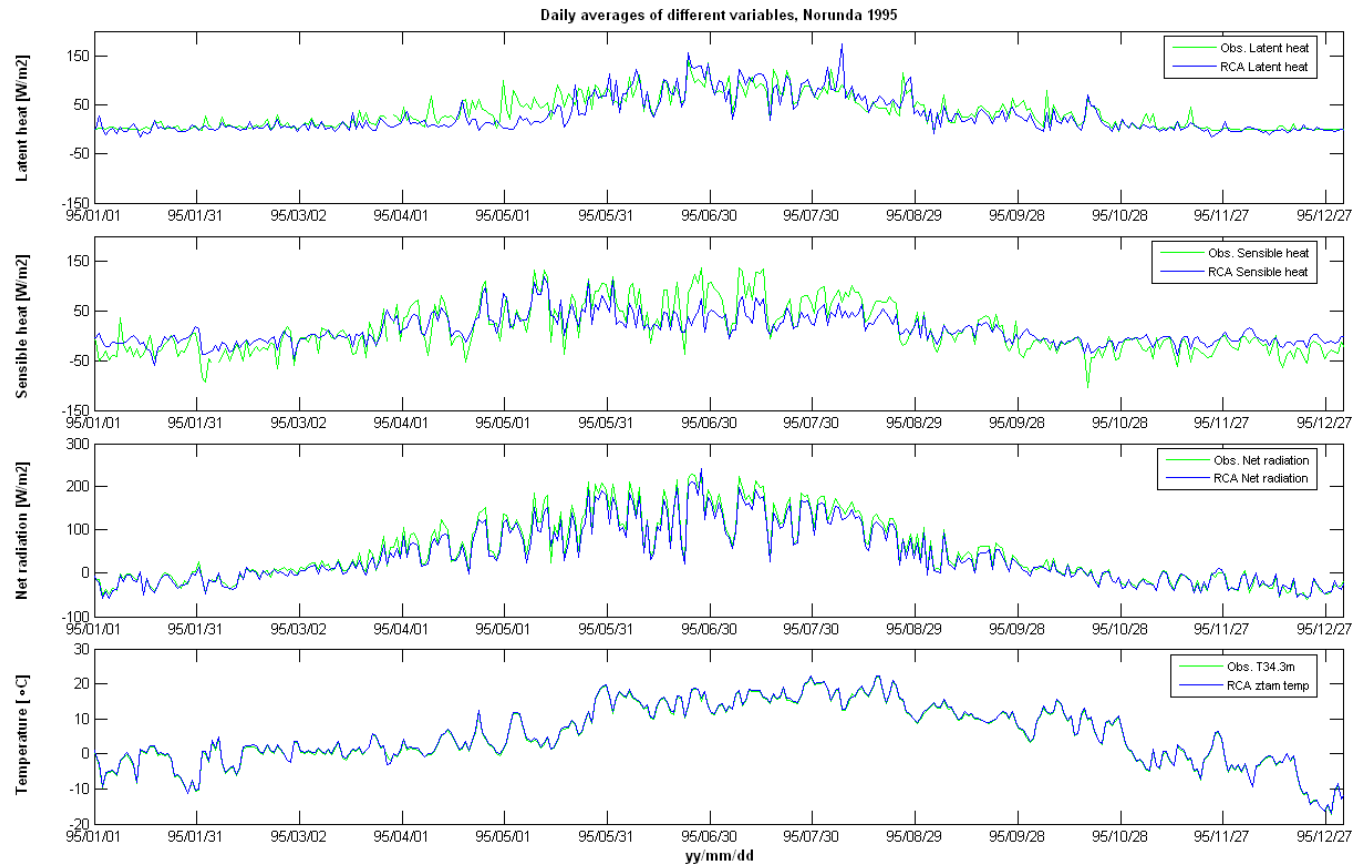


Figure C6. Daily averages for different variables at Norunda 1995. From top to bottom: Latent heat, Sensible heat, Net radiation and temperature at the reference level (ztam). Green lines are observations and blue lines are modelled values.

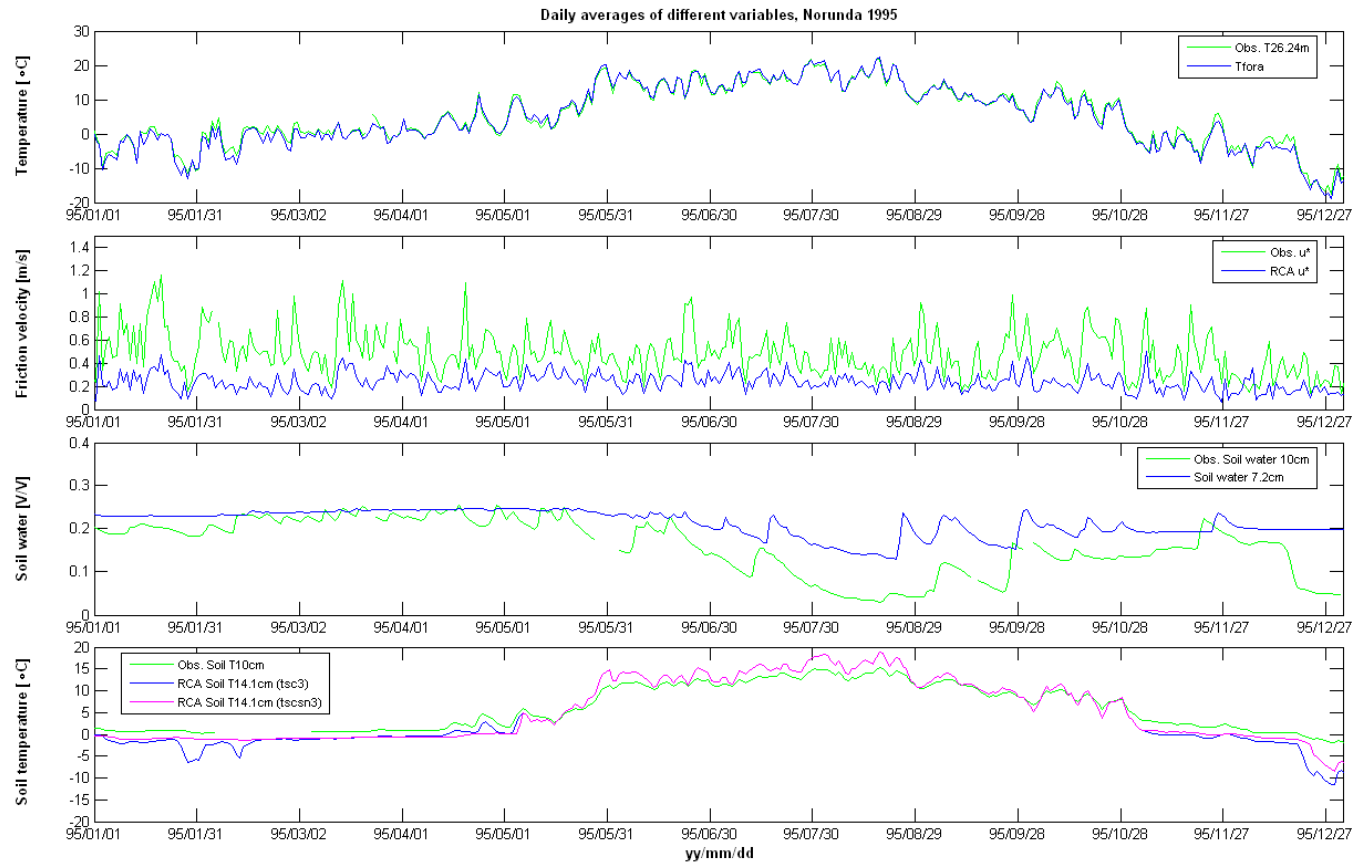


Figure C7. Daily averages for different variables at Norunda 1995. From top to bottom: canopy temperature (tfora), friction velocity, top soil water, third layer soil temperature without snow (blue) and with snow (magenta). All observations are green.

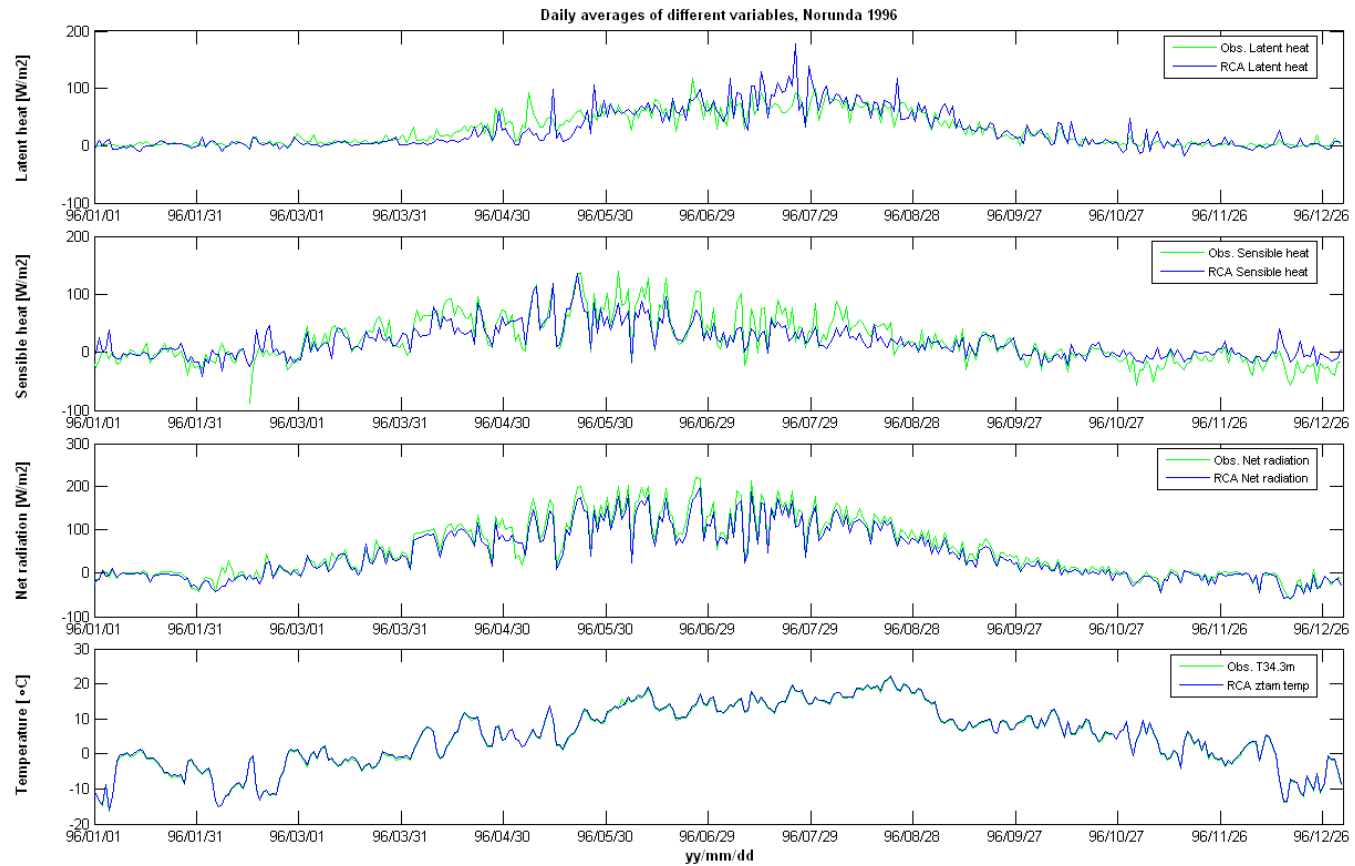


Figure C8. Daily averages for different variables at Norunda 1994. From top to bottom: Latent heat, Sensible heat, Net radiation and temperature at the reference level (ztam). Green lines are observations and blue lines are modelled values.

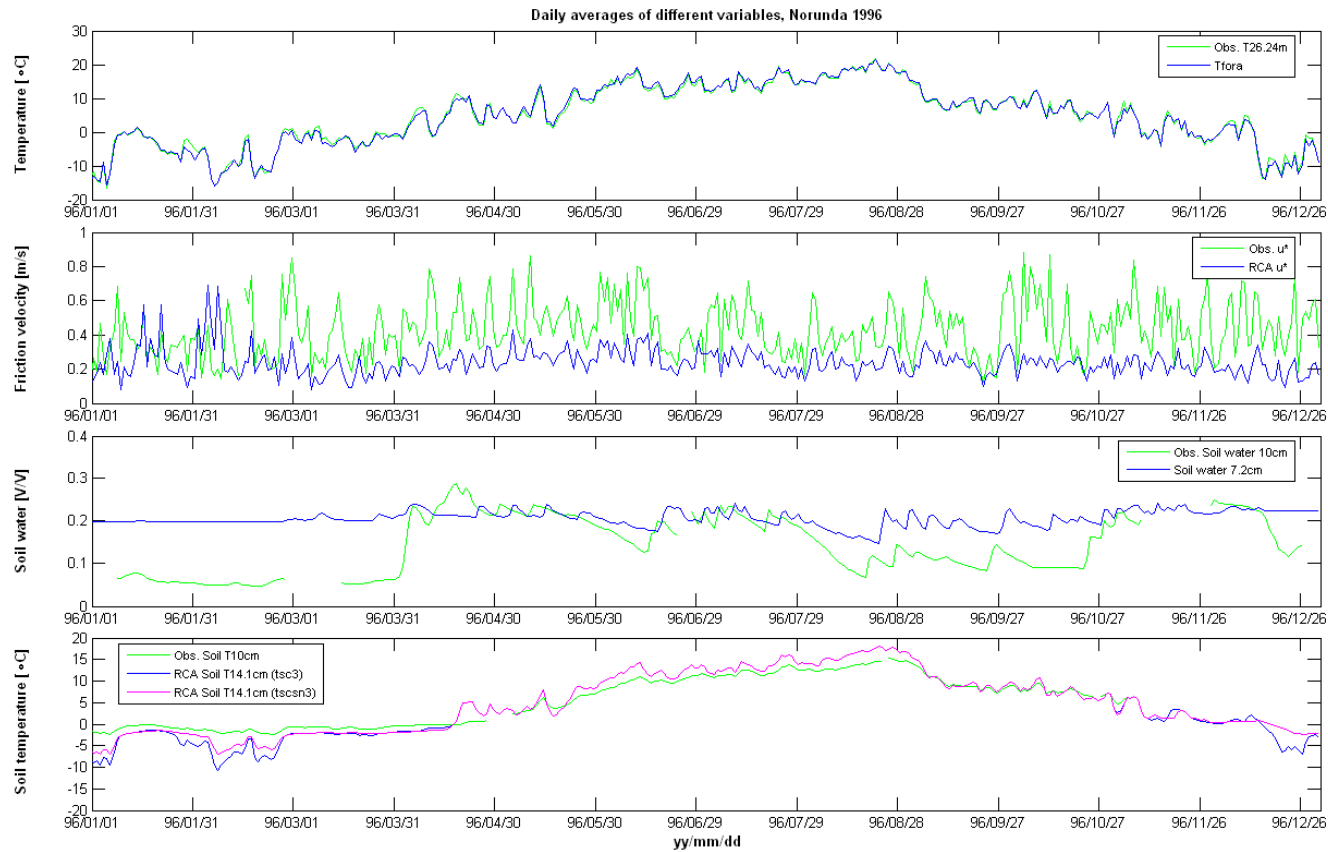


Figure C9. Daily averages for different variables at Norunda 1996. From top to bottom: canopy temperature (tfora), friction velocity, top soil water, third layer soil temperature without snow (blue) and with snow (magenta). All observations are green.

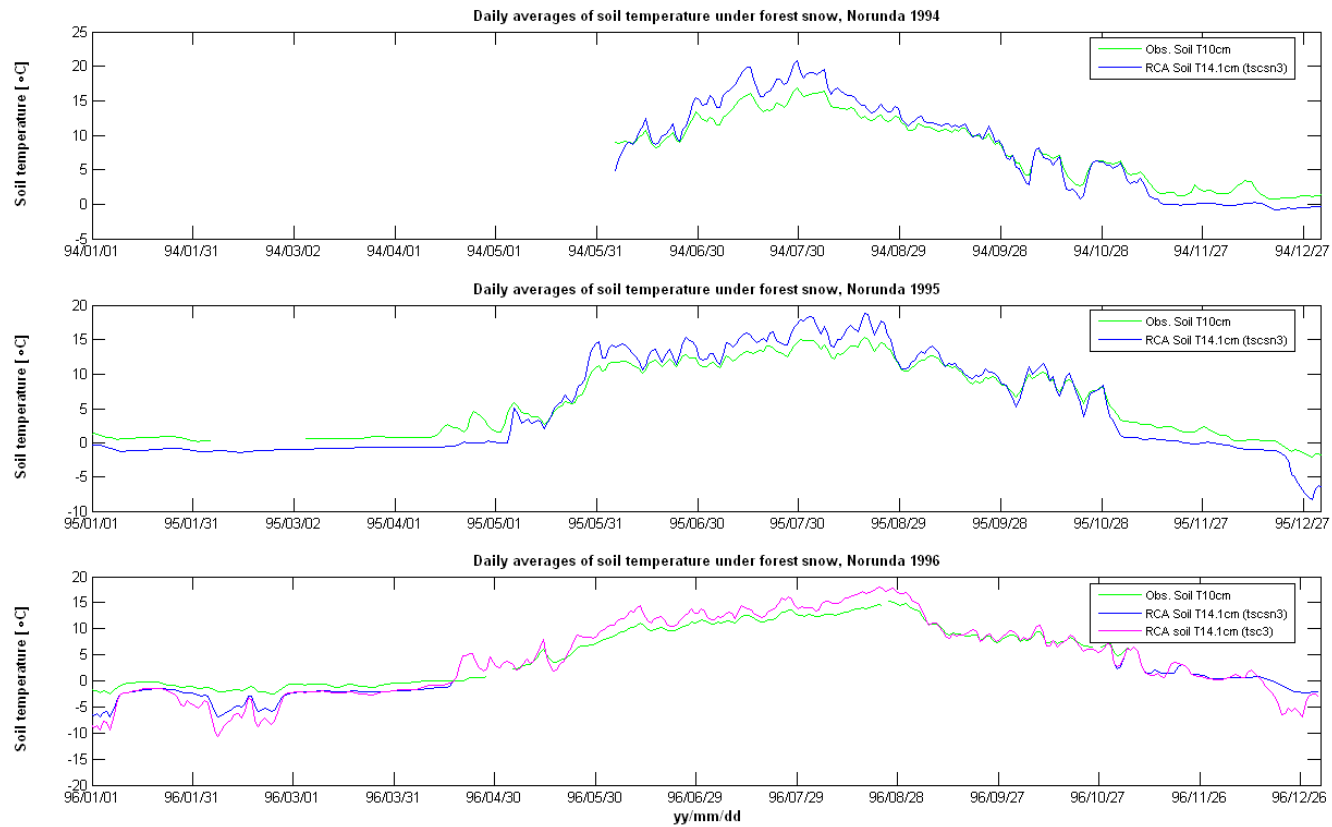


Figure C10. Daily averages for third layer soil temperatures at Norunda. From top to bottom: 1994 with snow, 1995 with snow, 1996 with snow (blue) and without snow (magenta). All observations are green

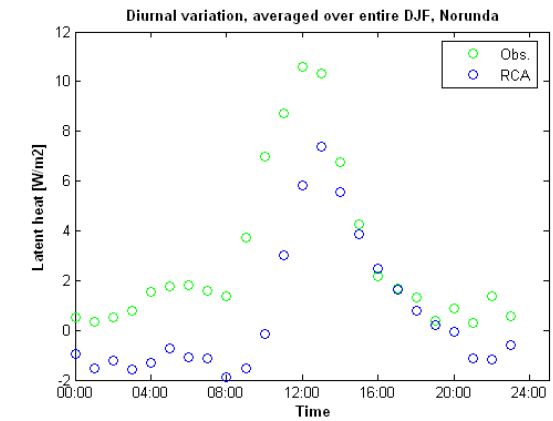
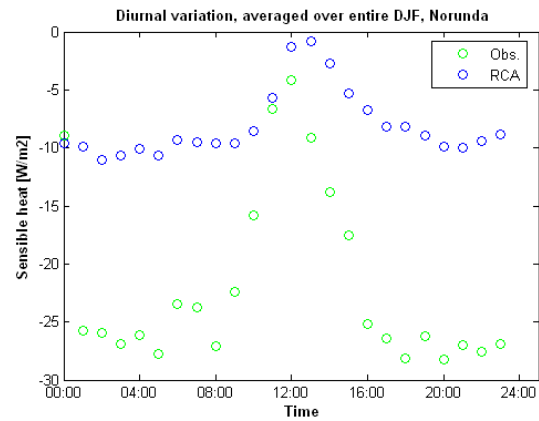
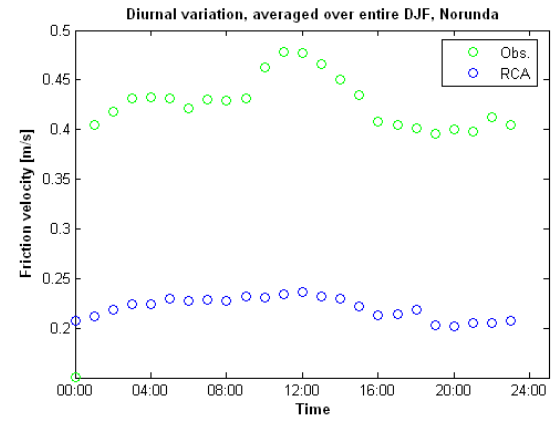
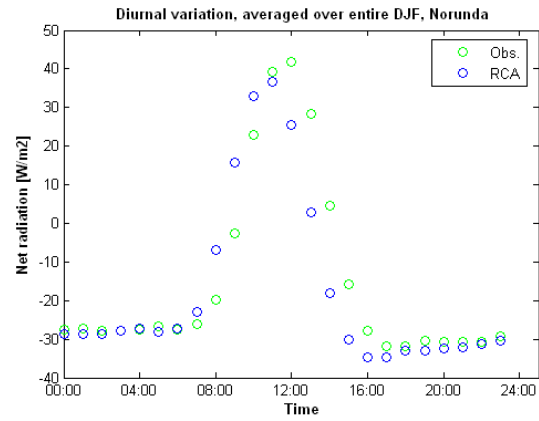


Figure C11. Diurnal variation for different variables at Norunda during DJF 1994-96. Top left: Net radiation. Top right: Friction velocity. Bottom left: Sensible heat. Bottom right: Latent heat. Modelled values are blue and observations are green.

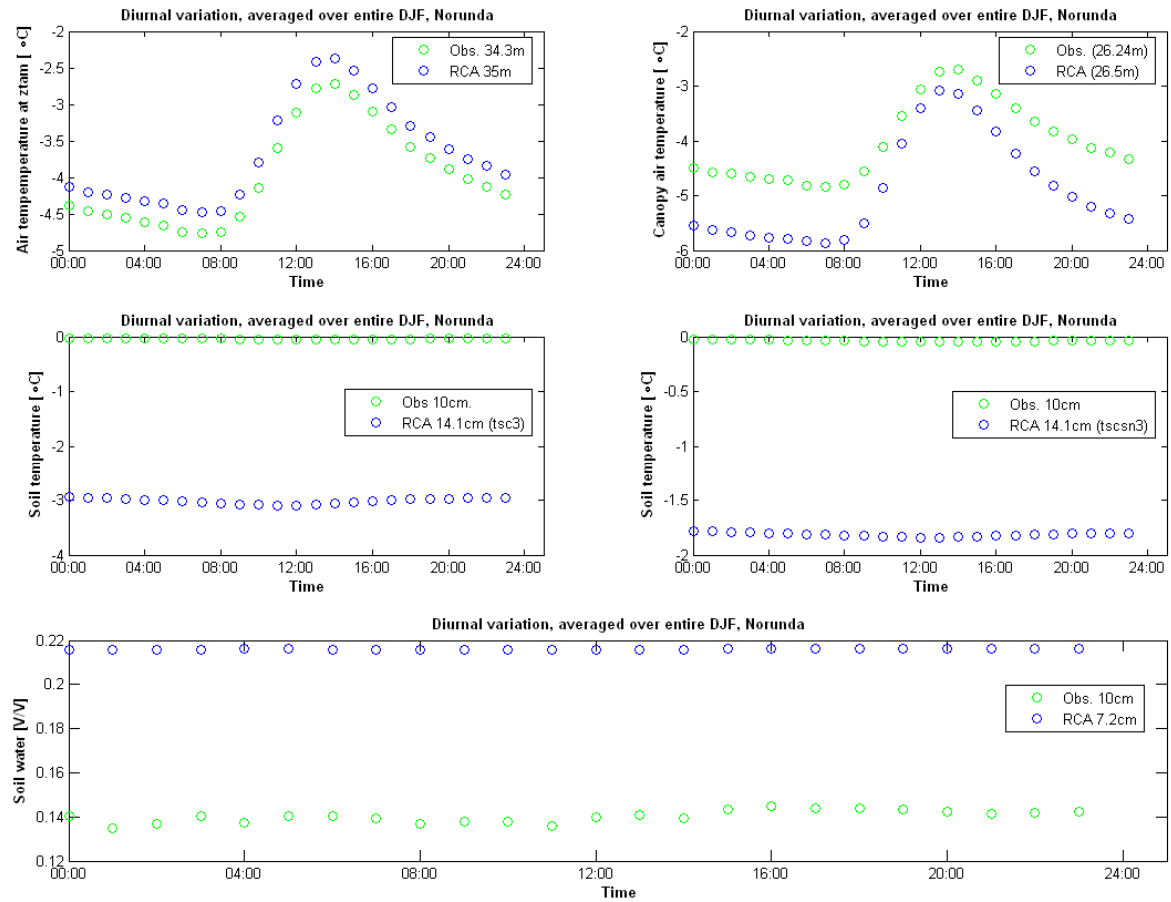


Figure C12 Diurnal variation for different variables at Norunda during DJF 1994-96. Top left: Air temperature at reference level (z_{tram}). Top right: Canopy air temperature. Middle left: third layer soil temperature without snow. Middle right: third layer soil temperature with snow. Bottom: top soil water.

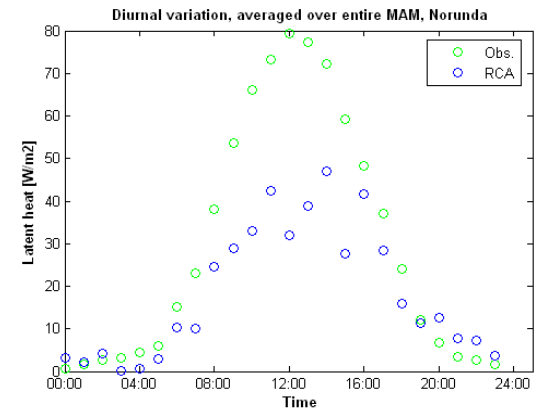
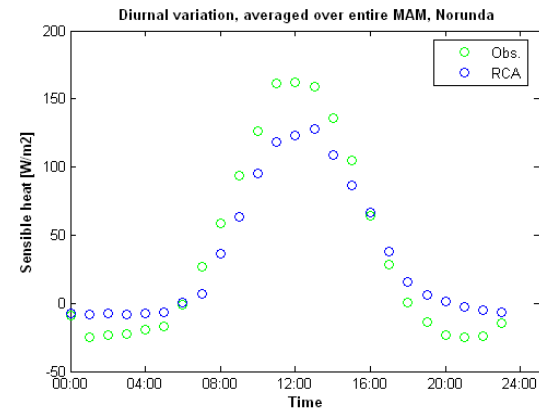
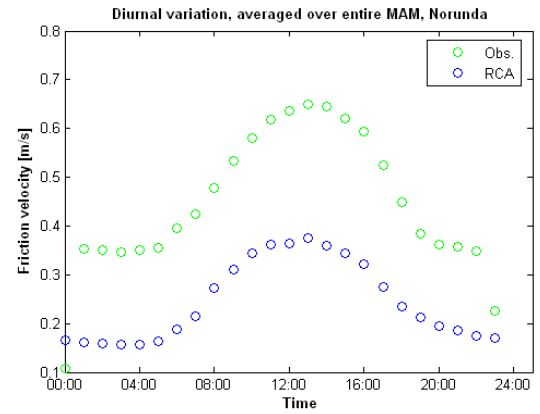
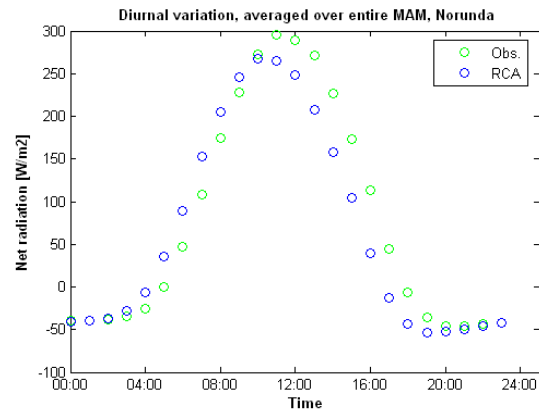


Figure C13. Diurnal variation for different variables at Norunda during MAM 1994-96. Top left: Net radiation. Top right: Friction velocity. Bottom left: Sensible heat. Bottom right: Latent heat. Modelled values are blue and observations are green.

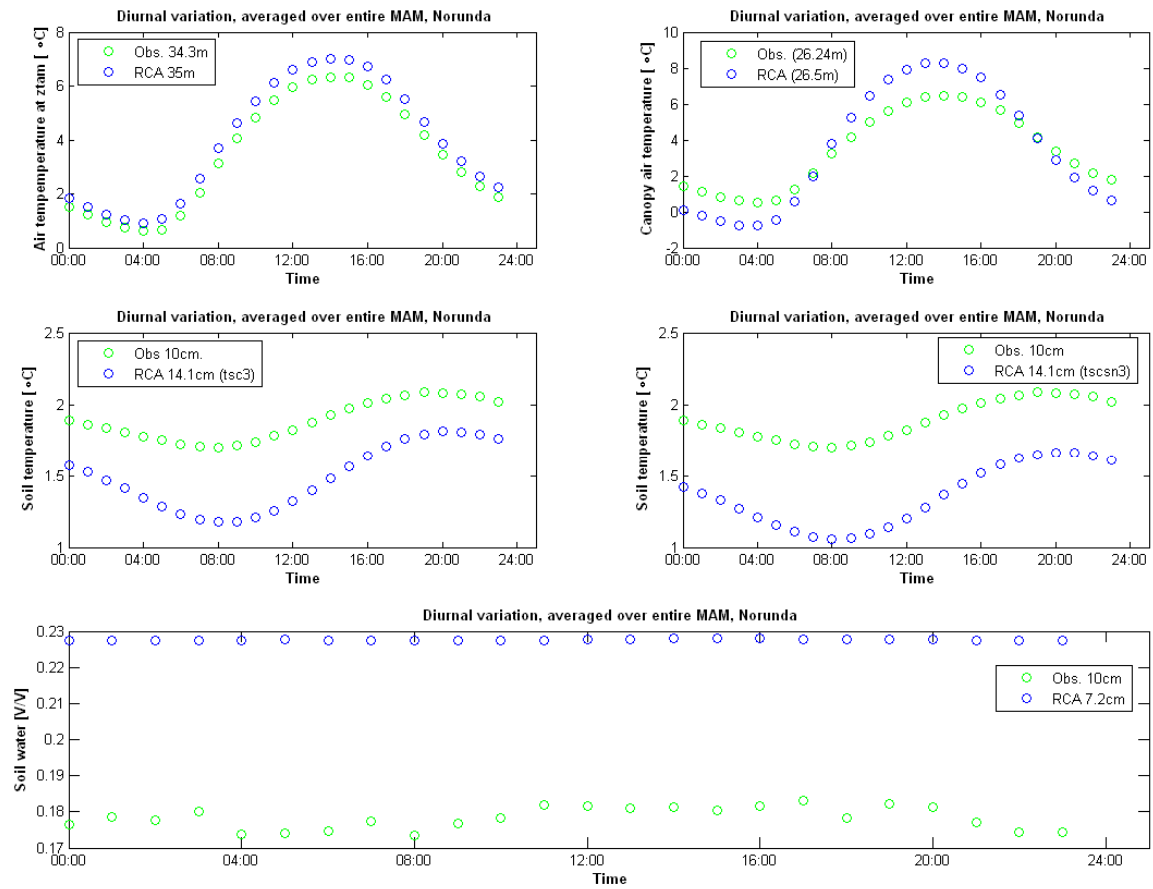


Figure C14. Diurnal variation for different variables at Norunda during MAM 1994-96. Top left: Air temperature at reference level (z_{tam}). Top right: Canopy air temperature. Middle left: third layer soil temperature without snow. Middle right: third layer soil temperature with snow. Bottom: top soil water.

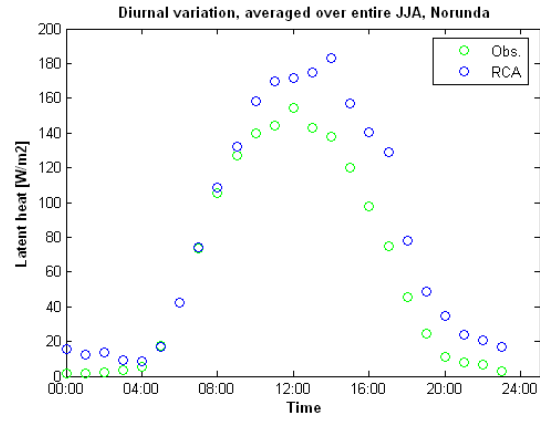
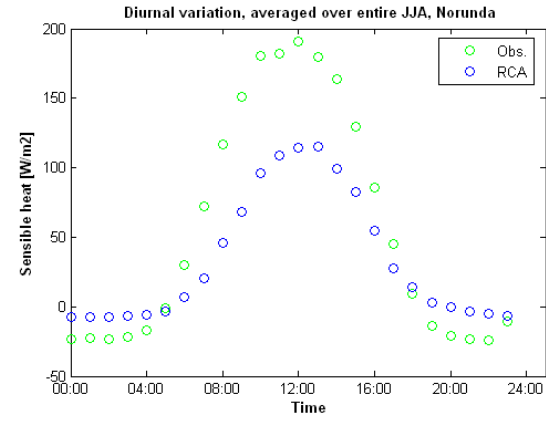
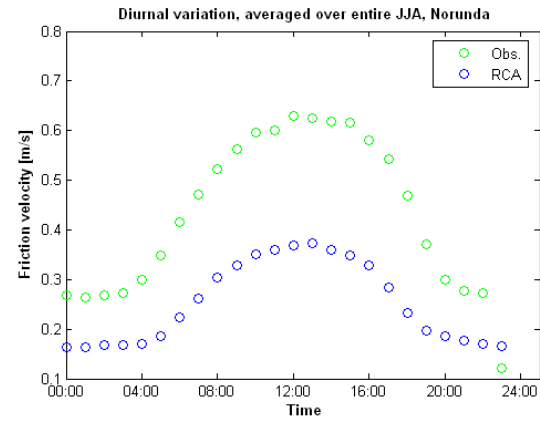
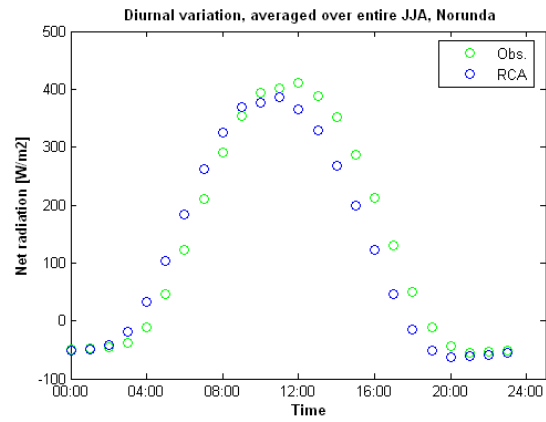


Figure C15. Diurnal variation for different variables at Norunda during JJA 1994-96. Top left: Net radiation. Top right: Friction velocity. Bottom left: Sensible heat. Bottom right: Latent heat. Modelled values are blue and observations are green.

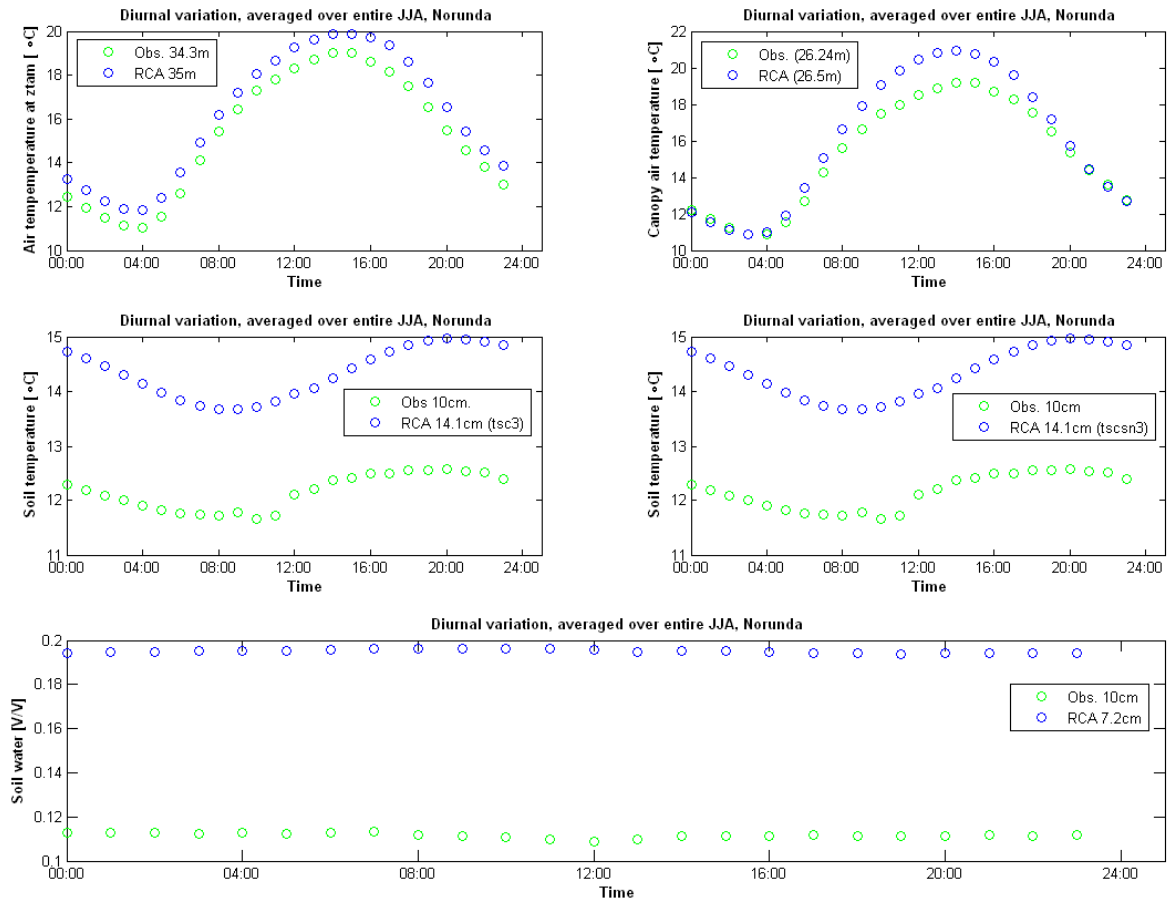


Figure C16 Diurnal variation for different variables at Norunda during JJA 1994-96. Top left: Air temperature at reference level (ztam). Top right: Canopy air temperature. Middle left: third layer soil temperature without snow. Middle right: third layer soil temperature with snow. Bottom: top soil water.

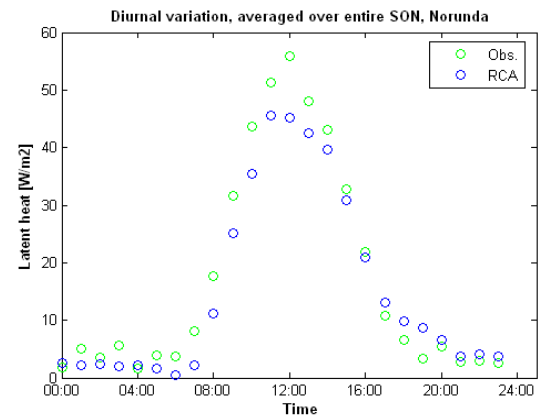
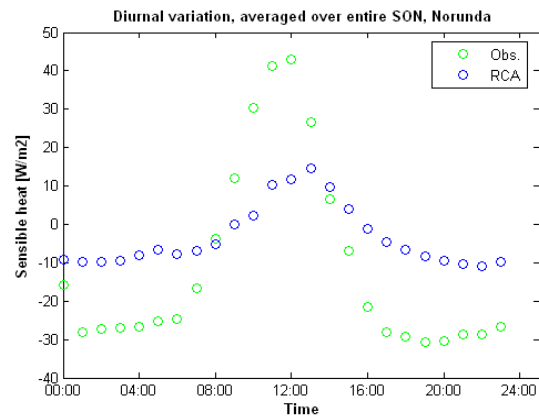
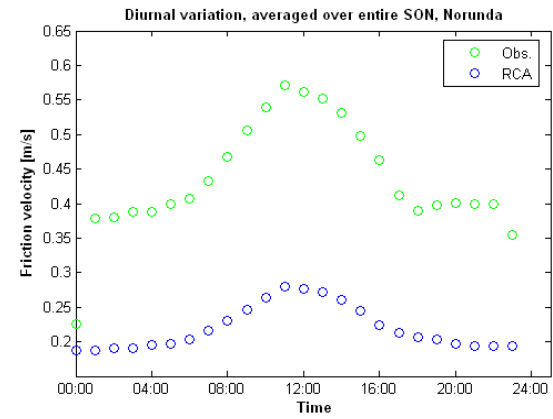
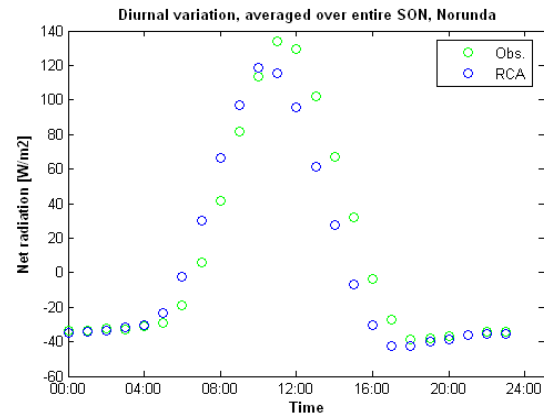


Figure C17. Diurnal variation for different variables at Norunda during SON 1994-96. Top left: Net radiation. Top right: Friction velocity. Bottom left: Sensible heat. Bottom right: Latent heat. Modelled values are blue and observations are green.

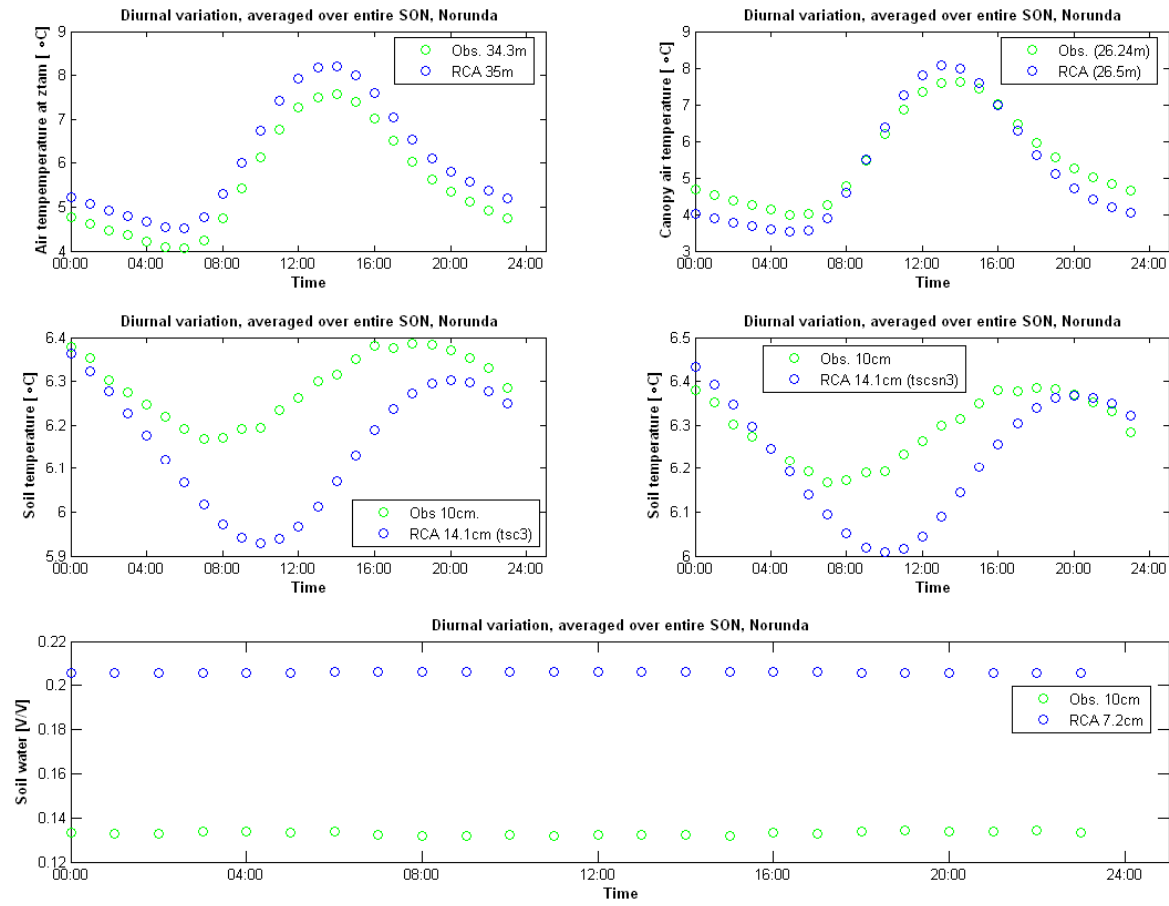


Figure C18 Diurnal variation for different variables at Norunda during SON 1994-96. Top left: Air temperature at reference level (ztam). Top right: Canopy air temperature. Middle left: third layer soil temperature without snow. Middle right: third layer soil temperature with snow. Bottom: top soil water.

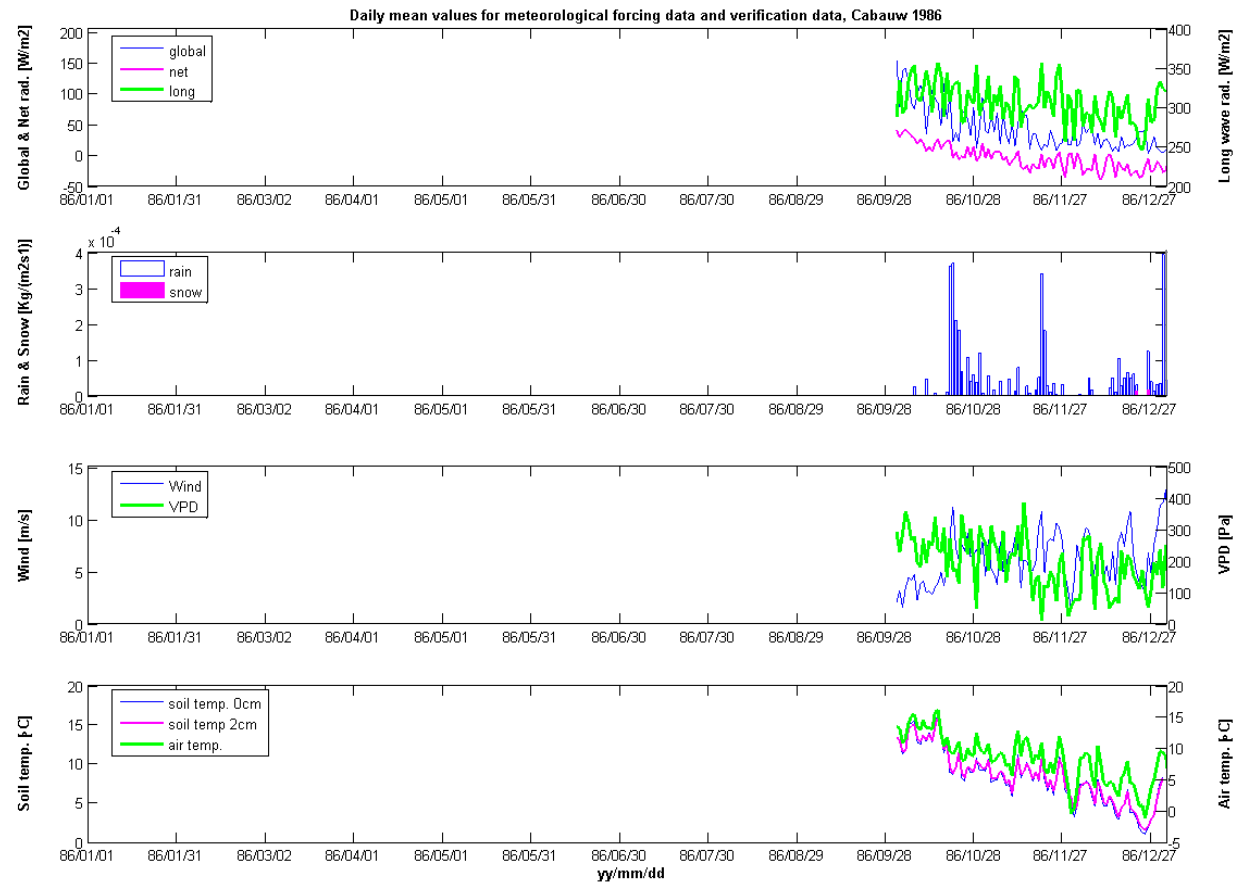


Figure C19. Daily averages of driving- and verification data at Cabauw 1986. From top to bottom: global (blue)- net (magenta)- and long wave (green)- radiation, rain (blue)- and snow (magenta)- bars, wind (blue) and VPD (green), air temperature (green) and soil temperatures at 0 cm-(blue) and 2 cm-(magenta) depths.

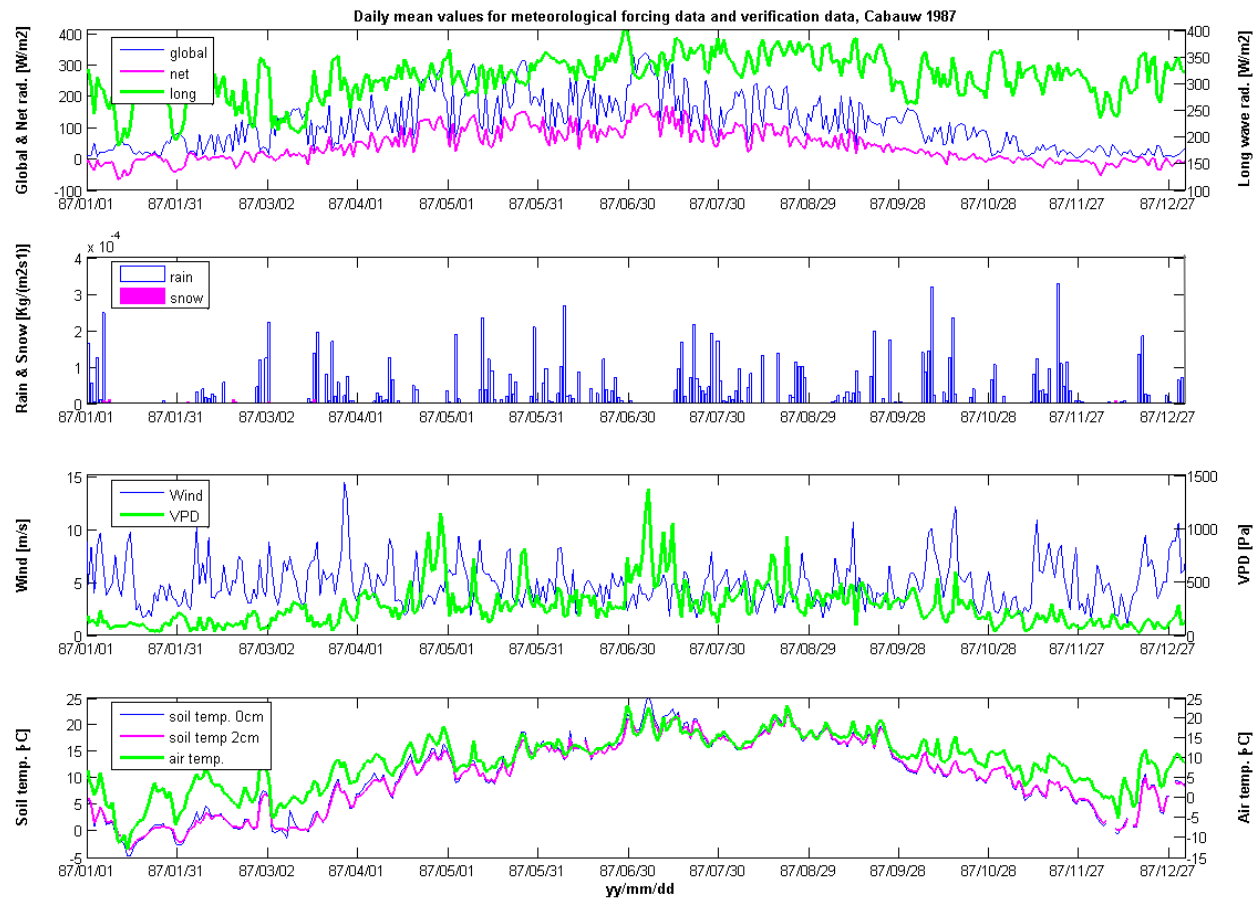


Figure C20. Daily averages of driving- and verification data at Cabauw 1987. From top to bottom: global (blue)- net (magenta)- and long wave (green)- radiation, rain (blue)- and snow (magenta)- bars, wind (blue) and VPD (green), air temperature (green) and soil temperatures at 0 cm-(blue) and 2 cm-(magenta) depths.

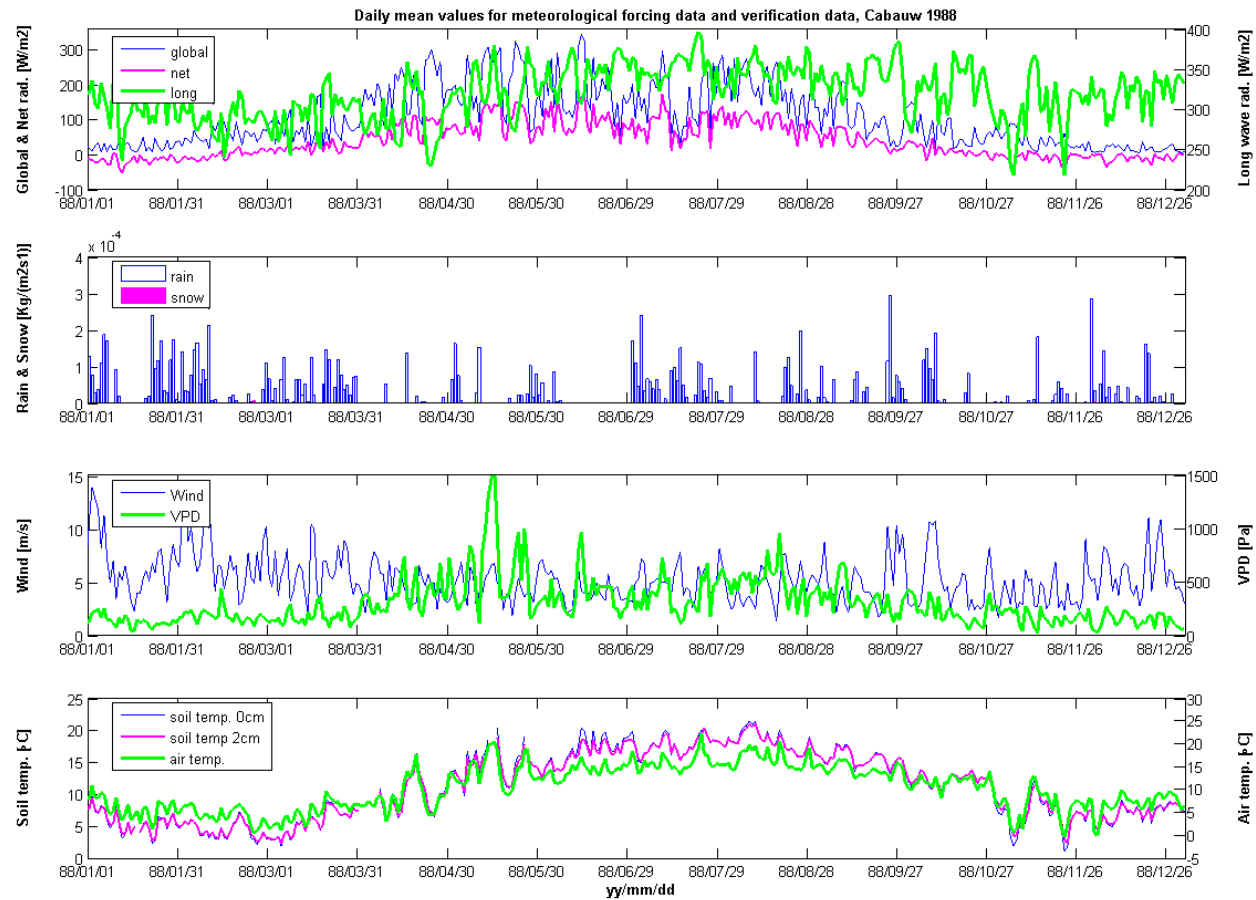


Figure C21. Daily averages of driving- and verification data at Cabauw 1988. From top to bottom: global (blue)- net (magenta)- and long wave (green)- radiation, rain (blue)- and snow (magenta)- bars, wind (blue) and VPD (green), air temperature (green) and soil temperatures at 0 cm- (blue) and 2 cm- (magenta) depths.

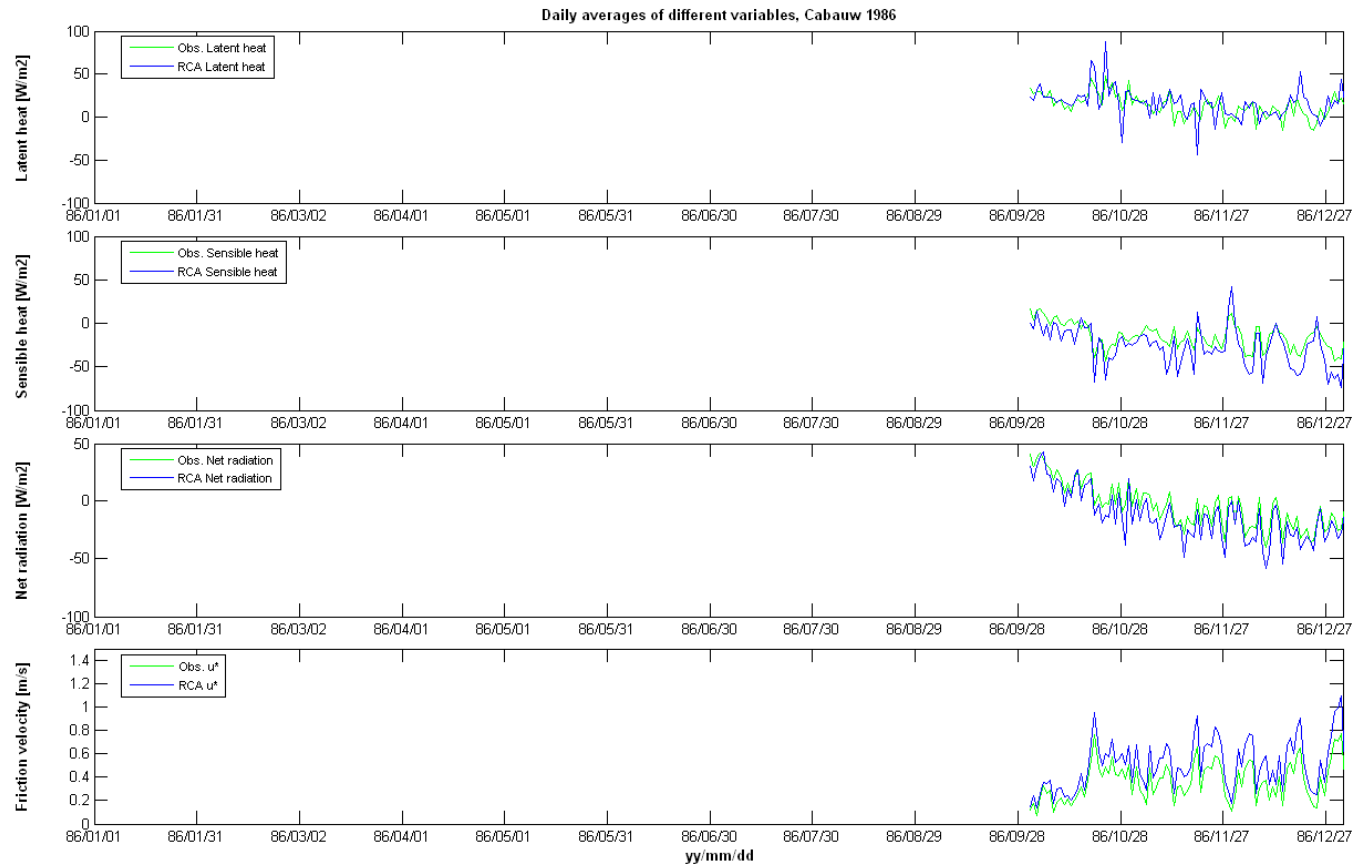


Figure C22. Daily averages for different variables at Cabauw 1986. From top to bottom: Latent heat, Sensible heat, Net radiation and friction velocity. Green lines are observations and blue lines are modelled values.

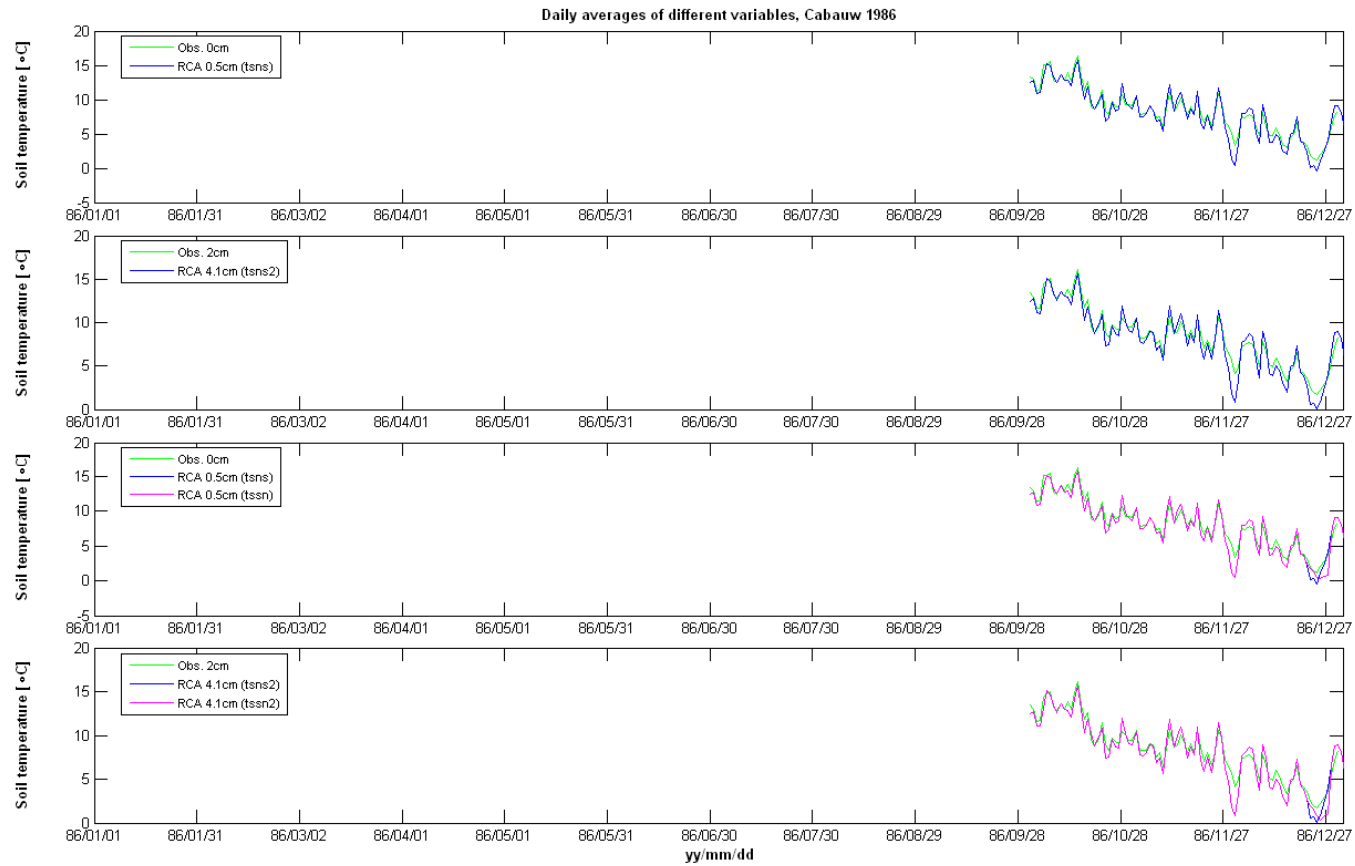


Figure C23. Daily averages for soil temperatures at Cabauw 1986. From top to bottom: first layer without snow, second layer without snow, first layer- without snow (blue) and with snow (magenta), second layer- without snow (blue) and with snow (magenta). All observations are green.

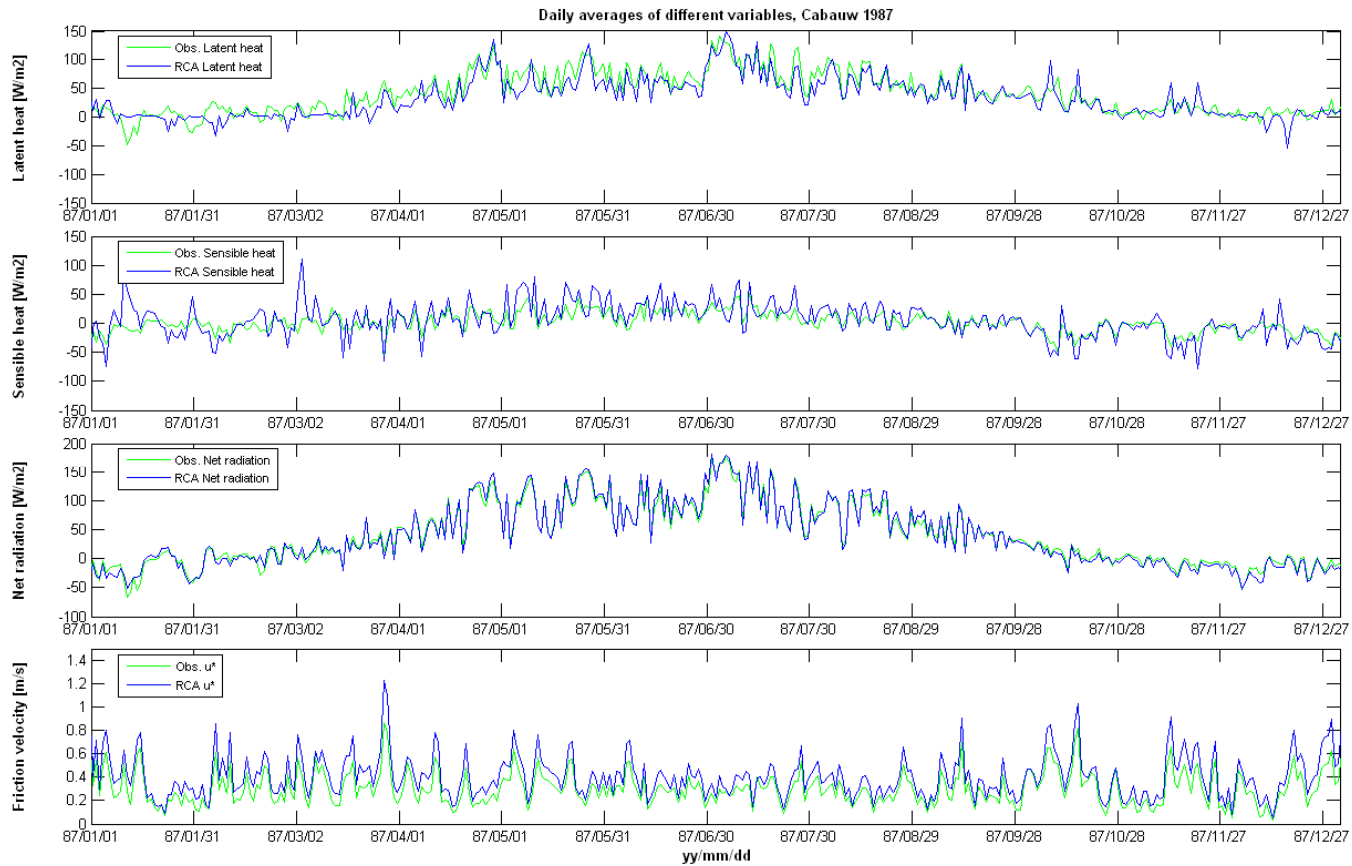


Figure C24. Daily averages for different variables at Cabauw 1987. From top to bottom: Latent heat, Sensible heat, Net radiation and friction velocity. Green lines are observations and blue lines are modelled values.

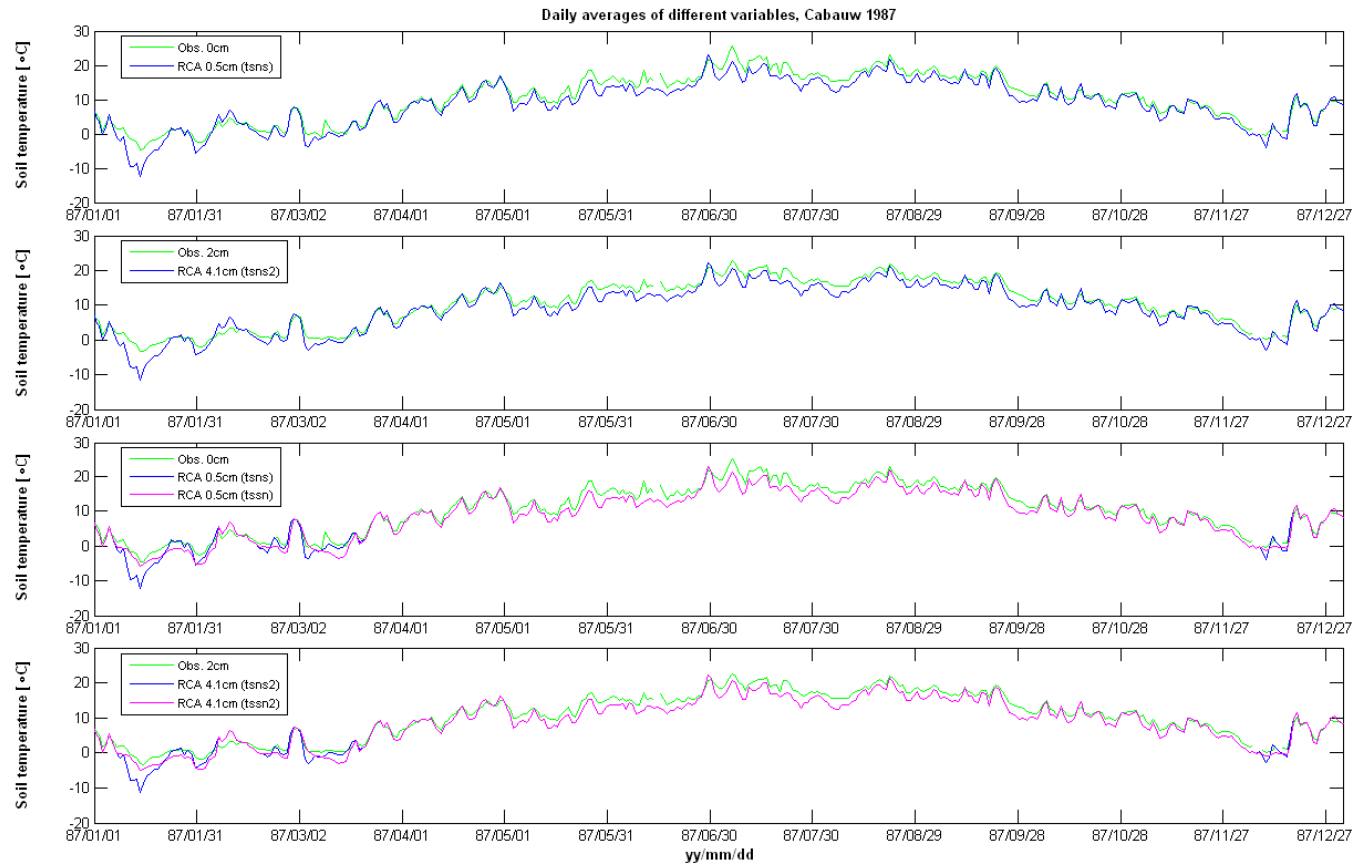


Figure C25. Daily averages for soil temperatures at Cabauw 1987. From top to bottom: first layer without snow, second layer without snow, first layer- without snow (blue) and with snow (magenta), second layer- without snow (blue) and with snow (magenta). All observations are green.

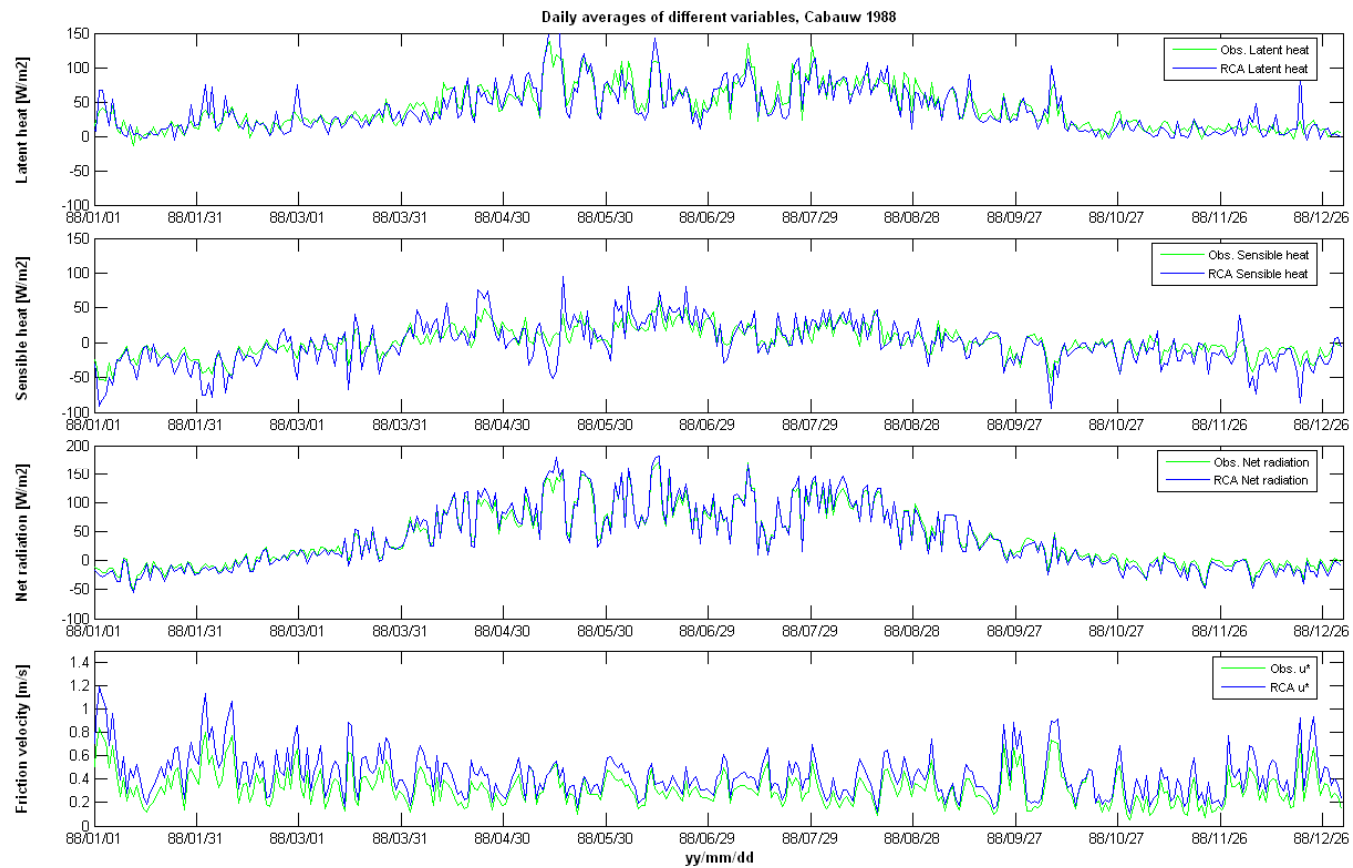


Figure C26. Daily averages for different variables at Cabauw 1988. From top to bottom: Latent heat, Sensible heat, Net radiation and friction velocity. Green lines are observations and blue lines are modelled values.

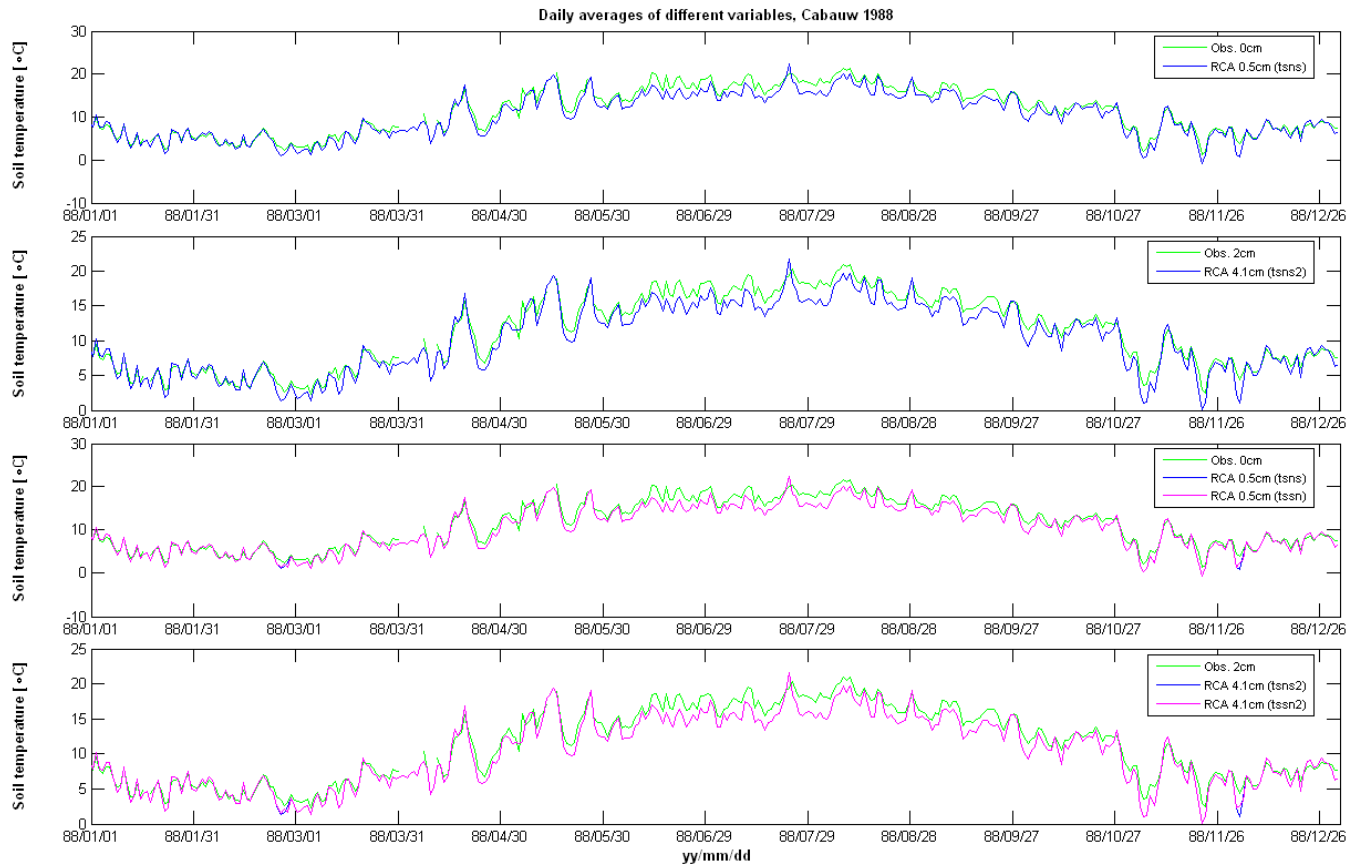


Figure C27. Daily averages for soil temperatures at Cabauw 1988. From top to bottom: first layer without snow, second layer without snow, first layer- without snow (blue) and with snow (magenta), second layer- without snow (blue) and with snow (magenta). All observations are green.

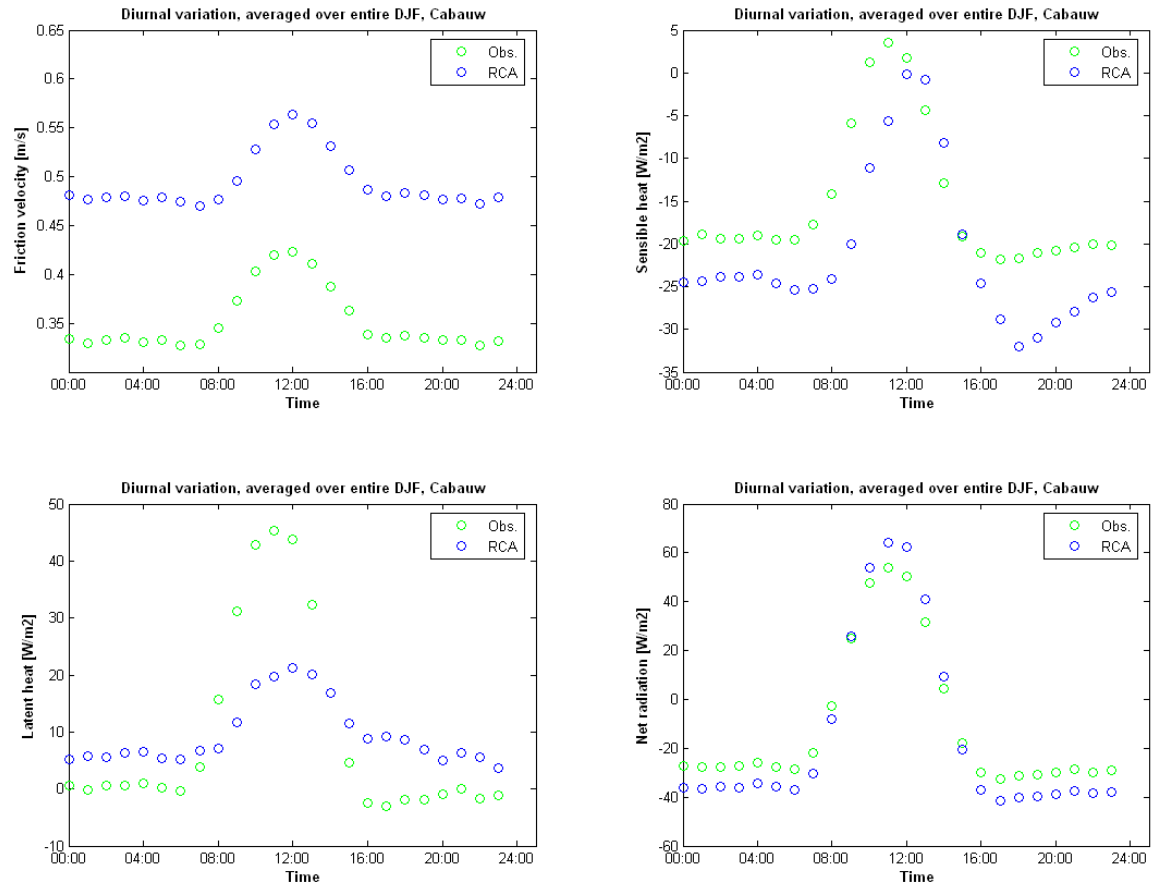


Figure C28. Diurnal variation for different variables at Cabauw during DJF 1986-88. Top left: Friction velocity. Top right: Sensible heat. Bottom left: Latent heat. Bottom right: Net radiation. All observations are green

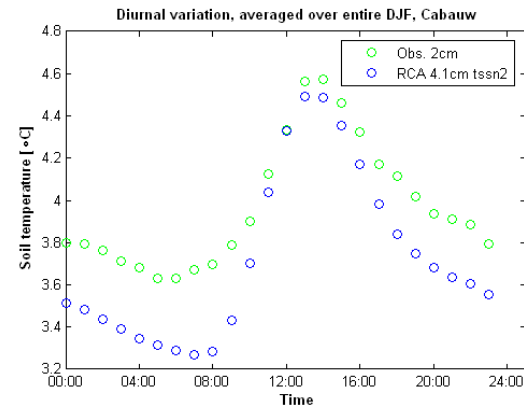
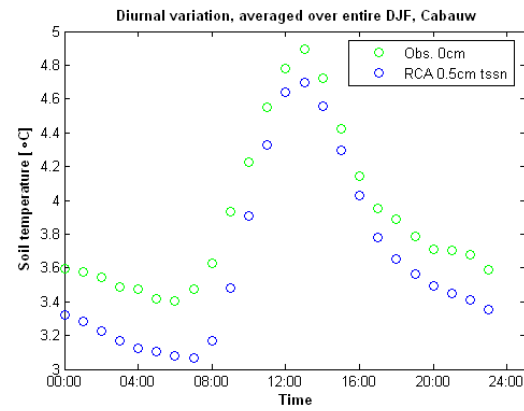
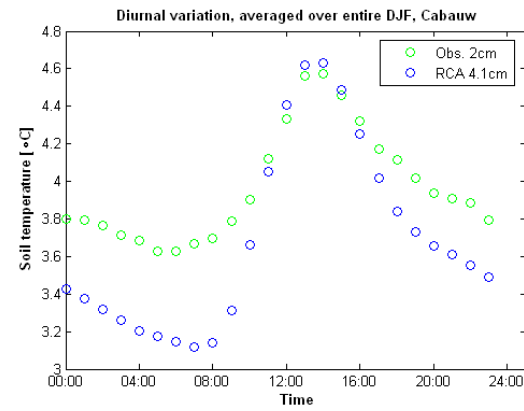
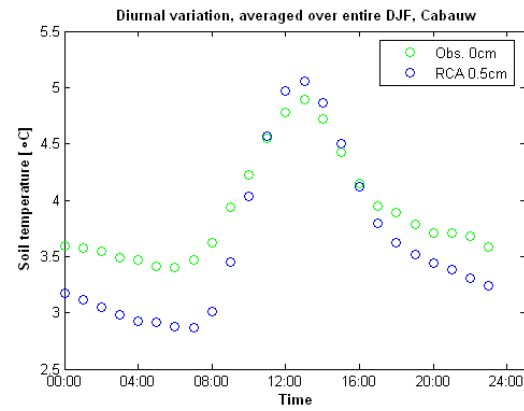


Figure C29. Diurnal variation for different soil temperatures at Cabauw during DJF 1986-88. Top left: first soil temperature layer without snow. Top right: second temperature soil layer without snow. Bottom left: first soil temperature layer with snow. Bottom right: second soil temperature layer with snow. All observations are green.

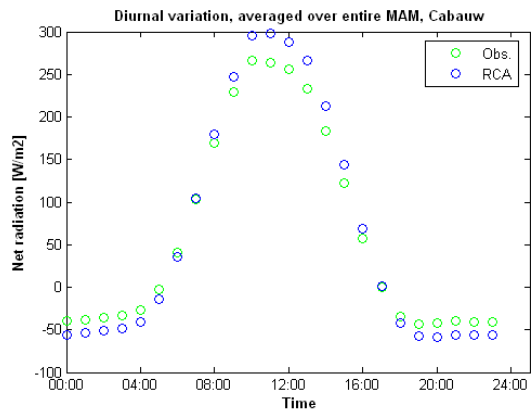
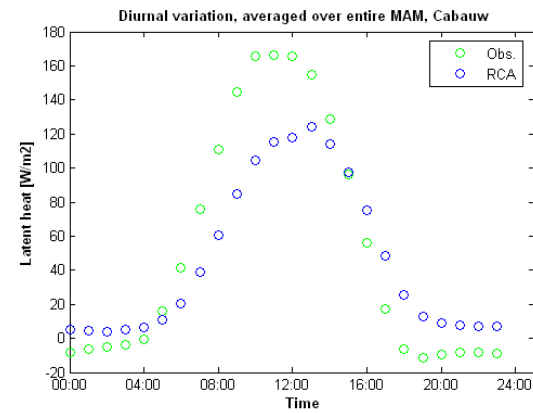
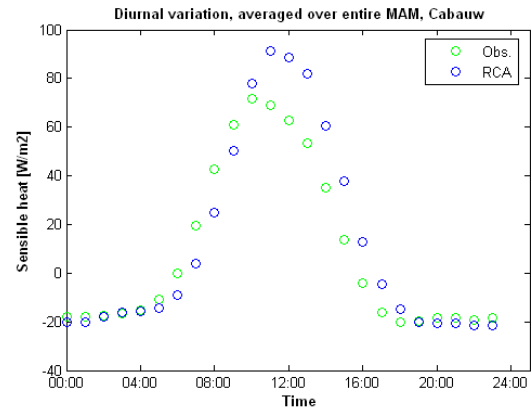
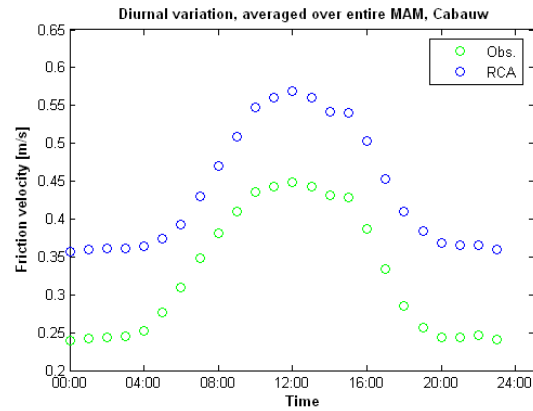


Figure C30. Diurnal variation for different variables at Cabauw during MAM 1986-88. Top left: Friction velocity. Top right: Sensible heat. Bottom left: Latent heat. Bottom right: Net radiation. All observations are green

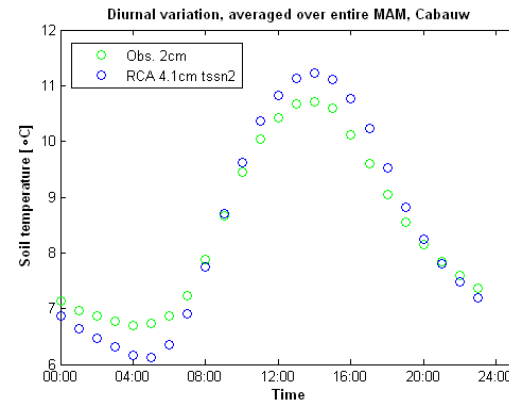
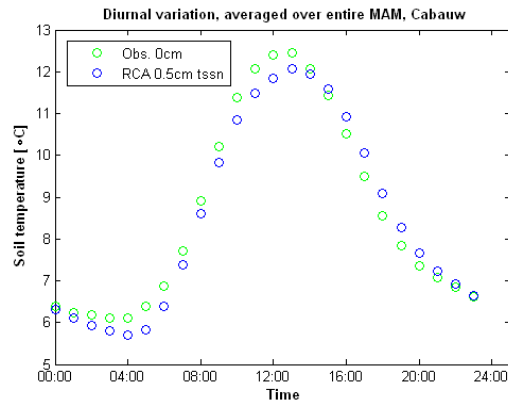
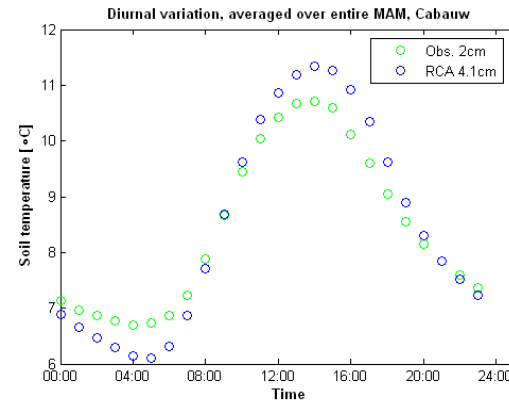
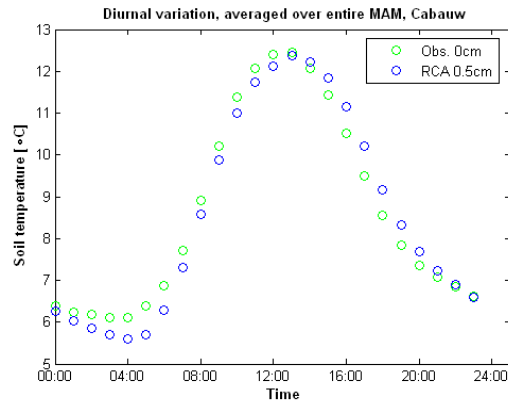


Figure C31. Diurnal variation for different soil temperatures at Cabauw during MAM 1986-88. Top left: first soil temperature layer without snow. Top right: second temperature soil layer without snow. Bottom left: first soil temperature layer with snow. Bottom right: second soil temperature layer with snow. All observations are green.

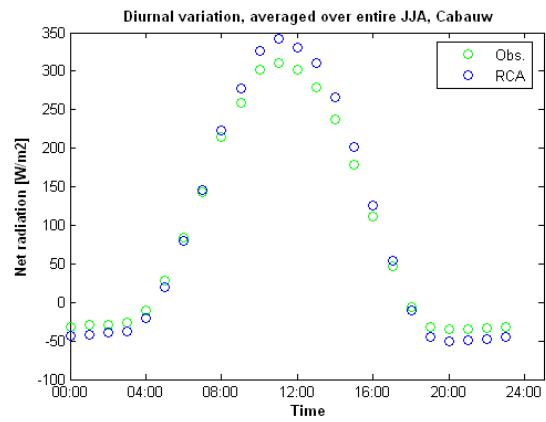
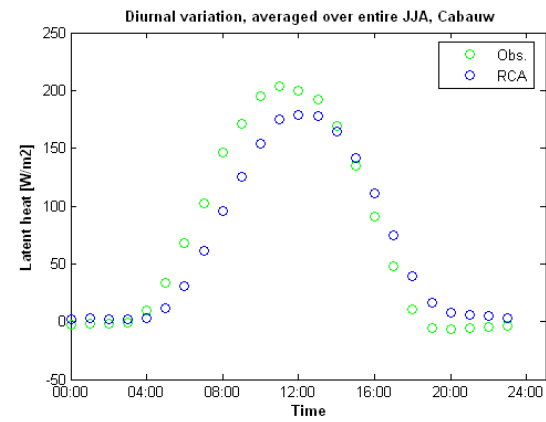
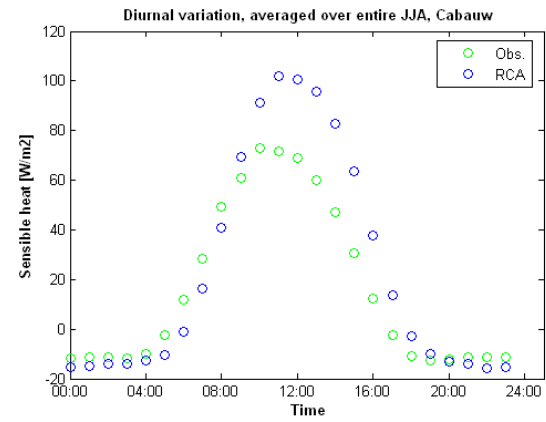
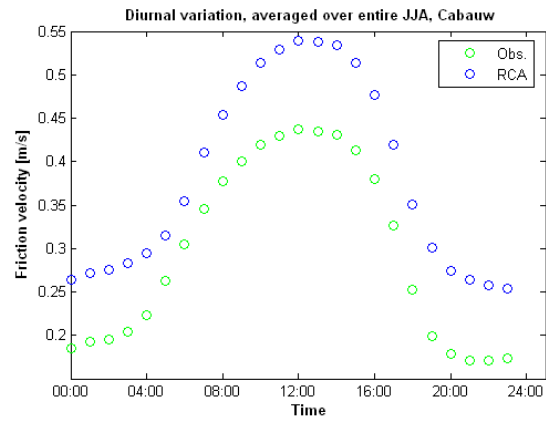


Figure C32. Diurnal variation for different variables at Cabauw during JJA 1986-88. Top left: Friction velocity. Top right: Sensible heat. Bottom left: Latent heat. Bottom right: Net radiation. All observations are green

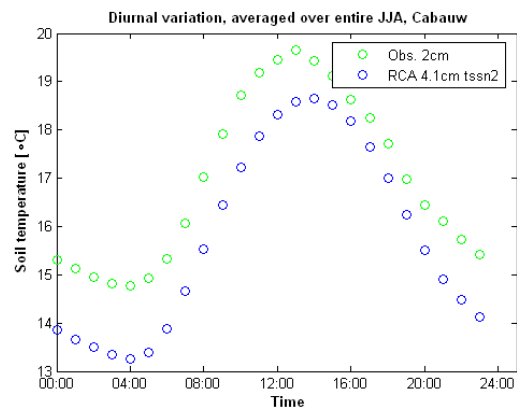
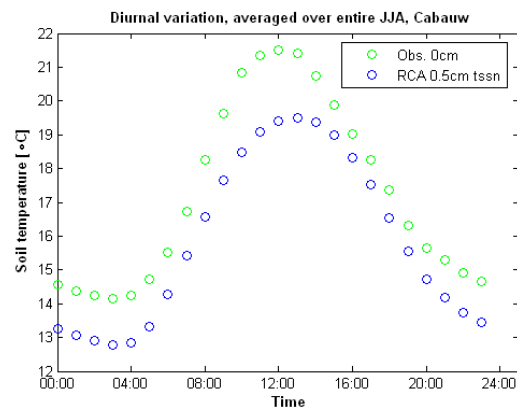
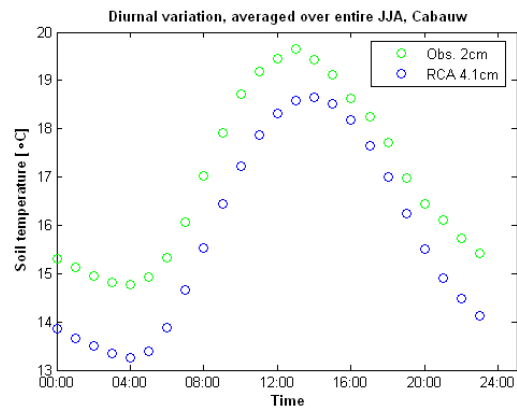
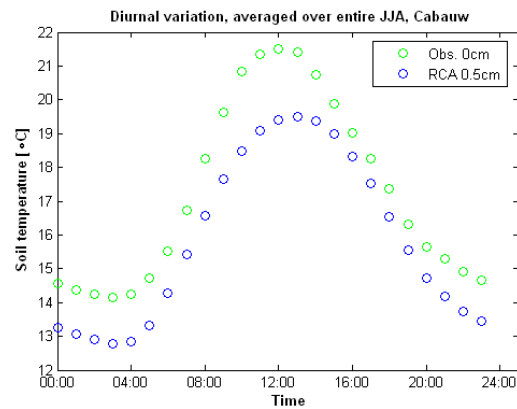


Figure C33. Diurnal variation for different soil temperatures at Cabauw during JJA 1986-88. Top left: first soil temperature layer without snow. Top right: second temperature soil layer without snow. Bottom left: first soil temperature layer with snow. Bottom right: second soil temperature layer with snow. All observations are green.

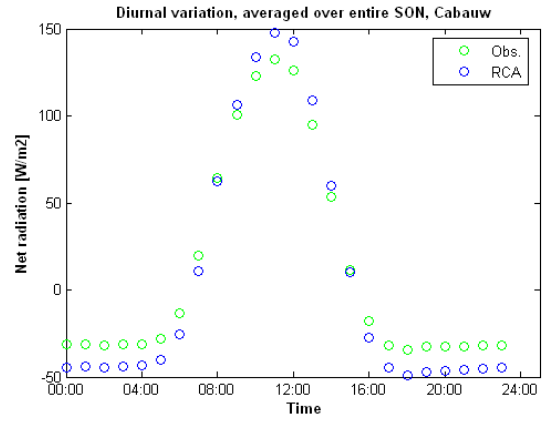
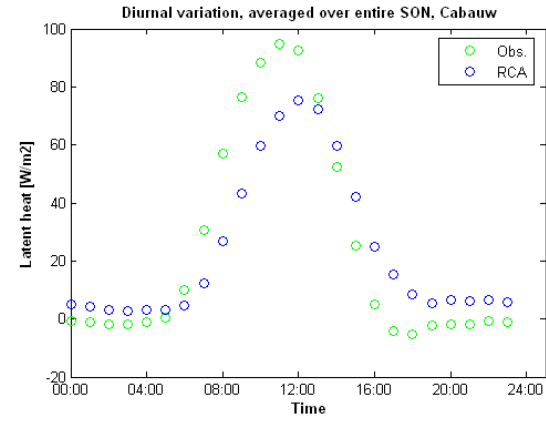
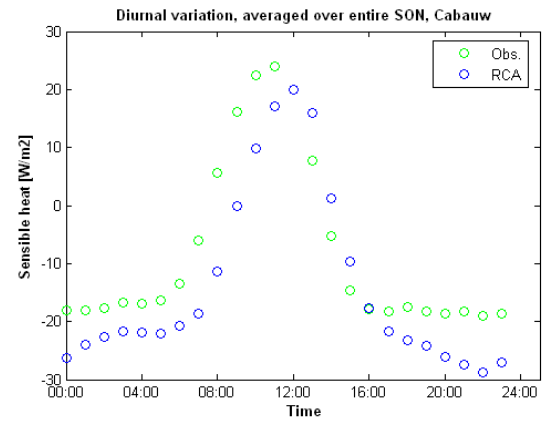
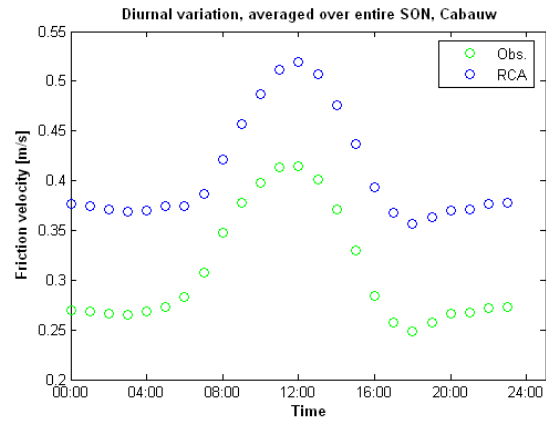


Figure C34. Diurnal variation for different variables at Cabauw during SON 1986-88. Top left: Friction velocity. Top right: Sensible heat. Bottom left: Latent heat. Bottom right: Net radiation. All observations are green.

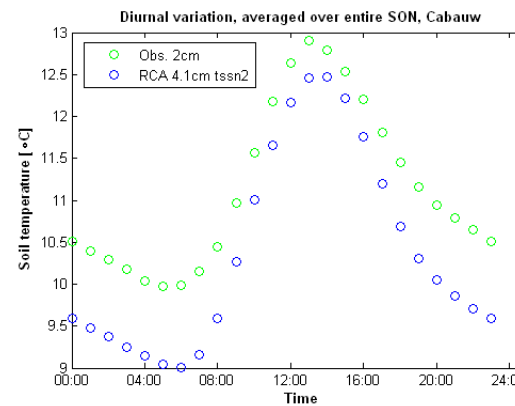
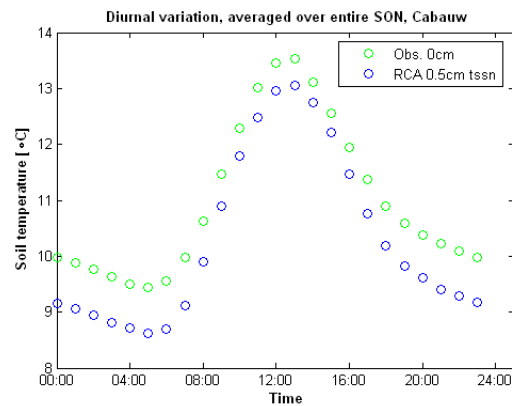
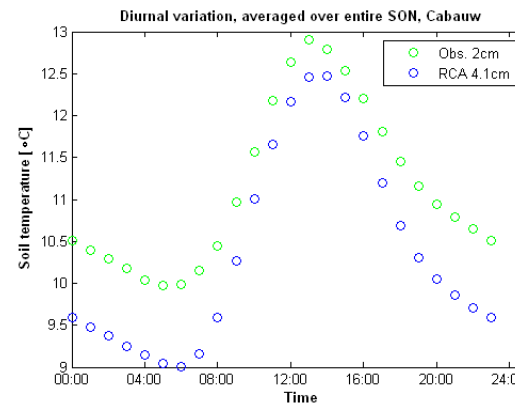
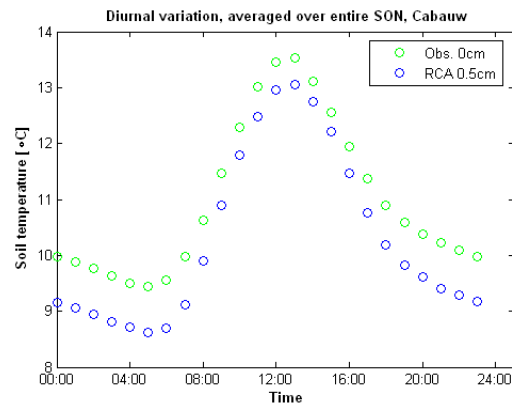


Figure C35. Diurnal variation for different soil temperatures at Cabauw during SON 1986-88. Top left: first soil temperature layer without snow. Top right: second temperature soil layer without snow. Bottom left: first soil temperature layer with snow. Bottom right: second soil temperature layer with snow. All observations are green.

